TIME-CONSISTENT APPROXIMATIONS OF RISK-AVERSE MULTISTAGE STOCHASTIC OPTIMIZATION PROBLEMS

BY TSVETAN ASAMOV

A dissertation submitted to the

Graduate School—New Brunswick

Rutgers, The State University of New Jersey

in partial fulfillment of the requirements

for the degree of

Doctor of Philosophy

Graduate Program in Operations Research

Written under the direction of

Andrzej Ruszczyński

and approved by

_____

_____

_____

_____

_____

New Brunswick, New Jersey

October, 2013

ABSTRACT OF THE DISSERTATION

TIME-CONSISTENT APPROXIMATIONS OF RISK-AVERSE MULTISTAGE STOCHASTIC OPTIMIZATION PROBLEMS

by Tsvetan Asamov

Dissertation Director: Andrzej Ruszczyński

In this work we study the concept of time consistency as it relates to multistage risk-averse stochastic optimization problems on finite scenario trees. We use dynamic time-consistent formulations to approximate problems having a single global coherent risk measure applied to the aggregated costs over all time periods. The duality of coherent risk measures is employed to create a time-consistent cutting plane algorithm for the construction of non-parametric time-consistent approximations where every one-step conditional risk measure is specified only by its dual representation. Moreover, we show that the method can be extended to generate parametric approximations involving compositions of risk measures from a specified family. Additionally, we also consider the case when the objective function is the mean-upper semideviation measure of risk and develop methods for the construction of universal time-consistent upper bounding functions. We prove that such functions provide time-consistent upper bounds to the global risk measure for an arbitrary feasible policy.

Finally, the quality of the approximations generated by the proposed methods is analyzed in multiple computational experiments involving two-stage scenario trees with both artificial data, as well as stock return data for the components of the Dow Jones

Industrial Average stock market index. Our numerical results indicate that the dynamic time-consistent formulations closely approximate the original problem for a wide range of risk aversion parameters.

Acknowledgements

I would like to thank my advisor Dr. Andrzej Ruszczyński for introducing me to the topic of time-consistent risk measures. His patient mentorship, enthusiasm and support created a work environment that was conducive to successful research. I greatly enjoyed our conversations and the challenges that we faced. I am also indebted to my committee members Dr. Adi Ben-Israel, Dr. Darinka Dentcheva, Dr. Elsayed Elsayed, and Dr. Fred Roberts for their careful reviews and helpful feedback. Additionally, I would like to express my gratitude and appreciation to Dr. András Prékopa, Dr. Endre Boros and all the faculty members of RUTCOR for giving me abundant knowledge, thoughtful guidance and considerate advice during my graduate studies.

Most of all, I would like to thank my family. My mother Ganka, father Ivan and brother Nikolay have always been there for me, and have provided me with love, care and inspiration throughout my life. I owe them more than words can express.

Finally, I would like to acknowledge the financial support that I received by the Excellence Fellowship and Teaching Assistantship awards at Rutgers University. My research was also supported by the Air Force Office of Scientific Research Award FA9550-11-1-0164: "Coherent Risk-Adjusted Decisions over Time: a Bilevel Programming Approach".

Dedication

To my parents...

Table of Contents

List of Tables

List of Figures

Chapter 1

Introduction and Preliminaries

1.1 Introduction

The increasing complexity and interdependence of the modern world have elevated the importance of risk management and turned risk-averse stochastic optimization into an active field of study in Operations Research. The mean-risk method for the optimization of portfolios with a finite number of assets was first introduced in the seminal work of Markowitz [30]. The mean-variance approach yields parametric formulations that can be solved efficiently as convex quadratic programming problems. However, there is a drawback of the method since the mean and the variance are measured in different units. Moreover, it penalizes overperformance in addition to underperformance. Markowitz recognized those issues and suggested that they can be fixed by the use of mean-semideviation [31]. While such an adjustment seemed reasonable for the mean-variance model, the more general question of what functions constitute suitable risk measures was still left unanswered. The problem was addressed by Artzner, Delbaen, Eber and Heath [3] who used an axiomatic approach to introduce the concept of coherent risk measures. They employed the term *coherent* to denote risk functions which satisfy several properties that are desirable for practical optimization. The theory of coherent risk measures has been an active area of study for over a decade and has established itself as and an alternative to expected utility models of risk averse preferences in stochastic optimization. The field was developed in numerous publications (see, e.g., [17, 20, 50] and the references therein). The subadditivity and positive homogeniety of coherent risk measures imply their convexity. Thus, using convex duality theory we can represent any coherent risk measure as the maximum of expected values, where the probability measure is chosen from a convex and closed set of probability

distributions. In addition, Kusuoka [28] showed that any coherent and law-invariant (depending only on the underlying distribution) risk measure can also be represented using a collection of integrals of Average Value at Risk measures. More specifically, his result implies that any coherent law-invariant risk measure can be expressed as the maximum expected value of Average Value at Risk functions at random level where the maximization is over a family of probability distributions on $(0, 1]$ for the different levels of risk. Complementing Kusuoka's work, Shapiro [51] demonstrated that such representations are unique in the case of comonotonic risk mesures. However, for general law invariant coherent risk measures uniqueness of the set of probability distributions is not guaranteed.

In addition to single-stage models, risk-aversion can also be considered in the case of multistage optimization problems. In the last decade, optimization models involving dynamic measures of risk, which allow for risk-averse evaluation of streams of future costs or rewards have gained popularity among researchers (see, e.g., [4, 10, 29, 37, 42, 49]). The application of dynamic risk measures in stochastic optimization models leads to a new class of problems, which are significantly more complex than their risk-neutral counterparts (see [50, 49, 1]). One reason is that multistage risk-averse optimization problems are more difficult to solve. More importantly, they are also more difficult to analyze because of the evolution of risk over different time periods. Still, it turns out that a certain class of dynamic risk measures, known as time-consistent risk measures [42, 11, 16, 53, 48, 21] remedy both of those challenges. If the risk measures are time-consistent, specialized decomposition methods can be developed, to facilitate the solution of the resulting optimization problems (see [32, 13]). In the case of time-inconsistent risk measures, no such methods exist so far. However, in general it is much easier to specify time-inconsistent risk measures. Our aim is to explore the possibility of constructing time-consistent approximations of time-inconsistent risk measures and using them in optimization problems.

The relations of risk measures and compositions of conditional risk measures (which are time-consistent by construction) has been considered in several recent works. Pichler and Pflug [39] use the dual representation of Average Value at Risk to show that for a

given random cost, one can constuct extended conditional risk functionals which allow for a temporal decomposition that preserves the initial risk preference accross time periods. Their analysis is focused on spectral risk measures, which were introduced by Artzner, et.al. in [4] and defined as a convex combination of Average Value at Risk at different levels. Thus using the Kusuoka representation theorem, Pichler and Pflug conclude that if we consider a given random variable as our random cost, then any coherent risk measure can be represented as a composition of extended conditional risk functionals without losing information or preferences.

Xin and Shapiro [54] consider upper bounds on compositions of Average Value at Risk measures and comonotonic measures by single measures of the same form. Their numerical results indicate that the quality of the approximations strongly depends on the covariance of the random costs in different time periods.

In the paper [25] Iancu, Petrik and Subramanian study the problem of upper and lower approximations of a time-inconsistent measure by a multiple of given time-consistent measure. They show that computing the optimal scaling factors for both upper and lower bounds is generally NP-hard even for law-invariant measures. When the measures are given by (compositions of) Average Value at Risk, an anlytical form of the tightest possible time-consistent upper bounds is specified. Even though the best time-consistent lower bounds are more difficult to compute, they provide closer approximations to a given time-inconsistent risk measure than the tightest time-consistent upper bounds.

Roorda and Schumacher discuss different definitions of time consistency in [44] and explore the relations between them. They extend a result of Artzner [5] and show that conditional Average Value at Risk does not satisfy even the weak notion of conditional consistency.

Despite its wide use in practice, in general the Value at Risk function is not a coherent risk measure. The issue has been studied extensively by Acerbi and Tasche [2], Delbaen [15], and Yamai and Yoshiba [55]. Additionally, Cheridito and Stadje [12] show that VaR is not time-consistent either. They propose two alternatives: a time-consistent composition of VaR functionals, and a composition of AVaR measures which

is both time-consistent and coherent.

The class of coherent risk measures can be extended to the class of convex risk measures that are not necessarily positively homogeneous. In that case a dual representation is still possible as has been shown by Föllmer and Schied [18] as well as Frittelli and Rosazza Gianin [22]. Ben-Tal and Teboulle [7, 8] employ utility functions to develop the concept of optimized certainty equivalent and show that it can be used to generate convex risk measures. Under their approach, a convex risk measure can be obtained by choosing a particular utility function, e.g., the Average Value at Risk can be derived using a piecewise linear function. One instance of convex measures that are not coherent is the class of entropic risk measures which have been studied by Föllmer and Schied [19, 17], Penner [35], and Rudloff, Sass and Wunderlich [45]. Detelefsen and Scandolo [16] consider the duality structure of convex risk functions for the construction of dynamic time-consistent risk measures and illustrate their approach for the class of entropic measures.

Our approach is different from all of the above. Given a coherent measure of risk for the total cost of a multistage optimization problem, we develop a time-consistent decomposition method. If the original measure is time-consistent, the method finds the optimal solution of the problem. If the risk measure is not time-consistent, the method will find a time-consistent upper bound on the optimal value of the problem. The decomposition method can be formulated and implemented in two versions: a non-parametric version, when the analytical form of the approximation is not specified, and a parametric form, which seeks the best approximation among a fixed family of measures. We also propose two algorithms for computing *universal* time-consistent upper bounds, when the analytical forms of the original measure and its approximations are specified.

1.1.1 Outline of the Dissertation

In the remaining sections of this chapter we introduce coherent risk measures and use an example to demonstrate the phenomenon of time inconsistency. In Sections 2.1 and 2.2 we quickly review basic concepts associated with risk-averse multistage optimization. Sections 2.3 and 2.4 present the main theoretical foundations of the

decomposition methods. In Section 2.5 we describe a new nested decomposition method for optimizing polyhedral time-consistent models, which extends to the multistage case the method of [32]. Section 3.2 describes a time-consistent decomposition method, which can be applied to both consistent and inconsistent problems. In Section 3.3 we derive its properties in the time-inconsistent case, and in Section 3.4 we describe its parametric version. In Chapter 4 we present two algorithms for calculating *universal* time-consistent upper bounds, that is, upper bounds which are valid for all values of the decision vector. Finally, in Chapter 5 we present a numerical illustration of the operation of the methods.

1.2 Coherent Risk Measures

Consider a probability space $(\Omega, \mathcal{F}, P)$ consisting of a sigma algebra $\mathcal{F}$ induced on the sample set Ω and a probability measure P defined on $\mathcal{F}$. We consider the space of random outcomes $\mathcal{Z} = \mathcal{L}_p(\Omega, \mathcal{F}, P)$, where $p \in [1, \infty)$. Every element $Z \in \mathcal{Z}$ is a random variable with a bounded p-th moment under the probability measure P. One can think of risk as the present value of a unknown (random) cost which would be observed in the future. Formally, we define a risk measure to be a function $\rho : \mathcal{Z} \to \mathbb{R}$. Additionally, *coherent* risk measures which were originally introduced by Artzner, et al. [3] are risk measures satisfying the following four axioms:

(A1) *Subadditivity*: $\rho(Z + V) \leq \rho(Z) + \rho(V)$, for all $Z, V \in \mathcal{Z}$.

(A2) *Monotonicity*: If $Z, V \in \mathcal{Z}$ and $Z \leq V$, then $\rho(Z) \leq \rho(V)$;

(A3) *Translation Equivariance*: If $Z \in \mathcal{Z}$ and $a \in \mathbb{R}$, then

$$\rho(a + Z) = a + \rho(Z).$$

(A4) *Positive Homogeneity*: If $\gamma \geq 0$ and $Z \in \mathcal{Z}$, then $\rho(\gamma Z) = \gamma \rho(Z)$.

We can interpret the risk as a "fair present value", or a deterministic equivalent amount of cash that we would be willing to pay to avoid incurring a random cost in the future. From this point of view the above axioms have straighforward interpretations. The

subadditivity axiom has the well-known interpretation that "a merger does not create extra risk" [3]. The monotonicity property implies that investments which would incur a greater cost in every possible future scenario, must result in a greater risk in the present. Axiom (A3) implies that if a certain cost needs to be taken into account under all possible scenarios, then we can consider it as a constant and separate it from the random component. Then the risk of the overall position is simply the sum of the constant cost and the risk associated with the remaining (stochastic) amount. Finally, the positive homogeneity property implies that the amount that we are willing to pay to avoid the random cost should be independent of the currency (or scale) that we use to measure risk. For example, if we scale up one hundred times the risk of an investment measured in dollars, then the result should be the same as the risk of the investment measured in cents.

The subadditivity and positive homogeneity properties imply that coherent risk measures are convex functions. To emphasize this fact, reserchers often use the following convexity axiom (A1') in the place of the subadditivity condition (A1). The axioms (A1'), (A2)-(A4) present an alternative definition that is equivalent to the original one given by Artzner, et al..

(A1') *Convexity*: $\rho\left(\alpha Z + (1-\alpha)\, V\right) \leq \alpha\rho(Z) + (1-\alpha)\rho(V)$, for all $Z, V \in \mathcal{Z}$ and all $\alpha \in [0,1]$;

Example 1. *Consider the mean–upper semideviation function $\rho(Z)$ defined as follows:*

$$\rho(Z) = \mathbb{E}[Z] + \kappa\mathbb{E}\left[\left(Z - \mathbb{E}[Z]\right)_+\right], \quad \kappa \in [0,1] \tag{1.1}$$

We can verify that all axioms (A1)-(A4) hold for $\rho(Z)$. For details, please see Ruszczyński and Shapiro [49, Example 6.1], [50, Example 4.2], and Ogryczak and Ruszczyński [33, 34].

Example 2. *The Value at Risk at level $\alpha \in (0,1)$ is given by*

$$VaR_\alpha(Z) = F_Z^{-1}(1-\alpha).$$

where F is the cumulative distribution function of the random variable Z. Despite its popularity in practical applications, the Value at Risk is not a coherent risk measure

since it does not satisfy the subadditivity axiom. Pflug [38] pointed out that in the case of comonotone random variables, the Value at Risk is additive. Furthermore, Danielsson, et al. [14] and Ibragimov [26] show that Value at Risk would be subadditive for random variables that do not involve heavy tails. More specifically, subadditivity would hold if the underliying distributions were log-concave, such as the uniform, normal and exponential distributions [26].

Another popular risk measure is the Average Value at Risk.

Example 3. *The Average Value at Risk at level $\alpha \in (0,1)$ is defined as*

$$AVaR_\alpha(Z) = \frac{1}{\alpha}\int_0^\alpha VaR_\beta(Z)d\beta \tag{1.2}$$

Furthermore, it can be computed using the following linear programming formulation:

$$AVaR_\alpha(Z) = \min_\xi \left\{ \xi + \frac{1}{\alpha}\mathbb{E}\left[\left(Z-\xi\right)_+ \right] \right\} \tag{1.3}$$

We can verify that $AVaR_\alpha(Z)$ satisfies axioms (A1)-(A4) and is therefore a coherent risk measure. For details, the reader is refered to Ruszczyński and Shapiro [49, Example 6.2], [50, Example 4.3], Ogryczak and Ruszczyński [33, 34], Rockafellar and Uryasev [43], and Pflug [38, 40].

Finally, we also mention that every coherent measure of risk $\rho(Z)$ has the following dual representation:

$$\rho(Z) = \max_{\mu\in\mathcal{A}} \mathbb{E}_\mu[Z] \tag{1.4}$$

where $\mathcal{A}$ is a closed and convex set of probability distributions [50, Theorem 2.2]. Furthermore, one can show that $\mathcal{A} = \partial\rho(0)$.

In some cases analytical descriptions of the sets $\mathcal{A}$ can be derived. For example, suppose there are n possible scenarios that we would like to consider for single stage risk-averse optimization. Then for a fixed allocation, our loss would be a discrete random variable Z which takes a value of z_i under the $i-$th scenario, which can occur with probability p_i, for $i \in \{1,..,n\}$. This setup is depicted in Figure 1.1. In this case we can arrive at the following results:

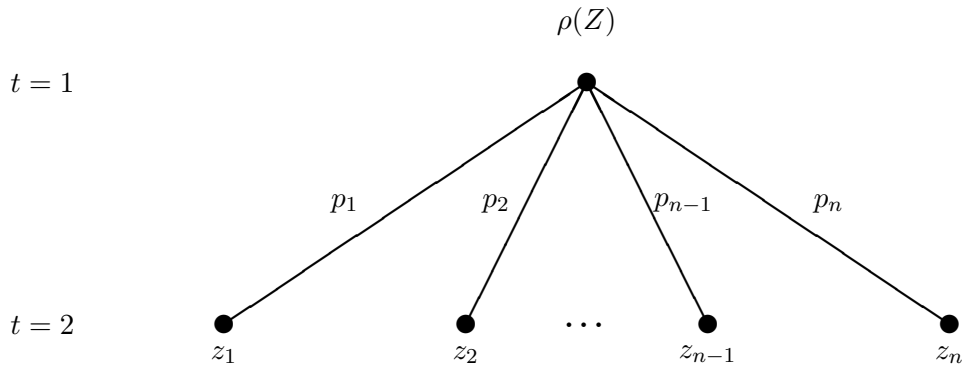

Figure 1.1: One-stage scenario tree.

Example 4. *The dual set of probability measures corresponding to the mean–upper semideviation function with a risk coefficient $\gamma \in (0,1)$ is given by:*

$$\mathcal{A} = \{\mu : \frac{\mu_i}{p_i} = 1 + h_i - \sum_{k=1}^{n} h_k p_k,\ 0 \le h_i \le \kappa\} \tag{1.5}$$

The result follows from [50, Example 4.2], and we also present a derivation based on linear programming in Section 1.2.1.

Example 5. *For the Average Value at Risk at level $\alpha \in (0,1)$ the dual set of probability measures is given by:*

$$\mathcal{A} = \{\mu : \frac{\mu_i}{p_i} \le \frac{1}{\alpha},\ \sum_{i=1}^{n} \mu_i = 1,\ \mu \ge 0\} \tag{1.6}$$

Please see [50, Example 4.3] for more details.

1.2.1 Dual Representation of Mean-Upper Semideviation

For the setup of Figure 1.1 the mean–upper semideviation function has the form

$$\rho(Z) = \sum_{i=1}^{n} p_i z_i + \kappa \sum_{i=1}^{n} p_i \left(z_i - \sum_{k=1}^{n} p_k z_k \right)_+ \tag{1.7}$$

However, we can also compute $\rho(Z)$ using the following linear programming formulation:

$$\begin{aligned} &\min_{s} \sum_{i=1}^{n} p_i z_i + \kappa \sum_{i=1}^{n} p_i s_i \\ &\text{s.t.} \\ &\sum_{k=1}^{n} p_k z_k + s_i \geq z_i, \quad \forall i \in \{1, \ldots, n\} \\ &s_i \geq 0, \quad \forall i \in \{1, ..., n\} \end{aligned} \tag{1.8}$$

Clearly, the optimal objective value is the value of the linear mean-semideviation, and the corresponding dual problem is given by:

$$\begin{aligned} &\max_{\lambda} \sum_{i=1}^{n} \lambda_i (z_i - \sum_{k=1}^{n} p_k z_k) + \sum_{i=1}^{n} p_i z_i \\ &\text{s.t.} \\ &\lambda_i \leq \kappa p_i, \quad \forall i \in \{1, ..., n\} \\ &\lambda_i \geq 0, \quad \forall i \in \{1, ..., n\} \end{aligned} \tag{1.9}$$

Now, we explore the primal-dual relationship a bit further. Assuming that we only consider scenarios with probabilities of occurence $p_i > 0$, we denote

$$h_i = \frac{\lambda_i}{p_i} \tag{1.10}$$

Then, we can rewrite the dual objective function as

$$\begin{aligned} \sum_{i=1}^{n} h_i p_i (z_i - \sum_{k=1}^{n} p_k z_k) + \sum_{i=1}^{n} p_i z_i &= \sum_{i=1}^{n} z_i (h_i p_i + p_i - \sum_{k=1}^{n} p_i h_k p_k) \\ &= \sum_{i=1}^{n} z_i p_i (1 + h_i - \sum_{k=1}^{n} p_k h_k) \end{aligned} \tag{1.11}$$

Hence we know,

$$\rho(Z) = \max_{\mu \in \mathcal{A}^{\kappa}} E_{\mu}[Z] \tag{1.12}$$

where

$$\begin{aligned} \mathcal{A}^{\kappa} &= \partial \rho(0) \\ &= \{\mu : \frac{\mu_i}{p_i} = 1 + h_i - \sum_{k=1}^{n} h_k p_k, \ 0 \leq h_i \leq \kappa\} \end{aligned} \tag{1.13}$$

Before we proceed, we show that $\mathcal{A}^\kappa$ is a family of probability measures. Denoting $\bar{h} = \sum_{i=1}^{n} h_i p_i$,

$$\begin{aligned}\sum_{i=1}^{n} \mu_i &= \sum_{i=1}^{n} p_i + p_i h_i - p_i \sum_{k=1}^{n} p_k h_k \\ &= 1 + \sum_{i=1}^{n} p_i \left(h_i - \sum_{k=1}^{n} p_k h_k \right) \\ &= 1 + \bar{h} - \sum_{i=1}^{n} p_i \bar{h} \\ &= 1\end{aligned} \tag{1.14}$$

Moreover, if $\kappa \leq 1$, then $0 \leq h_i \leq \kappa \leq 1$, and $\sum_{k=1}^{n} p_k h_k \leq 1$. Therefore,

$$\begin{aligned}\mu_i &= p_i(1 + h_i - \sum_{k=1}^{n} p_k h_k) \\ &\geq 0\end{aligned} \tag{1.15}$$

Thus we verify that $\mathcal{A}^\kappa$ is a family of probability measures and $\rho(Z)$ can be computed by finding $\mu^* \in \mathcal{A}^\kappa$ such that

$$E_{\mu^*}[Z] = \max_{\mu \in \mathcal{A}^\kappa} E_\mu[Z]$$

What is more, we can find a closed form expression for μ^*. Notice that the optimal solution of problem (1.8) has corresponding dual multipliers λ_i^* that are given by:

$$\lambda_i^* = \begin{cases} \kappa p_i & \text{if } z_i \geq \sum_{k=1}^{n} p_k z_k \\ 0 & \text{otherwise} \end{cases} \tag{1.16}$$

Thus, using equations (1.10) and (1.13), we know

$$\begin{aligned}\mu_i^* &= p_i(1 + h_i^* - \sum_{k=1}^{n} h_k^* p_k) \\ &= p_i \left(1 + \frac{\lambda_i^*}{p_i} - \sum_{k=1}^{n} \frac{\lambda_k^*}{p_k} p_k \right) \\ &= p_i + \lambda_i^* - p_i \sum_{k=1}^{n} \lambda_k^*\end{aligned} \tag{1.17}$$

1.3 The Paradox of Time Inconsistency

Time inconsistency is a remarkable phenomenon that is rather non-intuitive. In order to illustrate it, we consider a two stage decision tree with only two possible scenarios at each stage. We can either move left with probability of 0.3 or move right with probability of 0.7. At the end of the second stage, at time $t = 3$, we observe the realization of a random variable Z which reprsents costs or losses, so smaller values of Z are better for us. The described setup is presented in Figure 1.2.

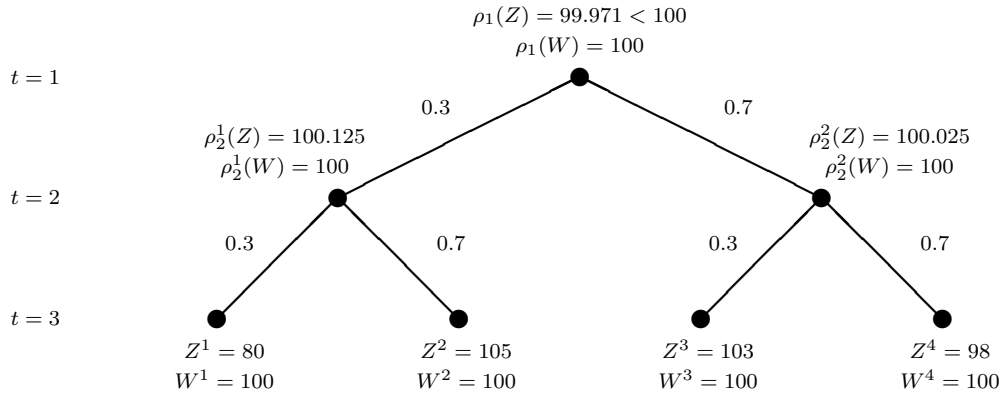

Figure 1.2: Time inconsistency when risk is measured by the mean–upper semideviation function with $\kappa = 0.5$

Now, suppose that we would like to make a decision which would involve the random cost Z. Then we would need a certain function to examine the possible realizations of Z and tell us just how good or how bad Z actually is. One possible such function is the expected value, and in this case $E[Z]$ would represent our expected cost. However, in practical applications it is often the case that cost over-runs are especially painful and undesirable. Still, the expected value function does not accurately represent such preferences. One possible approach to address this issue would be to consider the mean–upper semideviation function of Example 1.1.

Upon inspection, we can see that $\rho(Z)$ takes into account the expected cost, and in addition, it also introduces a penalty of κ for realizations of Z which are above the

mean. Further, by adjusting the value of κ we can control our risk preference, with larger values of κ implying greater risk-aversion. Now, suppose that we choose our risk aversion coefficient to be $\kappa = 0.5$, and we evaluate the risk of the random cost Z at time $t = 1$ using the realizations shown in Figure 1.2. Then,

$$\begin{aligned} E_1[Z] &= 0.3 \cdot 0.3 \cdot 80 + 0.3 \cdot 0.7 \cdot 105 + 0.7 \cdot 0.3 \cdot 103 + 0.7 \cdot 0.7 \cdot 98 \\ &= 98.9 \end{aligned} \tag{1.18}$$

and

$$\begin{aligned} \rho_1(Z) &= \mathbb{E}_1[Z] + \kappa \mathbb{E}\left[\left(Z - \mathbb{E}_1[Z]\right)_+\right] \\ &= 98.9 + 0.5 \cdot \big(0.3 \cdot 0.7 \cdot (105 - 98.9) + 0.7 \cdot 0.3 \cdot (103 - 98.9)\big) \\ &= 99.971 \\ &< 100 \\ &= \rho_1(W) \end{aligned} \tag{1.19}$$

Thus we know that at time $t = 1$, we would prefer the random cost Z rather than a fixed cost W which takes a value of 100 at time $t = 3$ under every possible scenario. However, as we move to a node at time period $t = 2$, parts of the scenario tree would become irrelevant and our risk evaluation would only depend on a smaller set of possible scenarios. Thus, if we consider the left node at time $t = 2$, we see that

$$\begin{aligned} E_2^1[Z] &= 0.3 \cdot 80 + 0.7 \cdot 105 \\ &= 97.5 \end{aligned} \tag{1.20}$$

and

$$\begin{aligned} \rho_2^1(Z) &= \mathbb{E}_2^1[Z] + \kappa \mathbb{E}\left[\left(Z - \mathbb{E}_2^1[Z]\right)_+\right] \\ &= 97.5 + 0.5 \cdot \big(0.7 \cdot (105 - 97.5)\big) \\ &= 100.125 \\ &> 100 \\ &= \rho_2^1(W) \end{aligned} \tag{1.21}$$

Similarly, at the right node at time $t = 2$ we observe

$$\begin{aligned} E_2^2[Z] &= 0.3 \cdot 103 + 0.7 \cdot 98 \\ &= 99.5 \end{aligned} \tag{1.22}$$

and

$$\begin{aligned} \rho_2^2(Z) &= \mathbb{E}_2^2[Z] + \kappa \mathbb{E}\left[\left(Z - \mathbb{E}_2^2[Z]\right)_+\right] \\ &= 99.5 + 0.5 \cdot \left(0.3 \cdot (103 - 99.5)\right) \\ &= 100.025 \\ &> 100 \\ &= \rho_2^2(W) \end{aligned} \tag{1.23}$$

Hence we know that under all possible scenarios, at time $t = 2$ we would prefer W over Z. But if that is the case, how could we make a decision? If we make the optimal decision at time $t = 1$ and choose Z over W, then at the next step our choice would certainly appear suboptimal. However, if at time $t = 1$ we take into account our future preferences and choose W over Z, then we would be making a suboptimal decision from the point of view of the root node. Hence, any decision that we make would involve a contradiction. This paradox is known as time inconsistency and it is an issue of paramount importance in practical multistage risk-averse optimization. In order to avoid it, we need to use specially constructed risk functions known as time-consistent risk measures.

Chapter 2

Multistage Risk-Averse Optimization

2.1 Introduction to Multistage Risk-Averse Optimization

In a multistage risk-averse stochastic linear programming problem, on a probability space $(\Omega, \mathcal{F}, P)$, with a sigma algebra $\mathcal{F}$ and probability measure P, we consider a filtration $\{\emptyset, \Omega\} = \mathcal{F}_1 \subset \mathcal{F}_2 \subset \cdots \subset \mathcal{F}_T = \mathcal{F}$. A *policy* is a random vector $x = (x_1, \ldots, x_T)$, where each x_t has values in $\mathbb{R}^{n_t}$, $t = 1, \ldots, T$. If each x_t is $\mathcal{F}_t$-measurable, $t = 1, \ldots, T$, a policy x is called *implementable*. The set of all implementable policies is denoted by I.

A policy x is *feasible*, if it satisfies the following system of linear equations and inclusions:

$$
\begin{array}{lllllllll}
A_1x_1 & & & & & & & = & b_1, \\
B_2x_1 & + & A_2x_2 & & & & & = & b_2, \\
 & & B_3x_2 & + & A_3x_3 & & & = & b_3, \\
\multicolumn{7}{l}{\cdots\cdots\cdots\cdots\cdots\cdots\cdots\cdots\cdots\cdots\cdots\cdots\cdots\cdots\cdots} \\
 & & & & & B_Tx_{T-1} & + \; A_Tx_T & = & b_T, \\
x_1 \in X_1, & & x_2 \in X_2, & & x_3 \in X_3, & \ldots & x_T \in X_T. & &
\end{array}
\tag{2.1}
$$

The matrices A_t of dimensions $m_t \times n_t$, the matrices B_t of dimensions $m_t \times n_{t-1}$, and the vectors b_t of dimensions m_t are $\mathcal{F}_t$-measurable data, for $t = 1, \ldots, T$. Each set X_t is an $\mathcal{F}_t$-measurable convex and closed polyhedron (for measurability of multifunctions, see [6]). The set of all feasible policies is denoted by F.

In the example in Section 1.3 we only considered final stage costs. However, in general we can consider costs at every stage. Suppose c_t, $t = 1, \ldots, T$, is a sequence of random cost vectors such that each c_t is $\mathcal{F}_t$-measurable. An implementable policy

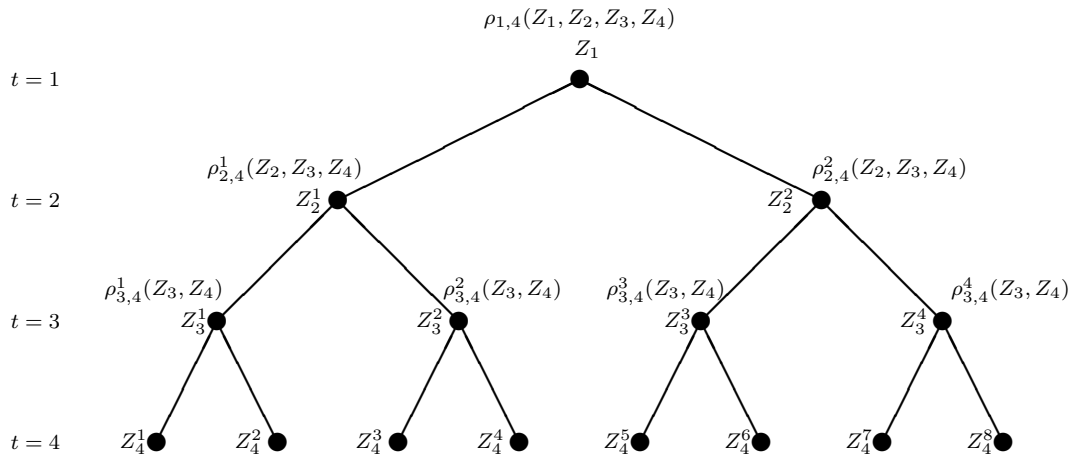

Figure 2.1: Dynamic measure of risk for a multistage scenario tree.

$x \in I$ results in a random cost sequence:

$$Z_t = \langle c_t, x_t \rangle, \quad t = 1, \ldots, T, \tag{2.2}$$

with each $z_t \in \mathcal{Z}_t$, where $\mathcal{Z}_t$ is the space of $\mathcal{F}_t$-measurable random variables. Our intention is to formulate and analyze a risk-averse multistage stochastic optimization problem:

$$\min_{x \in I \cap F} \varrho(Z_1, Z_2, \ldots, Z_T), \tag{2.3}$$

where $\varrho : \mathcal{Z}_1 \times \mathcal{Z}_2 \times \cdots \times \mathcal{Z}_T \to \mathbb{R}$ is a dynamic measure of risk.

2.2 Time Consistency

As time goes on, we have to consider tail subsequences $Z_t, \ldots, Z_T$ of the sequence of future costs, where $1 \leq t \leq T$. They are elements of the spaces $\mathcal{Z}_{t,T} = \mathcal{Z}_t \times \cdots \times \mathcal{Z}_T$. It is, therefore, necessary to consider the corresponding *conditional risk measures* $\varrho_{t,T} : \mathcal{Z}_{t,T} \to \mathcal{Z}_t$, where $t = 1, \ldots, T$. The value of the conditional risk measure $\rho_{t,T}(Z_t, \ldots, Z_T)$ can be interpreted as a fair one-time $\mathcal{F}_t$-measurable charge we would be willing to incur at time t, instead of the sequence of random future costs $Z_t, \ldots, Z_T$.

As smaller realizations of outcomes $Z_1, \ldots, Z_T$ are preferred (they are "costs" or "losses"), it is natural to assume the following *monotonicity condition*: for every $t =$

$1, \ldots, T$

$$\varrho_{t,T}(Z) \leq \varrho_{t,T}(W) \text{ for all } Z, W \in \mathcal{Z}_{t,T} \text{ such that } Z \leq W. \tag{2.4}$$

Here and elsewhere in the paper, inequalities between random vectors are understood component-wise and in the almost sure sense. A collection of conditional measures of risk, $\{\varrho_{t,T}\}_{t=1}^{T}$, is a *dynamic measure of risk*.

The key issue associated with dynamic preferences is the question of their consistency over time. It has been studied in various contexts in the past (see, e.g., [4, 10]); here, we adapt the perspective of [48].

Definition 6. *A dynamic risk measure* $\{\varrho_{t,T}\}_{t=1}^{T}$ *is called* time-consistent *if for all* $1 \leq \tau < \theta \leq T$ *and all sequences* $Z, W \in \mathcal{Z}_{\tau,T}$ *the conditions*

$$Z_k = W_k, \ k = \tau, \ldots, \theta - 1 \quad \textit{and} \quad \varrho_{\theta,T}(Z_\theta, \ldots, Z_T) \leq \varrho_{\theta,T}(W_\theta, \ldots, W_T) \tag{2.5}$$

imply that

$$\varrho_{\tau,T}(Z_\tau, \ldots, Z_T) \leq \varrho_{\tau,T}(W_\tau, \ldots, W_T). \tag{2.6}$$

For a dynamic risk measure $\{\rho_{t,T}\}_{t=1}^{T}$ we can define *one-step conditional risk measures* $\rho_t : \mathcal{Z}_{t+1} \to \mathcal{Z}_t$, $t = 1, \ldots, T-1$ as follows:

$$\rho_t(Z_{t+1}) = \varrho_{t,T}(0, Z_{t+1}, 0, \ldots, 0).$$

We can derive the following structure of a time-consistent dynamic risk measure.

Theorem 7 (Ruszczyński [48])**.** *Suppose a dynamic risk measure* $\{\varrho_{t,T}\}_{t=1}^{T}$ *satisfies for all* $Z \in \mathcal{Z}$ *and all* $t = 1, \ldots, T$ *the conditions:*

$$\varrho_{t,T}(Z_t, Z_{t+1}, \ldots, Z_T) = Z_t + \varrho_{t,T}(0, Z_{t+1}, \ldots, Z_T), \tag{2.7}$$

$$\varrho_{t,T}(0, \ldots, 0) = 0. \tag{2.8}$$

Then it is time-consistent if and only if for all $1 \leq t \leq T$ *and all* $Z \in \mathcal{Z}_{1,T}$ *the following identity is true:*

$$\begin{aligned} &\varrho_{t,T}(Z_t, \ldots, Z_T) \\ &\quad = Z_t + \rho_t\Big(Z_{t+1} + \rho_{t+1}\Big(Z_{t+2} + \cdots + \rho_{T-2}\big(Z_{T-1} + \rho_{T-1}(Z_T)\big)\cdots\Big)\Big). \end{aligned} \tag{2.9}$$

Condition (2.7) is a form of the *translation property*, discussed in various settings in [4, 29, 37]. Our version is weaker, because Z_t is $\mathcal{F}_t$-measurable.

It follows that a time-consistent dynamic risk measure is completely defined by one-step conditional risk measures ρ_t, $t = 1, \ldots, T-1$. For $t = 1$ formula (2.9) defines a risk measure of the *entire* sequence $Z \in \mathcal{Z}_{1,T}$ (with a deterministic Z_1).

We shall assume the property of *coherency* of conditional risk measures. Let $1 \leq t \leq T-1$. A *coherent conditional risk measure* is a function $\varrho_{t,T} : \mathcal{Z}_{t,T} \to \mathcal{Z}_t$ satisfying the following axioms:

(B1) *Convexity*: $\varrho_{t,T}(\alpha Z + (1-\alpha) V) \leq \alpha \varrho_{t,T}(Z) + (1-\alpha)\varrho_{t,T}(V)$, for all $Z, V \in \mathcal{Z}_{t,T}$ and all $\alpha \in [0,1]$;

(B2) *Monotonicity*: If $Z, V \in \mathcal{Z}_{t,T}$ and $Z \leq V$, then $\varrho_{t,T}(Z) \leq \varrho_{t,T}(V)$;

(B3) *Predictable Translation Equivariance*: If $Z \in \mathcal{Z}_{t,T}$, then

$$\varrho_{t,T}(Z_t, Z_{t+1}, \ldots, Z_T) = \varrho_{t,T}(0, Z_t + Z_{t+1}, \ldots, Z_T);$$

(B4) *Positive Homogeneity*: If $\gamma \geq 0$ and $Z \in \mathcal{Z}_{t,T}$, then $\rho_{t,T}(\gamma Z) = \gamma \rho_{t,T}(Z)$.

Condition (B3) can be interpreted as follows. At time t, we know the value of the $\mathcal{F}_t$-measurable cost Z_t, and therefore we can take it into account when evaluating the risk function $\varrho_{t,T}(Z_t, Z_{t+1}, \ldots, Z_T)$. Another way to obtain the same risk value would be to consider the cost at time t to be 0, while adding Z_t to the random cost of one of the future time periods. In the case of one-step conditional risk measures, we define coherence by conditions (B1), (B2), (B4), and the following condition

(B3') *Predictable Translation Equivariance*: If $Z_{t+1} \in \mathcal{Z}_{t+1}$ and $V_t \in \mathcal{Z}_t$, then

$$\rho_t(V_t + Z_{t+1}) = V_t + \rho_t(Z_{t+1}).$$

It combines (B3) with condition (2.7).

If the assumptions of Theorem 7 are satisfied, then all conditional risk measures are coherent if and only if all one-step conditional risk measures are coherent.

Example 8. *For example, the* conditional mean–upper semideviation *model defined by*

$$\rho_t(Z) = \mathbb{E}[Z|\mathcal{F}_t] + \kappa_t \, \mathbb{E}\left[\left(Z - \mathbb{E}[Z|\mathcal{F}_t]\right)_+ \middle| \mathcal{F}_t\right], \tag{2.10}$$

with an $\mathcal{F}_t$-measurable $\kappa_t \in [0,1]$, is a coherent one-step conditional risk measure [1, page 277].

Example 9. *Furthermore, the* conditional Average Value at Risk *given by*

$$AVaR_{\alpha_t}(Z) = \min_{\xi}\left\{\xi + \frac{1}{\alpha_t}\mathbb{E}\left[\left(Z-\xi\right)_+ \middle| \mathcal{F}_t\right]\right\} \tag{2.11}$$

with an $\mathcal{F}_t$-measurable $\alpha_t \in (0,1)$ is also a coherent one-step conditional risk measure [1, page 272].

Therefore, compositions of conditional mean–upper semideviation and conditional Average Value at Risk measures are coherent.

2.2.1 Solution to The Paradox of Time Inconsistency

In this section we revisit the example of Section 1.3.

Suppose that we still use the same value of $\kappa = 0.5$ at all nodes, i.e. $\kappa_1 = \kappa_2^1 = \kappa_2^2 = \kappa = 0.5$. Then, we would still have $\rho_2^1(Z) = 100.125$ and $\rho_2^2(Z) = 100.025$, while $\rho_2^1(W) = \rho_2^2(W) = 100$. Thus, at time $t = 2$, we would still prefer the fixed cost W over Z, since W carries less risk than Z. However, rather than evaluating the risk of the entire tree using the function $\rho_1(Z)$, now we follow the insight of Theorem 7 and use the nested composition of risk measures $\rho_1(\rho_2(Z))$ instead. This approach is illustrated in Figure 2.2.

Thus we have,

$$\begin{aligned} E_1[\rho_2(Z)] &= 0.3 \cdot 100.125 + 0.7 \cdot 100.025 \\ &= 100.055 \end{aligned} \tag{2.12}$$

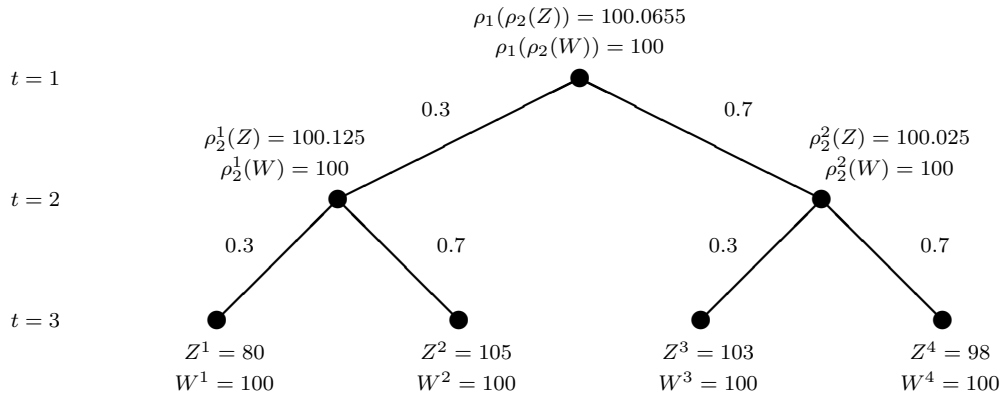

Figure 2.2: Time consistency when risk is measured by aggregated one-step conditional mean–upper semideviation measures with $\kappa_1 = \kappa_2^1 = \kappa_2^2 = \kappa = 0.5$. We can see that W is preferable to Z at both t_1 and t_2.

and

$$\begin{aligned}
\rho_1(\rho_2(Z)) &= \mathbb{E}_1[\rho_2(Z)] + \kappa_1 \mathbb{E}_1\left[\big(\rho_2(Z) - \mathbb{E}_1[\rho_2(Z)]\big)_+\right] \\
&= 100.055 + 0.5 \cdot \big(0.3 \cdot (100.125 - 100.055)\big) \\
&= 100.0655 \\
&> 100 \\
&= \rho_1(\rho_2(W))
\end{aligned} \tag{2.13}$$

Now, we can see that from the point of view of the root node at time $t = 1$, we would also prefer W over Z. Therefore, our decisions are consistent accross different time periods. Furthermore, as long as we use the nested composition of Theorem 7, our decisions would be guaranteed to be time-consistent, regardless of what the decisions actually are! This is nice but there is a caveat. The decisions depend on the risk measures that we use in the nested composition, which in this case are determined by the values of the risk aversion coefficients κ. For example, if we adjust our preferences

and choose $\kappa_1 = 0.6$, $\kappa_2^1 = 0.2$, and $\kappa_2^2 = 0$, then we would have

$$\begin{aligned}\rho_2^1(Z) &= E_2^1[Z] + \kappa_2^1 \cdot \mathbb{E}_2^1\left[\big(Z - \mathbb{E}_1[Z]\big)_+\right] \\ &= 97.5 + 0.2 \cdot \big(0.7 \cdot (105 - 97.5)\big) \\ &= 98.55 \\ &< \rho_2^1(W)\end{aligned} \tag{2.14}$$

and

$$\begin{aligned}\rho_2^2(Z) &= E_2^2[Z] \\ &= 99.5 \\ &< \rho_2^2(W)\end{aligned} \tag{2.15}$$

Further,

$$\begin{aligned}E_1[\rho_2(Z)] &= 0.3 \cdot 98.55 + 0.7 \cdot 99.5 \\ &= 99.215\end{aligned} \tag{2.16}$$

and

$$\begin{aligned}\rho_1(\rho_2(Z)) &= \mathbb{E}_1[\rho_2(Z)] + \kappa_1 \mathbb{E}_1\left[\big(\rho_2(Z) - \mathbb{E}_1[\rho_2(Z)]\big)_+\right] \\ &= 99.215 + 0.6 \cdot \big(0.7 \cdot (99.5 - 99.215)\big) \\ &= 99.3347 \\ &< \rho_1(\rho_2(W))\end{aligned} \tag{2.17}$$

This example is illustrated in Figure 2.3. We can see that our preferences are again time-consistent but now we make the opposite choice as we favor Z over W. Thus, before we can use time-consistent compositions to make decisions, it is imperative that we choose the "best" risk measure for every node in the tree. We address this question in Chapter 3 after introducing the essential notation and terminology in the remainder of the current chapter.

2.3 Scenario Trees and Recursive Risk Evaluation for Time-Consistent Models

Throughout this dissertation we assume that all sigma-algebras are finite and thus all vector spaces $\mathcal{Z}_t$ are finite-dimensional. In this setting, the realizations of data

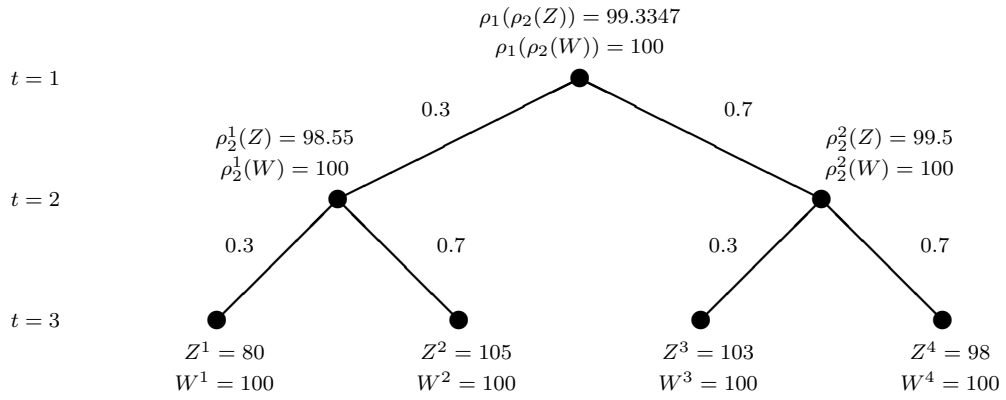

Figure 2.3: Time consistency when risk is measured by aggregated one-step conditional mean–upper semideviation measures with $\kappa_1 = 0.6$, $\kappa_2^1 = 0.2$, $\kappa_2^2 = 0$. We can see that Z is superior to W at both t_1 and t_2.

form a *scenario tree*. Our notation is consistent with the paper of Collado, Papp and Ruszczynski [13]. The nodes of the tree are organized in levels associated with stages $1, \ldots, T$; they correspond to the nested partitions of Ω given by the filtration $\mathcal{F}_1 \subset \mathcal{F}_2 \subset \cdots \subset \mathcal{F}_T$.

Level $t = 1$ consists of only one node, called the *root node*. We index the nodes by the symbol ν and assign $\nu = 1$ to the root node. The nodes located at further levels $t = 2, \ldots, T$ correspond to elementary events in $\mathcal{F}_t$. Every node ν at level $t = 2, \ldots, T$ is connected to its unique *ancestor node* $a(\nu)$ at level $t - 1$. The ancestor node corresponds to the elementary event in $\mathcal{F}_{t-1}$ containing the event associated with ν. Every node ν at levels $t = 1, \ldots, T - 1$ is connected to a collection $C(\nu)$ of *children nodes* at level $t + 1$. The children nodes correspond to the elementary events in $\mathcal{F}_{t+1}$ included in the event associated with ν. The set of all nodes at stage t is denoted by Ω_t, $t = 1, \ldots, T$. A *scenario* is a path s from the root to a node at the last stage T. We use the symbol $\mathcal{S}(\nu)$ to denote the set of scenarios passing through node ν. In this setting, the measure P can be specified by conditional probabilities $p_{\nu\eta} = P[\eta|\nu]$, where $\nu \in \Omega_t$, $\eta \in C(\nu)$, and $t = 1, \ldots, T - 1$. Every node ν at level t has a *history*: the path $(\nu_1, \ldots, \nu_{t-1}, \nu)$ from the root to ν. The probability of ν is the product of the corresponding conditional probabilities in its history: $p_\nu = p_{\nu_1\nu_2} p_{\nu_2\nu_3} \cdots p_{\nu_{t-1}\nu}$. When

$t = T$, this formula describes the probability of a scenario $s \in \Omega_T$.

For every node $\nu \in \Omega_t$, an $\mathcal{F}_t$-measurable random variable Z has identical values on all scenarios $s \in \mathcal{S}(\nu)$. It can, therefore, be equivalently represented as a function of a node in Ω_t; we write this function as Z^{Ω_t}.

The value of a coherent one-step conditional measure of risk $\rho_t(\cdot)$ is $\mathcal{F}_t$-measurable, and is also a function of a node ν at level t. It follows from [49, Thm. 3.2] that the value of $\rho_t(Z_{t+1})$ at node ν depends only on the values of $Z_{t+1}^{\Omega_{t+1}}$ at nodes $\eta \in C(\nu)$, which is a feature known as the *local property*. We denote the vector of these values by $Z^{C(\nu)}$, and we write the conditional risk measure equivalently as $\rho^\nu\big(Z_{t+1}^{C(\nu)}\big)$. We would like to emphasize that time consistency only implies the telescoping property (2.9), while the local property follows from positive homogeneity. If our risk measures were not positively homogeneous, then we would need to additionally assume the local property.

It follows from the above discussion that the random variables

$$V_t = \rho_t\Big(Z_{t+1} + \rho_{t+1}\big(Z_{t+2} + \cdots + \rho_{T-1}(Z_T)\ldots\big)\Big), \tag{2.18}$$

are $\mathcal{F}_t$-measurable, and thus we only need to consider their values V_t^ν at nodes $\nu \in \Omega_t$, $t = 1, \ldots, T$.

Consequently, the value of a time-consistent measure of risk (2.9) can be written recursively as follows:

$$\begin{aligned} &V^\nu = Z^\nu, \quad \nu \in \Omega_T, \\ &V^\nu = Z^\nu + \rho^\nu\big(V^{C(\nu)}\big), \quad \nu \in \Omega_t, \quad t = T-1, \ldots, 1. \end{aligned} \tag{2.19}$$

The recursive character of time-consistent measures of risk can be also used to derive optimality conditions in the form of *dynamic programming equations*. Let us consider a node $\nu \in \Omega_t$ and assume that the value of $x^{a(\nu)}$ is fixed. Owing to the local property, we can consider the subproblem of minimizing V^ν with respect to $x^\nu, x^{C(\nu)}, \ldots, x^{C^{T-t}(\nu)}$, subject to the corresponding subset of conditions (2.1) involving these variables. We call the optimal value of this subproblem the *value function*, and denote it by the symbol $\mathcal{Q}^\nu\big(x^{a(\nu)}\big)$. Except for the case of $t = 1$, it is a function of $x^{a(\nu)}$. Similarly to (2.19), we

use the symbol $\mathcal{Q}^{C(\nu)}\big(x^\nu\big)$ to represent a random variable with values $\mathcal{Q}^\eta\big(x^\nu\big)$, $\eta \in C(\nu)$, attained with probabilities $p_{\nu\eta}$.

Proceeding exactly as in [1, sec. 6.7.3], we obtain the following result.

Theorem 10. *The value functions $\mathcal{Q}_t^\nu\big(\,\cdot\,\big)$ satisfy the following equations:*

$$\begin{aligned}
\mathcal{Q}^\nu\big(x^{a(\nu)}\big) &= \min_{x^\nu}\Big\{\langle c^\nu, x^\nu\rangle : B^\nu x^{a(\nu)} + A^\nu x^\nu = b^\nu,\ x^\nu \in X^\nu\Big\}, \quad \nu \in \Omega_T,\\
\mathcal{Q}^\nu\big(x^{a(\nu)}\big) &= \min_{x^\nu}\Big\{\langle c^\nu, x^\nu\rangle + \rho^\nu\Big(\mathcal{Q}^{C(\nu)}\big(x^\nu\big)\Big) :\\
&\qquad\qquad B^\nu x^{a(\nu)} + A^\nu x^\nu = b^\nu,\ x^\nu \in X^\nu\Big\}, \quad \nu \in \Omega_t, \quad t = T-1,\dots,1,
\end{aligned} \tag{2.20}$$

with the convention that $\mathcal{Q}^1$ has no arguments. The value of $\mathcal{Q}^1$ is the optimal value of the problem, and the optimal decisions in problems (2.20) *constitute the optimal policy.*

The optimal value functions $\mathcal{Q}^\nu(\cdot)$ are convex, because their arguments appear as parameters in the constraints of convex optimization problems.

Theorem 10 is the theoretical foundation of an efficient computational method for solving two-stage time-consistent risk-averse problems, proposed in [32].

2.4 Transition Multikernels and Their Composition

We denote by $\mathcal{P}(C)$ the set of probability distributions on a collection of nodes $C \subset \Omega$. By [49, Remark 4.3], for every $t = 1,\dots,T-1$ and every node $\nu \in \Omega_t$ a convex closed set $\mathcal{A}_t(\nu) \subset \mathcal{P}(C(\nu))$ exists such that

$$\rho^\nu\big(Z^{C(\nu)}\big) = \max_{\mu \in \mathcal{A}_t(\nu)} \big\langle \mu, Z^{C(\nu)}\big\rangle. \tag{2.21}$$

Moreover, $\mathcal{A}_t(\nu) = \partial\rho^\nu\big(0\big)$.

We call the mappings $\mathcal{A}_t : \Omega_t \rightrightarrows \mathcal{P}(\Omega_{t+1})$ *multikernels*. Their values are convex and closed (as subdifferentials). They also satisfy the *local property*:

$$\mathcal{A}_t(\nu) \subset \mathcal{P}(C(\nu)), \quad \forall\, \nu \in \Omega_t. \tag{2.22}$$

If a kernel μ_t satisfies the relation $\mu_t(\nu) \in \mathcal{A}_t(\nu)$ for all $\nu \in \Omega_t$, we call it a *selector* of $\mathcal{A}_t$ and write $\mu_t \lessdot \mathcal{A}_t$. The value of $\mu(\nu)$ at a node $\eta \in C(\nu)$ is written as $\mu(\nu,\eta)$.

Much of our analysis uses compositions of multikernels. For a probability measure $q_t \in \mathcal{P}(\Omega_t)$ and a kernel $\mu_t \lessdot \mathcal{A}_t$, their composition is a probability measure on Ω_{t+1} satisfying the following equations:

$$(q_t \circ \mu_t)(\eta) = q_t(a(\eta))\mu_t(a(\eta), \eta),\ \eta \in \Omega_{t+1}.$$

The composition of a set of probability distributions $\mathcal{Q}_t \subset \mathcal{P}(\Omega_t)$ with a multikernel $\mathcal{A}_t : \Omega_t \rightrightarrows \mathcal{P}(\Omega_{t+1})$ satisfying (2.22), is the following set of probability measures on Ω_{t+1}:

$$Q_t \circ \mathcal{A}_t = \big\{q_t \circ \mu_t : q_t \in Q_t,\ \mu_t \lessdot \mathcal{A}_t\big\}.$$

If Q_t and $\mathcal{A}_t$ are convex and compact, then their composition $\mathcal{Q}_t \circ A_t$ is convex and compact as well.

We can now recall a useful dual representation of a dynamic measure of risk [13].

Theorem 11 (Collado, Papp and Ruszczynski [13])**.** *Suppose a dynamic risk measure $\varrho(\cdot)$ is given by* (2.9) *with conditional risk measures $\rho_t(\cdot)$ satisfying conditions (B1), (B2), (B3'), and (B4). Then for every adapted sequence $Z_1, \ldots, Z_T$ we have the relation*

$$\varrho(Z_1, \ldots, Z_T) = \max_{q \in \mathcal{A}_{1,T}} \big\langle q, Z_1 + Z_2 + \cdots + Z_T \big\rangle, \tag{2.23}$$

where

$$\mathcal{A}_{1,T} = \mathcal{A}_1 \circ \mathcal{A}_2 \cdots \circ \mathcal{A}_{T-1} \tag{2.24}$$

is a convex and closed set of probability measures on Ω.

Owing to this representation, we can rewrite the problem (2.3) as follows:

$$\min_{x \in I \cap F} \max_{q \in \mathcal{A}_{1,T}} \big\langle\, q, \langle c_1, x_1\rangle + \langle c_2, x_2\rangle + \cdots + \langle c_T, x_T\rangle \,\big\rangle. \tag{2.25}$$

This result is the theoretical foundation of a scenario decomposition method for solving time-consistent risk-averse optimization problems, proposed in [13].

2.4.1 Illustrative Example

Let us consider again the second example of Section 2.2.1 and adopt the notation of Section 2.4. We label the nodes as shown in Figure 2.4.

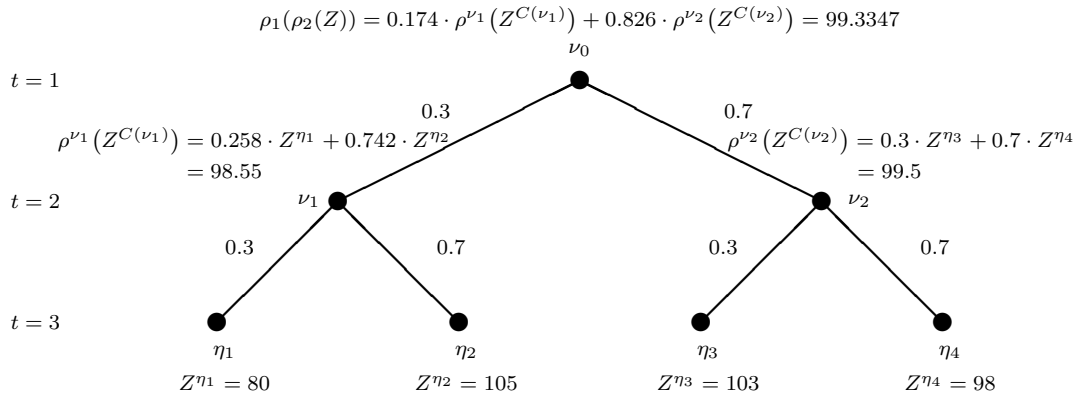

Figure 2.4: Dual representation of risk measures for $\kappa^{\nu_0} = 0.6$, $\kappa^{\nu^1} = 0.2$, $\kappa^{\nu^2} = 0$.

Hence, $\kappa^{\nu_0} = 0.6$, $\kappa^{\nu_1} = 0.2$, and $\kappa^{\nu_2} = 0$. The multikernel $\mathcal{A}_2(\cdot)$ has only two possible arguments, ν_1 and ν_2, since those are the only nodes for time $t = 2$. Thus,

$$\begin{aligned}\mathcal{A}_2(\nu_1) &= \left\{ \mu(\nu_1) : \begin{array}{l} \mu(\nu_1, \eta_1) = 0.3(1 + h_1 - 0.3h_1 - 0.7h_2) \\ \mu(\nu_1, \eta_2) = 0.7(1 + h_2 - 0.3h_1 - 0.7h_2) \\ 0 \le h_1 \le \kappa^{\nu_1} \\ 0 \le h_2 \le \kappa^{\nu_1} \end{array} \right\} \\ &= \left\{ \mu(\nu_1) : \begin{array}{l} \mu(\nu_1, \eta_1) = 0.3 + 0.21h_1 - 0.21h_2 \\ \mu(\nu_1, \eta_2) = 0.7 - 0.21h_1 + 0.21h_2 \\ 0 \le h_1 \le 0.2 \\ 0 \le h_2 \le 0.2 \end{array} \right\} \end{aligned} \tag{2.26}$$

Then,

$$\begin{aligned}\rho^{\nu_1}\left(Z^{C(\nu_1)}\right) &= \max_{\mu \in \mathcal{A}_2(\nu_1)} \left\langle \mu, Z^{C(\nu_1)} \right\rangle \\ &= 0.258 \cdot Z^{\eta_1} + 0.742 \cdot Z^{\eta_2} \\ &= 98.55 \end{aligned} \tag{2.27}$$

Further,

$$\begin{aligned}\mathcal{A}_2(\nu_2) &= \left\{ \mu(\nu_2): \begin{array}{l} \mu(\nu_2,\eta_3) = 0.3(1+h_1-0.3h_1-0.7h_2) \\ \mu(\nu_2,\eta_4) = 0.7(1+h_2-0.3h_1-0.7h_2) \\ 0 \le h_1 \le \kappa^{\nu_2} \\ 0 \le h_2 \le \kappa^{\nu_2} \end{array} \right\} \\ &= \left\{ \mu(\nu_2): \begin{array}{l} \mu(\nu_2,\eta_3) = 0.3 \\ \mu(\nu_2,\eta_4) = 0.7 \end{array} \right\} \end{aligned} \tag{2.28}$$

and

$$\begin{aligned}\rho^{\nu_2}\big(Z^{C(\nu_2)}\big) &= \max_{\mu \in \mathcal{A}_2(\nu_2)} \big\langle \mu, Z^{C(\nu_2)} \big\rangle \\ &= 0.3 \cdot Z^{\eta_3} + 0.7 \cdot Z^{\eta_4} \\ &= 99.5 \end{aligned} \tag{2.29}$$

Now we can find a selector $\mu_2 \lessdot \mathcal{A}_2$. For example, if μ_2 is such that

$$\begin{aligned} &\mu_2(\nu_1,\eta_1) = 0.258 \\ &\mu_2(\nu_1,\eta_2) = 0.742 \\ &\mu_2(\nu_2,\eta_3) = 0.3 \\ &\mu_2(\nu_2,\eta_3) = 0.7 \end{aligned} \tag{2.30}$$

then μ_2 would be a selector of $\mathcal{A}_2$ since $\mu_2(\nu_1) \in \mathcal{A}_2(\nu_1)$ and $\mu_2(\nu_2) \in \mathcal{A}_2(\nu_2)$.

Moreover, the multikernel $\mathcal{A}_1(\cdot)$ consists of a single probability distribution for the node ν_0.

$$\begin{aligned}\mathcal{A}_1(\nu_0) &= \left\{ \mu(\nu_0): \begin{array}{l} \mu(\nu_0,\nu_1) = 0.3(1+h_1-0.3h_1-0.7h_2) \\ \mu(\nu_0,\nu_2) = 0.7(1+h_2-0.3h_1-0.7h_2) \\ 0 \le h_1 \le \kappa^{\nu_0} \\ 0 \le h_2 \le \kappa^{\nu_0} \end{array} \right\} \\ &= \left\{ \mu(\nu_0): \begin{array}{l} \mu(\nu_0,\nu_1) = 0.3 + 0.21h_1 - 0.21h_2 \\ \mu(\nu_0,\nu_2) = 0.7 - 0.21h_1 + 0.21h_2 \\ 0 \le h_1 \le 0.6 \\ 0 \le h_2 \le 0.6 \end{array} \right\} \end{aligned} \tag{2.31}$$

Therefore,

$$\begin{aligned}
\rho_1(\rho_2(Z)) &= \max_{\mu\in\mathcal{A}_1}\left\{\mu(\nu_0,\nu_1)\cdot\rho^{\nu_1}\left(Z^{C(\nu_1)}\right)+\mu(\nu_0,\nu_2)\cdot\rho^{\nu_2}\left(Z^{C(\nu_2)}\right)\right\}\\
\rho_1(\rho_2(Z)) &= \max_{\mu\in\mathcal{A}_1}\left\{\mu(\nu_0,\nu_1)\cdot 98.55+\mu(\nu_0,\nu_2)\cdot 99.5\right\}\\
&= 0.174\cdot 98.55+0.826\cdot 99.5\\
&= 99.3347
\end{aligned} \tag{2.32}$$

Let us consider the probability distribution $q_2\in\mathcal{A}_1(\nu_0)$ on the set of nodes at time $t=2$ such that $q_2(\nu_1)=0.174$ and $q_2(\nu_2)=0.826$. Then the composition

$$q(\eta)=(q_2\circ\mu_2)(\eta)=q_2(a(\eta))\mu_2(a(\eta),\eta),\ \eta\in\Omega_3.$$

is a probability distribution on the set of nodes $\eta\in\Omega_3$. Furthermore,

$$q=\arg\max_{q\in\mathcal{A}_1\circ\mathcal{A}_2}\left\langle q,Z\right\rangle, \tag{2.33}$$

where the composition of the multikernel $\mathcal{A}_1$ (which is a single set of probability distributions $\mathcal{A}_1(\nu_0)\subset\mathcal{P}(\Omega_2)$ on the set of nodes at time $t=2$) with the multikernel $\mathcal{A}_2$ produces the set of probability measures on Ω_3 given by:

$$\mathcal{A}_1\circ\mathcal{A}_2=\left\{q_2\circ\mu_2 : q_2\in\mathcal{A}_1(\nu_0),\ \mu_2\lessdot\mathcal{A}_2\right\}.$$

Indeed, we can verify that

$$\begin{aligned}
\max_{q\in\mathcal{A}_1\circ\mathcal{A}_2}\left\langle q,Z\right\rangle &= 0.174\cdot(0.258\cdot Z^{\eta_1}+0.742\cdot Z^{\eta_2})+0.826\cdot(0.3\cdot Z^{\eta_3}+0.7\cdot Z^{\eta_4})\\
&= 0.044892\cdot 80+0.129108\cdot 105+0.2478\cdot 103+0.5782\cdot 98\\
&= 99.3347\\
&= \rho_1(\rho_2(Z))
\end{aligned} \tag{2.34}$$

2.5 Nested Decomposition of Time-Consistent Problems

We now extend the decomposition method proposed in [32] to multistage problems of form (2.3). Similar approaches are associated with the risk-averse extensions of the stochastic dual decomposition method of [36], proposed in [27, 41, 52].

To avoid technical difficulties, and in view of the application in the next section, we assume that all one-step conditional risk measures $\rho_t(\cdot)$ are *polyhedral*, that is, the sets $\mathcal{A}_t(\nu)$ are polyhedra, for all $\nu \in \Omega_t$ and all $t = 1, \ldots, T-1$.

In the nested decomposition method a subproblem is associated with every node of the scenario tree. The subproblems communicate along the arcs of the tree. A typical subproblem at a node $\nu \in \Omega_t$ will get the value of $x_{t-1}^{a(\nu)}$ from the ancestor node $a(\nu)$ and pass its current solution x_t^ν to its children nodes $\eta \in C(\nu)$. The subproblems will also pass the values of Lagrange multipliers associated with the constraints to their ancestor nodes, and receive the corresponding multipliers from their children nodes.

Consider a node ν at level $1 < t < T$ and suppose a new value $\bar{x}^{a(\nu)}$ has been received from the ancestor node. The information passed between the node subproblems depends on the result of a feasibility test, which amounts to solving the following problem:

$$\begin{array}{ll} \min\limits_{x^\nu, s} & \|s\|_1 \\ \text{s.t.} & B^\nu \bar{x}^{a(\nu)} + A^\nu x^\nu + s = b^\nu, \\ & x^\nu \in X^\nu. \end{array} \tag{2.35}$$

If the optimal value β of this problem is positive, the point $\bar{x}^{a(\nu)}$ is infeasible. Then, denoting by π the vector of Lagrange multipliers associated with the equality constraints, we can construct the following *feasibility cut*:

$$\beta + \left\langle g^\nu, x^{a(\nu)} - \bar{x}^{a(\nu)} \right\rangle \leq 0. \tag{2.36}$$

with

$$g^\nu = -\left(B^\nu\right)^{\mathsf{T}} \pi. \tag{2.37}$$

The feasibility cut (2.36) is passed to the ancestor node $a(\nu)$. No new information is passed to the children nodes.

If $\beta = 0$, we can solve the following *master problem*:

$$\begin{aligned}
\min_{x^\nu, U, W} \quad & U \\
\text{s.t} \quad & U \geq \langle c^\nu, x^\nu \rangle + \langle \mu_\ell^\nu, W \rangle, && \ell \in \bigcap_{\eta \in C(\nu)} L_{\text{obj}}^\eta, \\
& W^\eta \geq \bar{U}_\ell^\eta + \langle g_\ell^\eta, x^\nu - \bar{x}_\ell^\nu \rangle, && \ell \in L_{\text{obj}}^\eta, \quad \eta \in C(\nu), \\
& \beta_\ell^\eta + \langle g_\ell^\eta, x^\nu - \bar{x}_\ell^\nu \rangle \leq 0, && \ell \in L_{\text{feas}}^\eta, \quad \eta \in C(\nu), \\
& B^\nu \bar{x}^{a(\nu)} + A^\nu x^\nu = b^\nu, \\
& x^\nu \in X^\nu, \quad U \geq W_{\min}, \quad W \geq W_{\min}.
\end{aligned} \tag{2.38}$$

In this problem, we use L_{obj}^η to denote the set of previous iterations at which the subproblem $\eta \in C(\nu)$ returned an objective cut with value $\bar{U}_\ell^\eta$ and subgradient g_ℓ^η at $\bar{x}_\ell^\nu$), and L_{feas}^η to denote the set of previous iterations at which the subproblem $\eta \in C(\nu)$ returned a feasibility cut with value β_ℓ^η and subgradient g_ℓ^η. The iterations are numbered locally, at node ν. The constant $W_{\min}$ is the uniform lower bound on the value functions $\mathcal{Q}^\nu(\cdot)$ in (2.20).

Denote by $\bar{U}^\nu$ the optimal value of problem (2.38), by $\bar{x}^\nu$ the optimal solution, and by π the vector of Lagrange multipliers associated with the equality constraints. The solution $\bar{x}^\nu$, if different from previously reported, is passed to the children nodes $\eta \in C(\nu)$. If the value $\bar{U}^\nu$ is strictly larger than the value previously reported, then it is used together with the multipliers π to construct an objective cut

$$V^\nu \geq \bar{U}^\nu + \left\langle g^\nu, x^{a(\nu)} - \bar{x}^{a(\nu)} \right\rangle.$$

The subgradient g^ν is defined as in (2.37). The objective cut is passed to the ancestor problem $a(\nu)$.

If new objective or feasibility cuts are received from the children nodes $\eta \in C(\nu)$, then the sets of indices L_{obj}^η and L_{feas}^η are updated. Moreover, at any iteration ℓ at which all subproblems $\eta \in C(\nu)$ return feasibility cuts, we also calculate the probability measure

$$\mu_\ell^\nu = \arg\max_{\mu \in \mathcal{A}_t(\nu)} \left\langle \mu, W \right\rangle. \tag{2.39}$$

After all these updates, the master problem (2.38) is resolved and the resulting information (if essentially new) is transmitted to the ancestor and children nodes.

If $\nu = 1$ (the root node of the tree), there is no ancestor node, and thus problem (2.35) is not needed. Also, the constraint involving $\bar{x}^{a(\nu)}$ in (2.38) has to be omitted. For $\nu \in \Omega_T$ problem (2.38) simplifies as follows:

$$\min_{x^\nu} \left\{ \langle c^\nu, x^\nu \rangle : B^\nu \bar{x}^{a(\nu)} + A^\nu x^\nu = b^\nu,\ x^\nu \in X^\nu \right\}. \tag{2.40}$$

The protocol by which the nodes are processed is not essential for convergence of the method, although it may affect its speed. We make the following assumptions:

- The original problem (2.20) has an optimal solution;
- The procedure starts from the root node;
- For every linear problem (2.35), (2.38), and (2.39) the optimal basic solution is found;
- If the previous solution of a problem remains optimal, it is not changed;
- Every node subproblem is resolved after it receives new information from its ancestor or its children;
- The method stops when no changes in the optimal solutions of all subproblems occur.

Under these conditions, the method finds an optimal solution of (2.20) after finitely many updates in every subproblem node.

The proof of the claim is very similar to proofs of convergence of the nested decomposition of expected-value multistage stochastic linear programming problems (see [9, 46] and the references therein).

Let us observe at first that the subproblems (2.40) at level T can generate only finitely many different cuts, because their dual problems have only finitely many possible basic solutions. Therefore, there can be only finitely many systems of cuts in subproblems at level $T-1$. As the sets $\mathcal{A}_t(\nu)$ are convex bounded polyhedra, subproblems at level $T-1$ may have only finitely many different systems of constraints. This, in turn, implies that finitely many different cuts can be generated. Arguing in this way, we conclude that every node subproblem may have only finitely many different sets of constraints. As constraints are never removed, after finitely many updates, all node subproblems will have fixed sets of constraints.

Consider the subproblem at the root node after all its constraints have stabilized. As it has no ancestor, and its constraints are fixed, its solution will not change. This, in turn, implies that the solutions of subproblems at level 2 will not change. Arguing in this way, we conclude that the systems of constraints and solutions of *all* subproblems will stabilize.

It remains to prove optimality of the solution at which the subproblems stabilize. To this end, observe that all value functions $\mathcal{Q}^\nu(\cdot)$ in (2.20) are convex, and the cuts in (2.38) provide their relaxations. Therefore, the optimal values $\bar{U}^\nu$ of the subproblems (2.38) satisfy the inequalities:

$$\bar{U}^1 \le \mathcal{Q}^1, \quad \bar{U}^\nu \le \mathcal{Q}^\nu\big(x^{a(\nu)}\big), \quad \nu \in \Omega_t, \quad t = 2, \dots, T.$$

By (2.40), $\bar{U}^\nu = \mathcal{Q}^\nu\big(x^{a(\nu)}\big)$, for $\nu \in \Omega_T$. Consider a node ν at level $T-1$. Then, among the objective cuts in (2.38), we have the inequalities $W^\eta \ge \bar{U}^\eta$, $\eta \in C(\nu)$, because the solution does not change. Then it follows from (2.39) that $\bar{U}^\nu = \mathcal{Q}^\nu\big(x^{a(\nu)}\big)$. In a similar way, feasibility of the optimal solution can be established. Proceeding in this way, we conclude that all optimal values of the subproblems are equal to the optimal value functions at this solution. As the optimal solutions minimize a convex relaxation of the original problem, they are optimal for the original problem.

Chapter 3

Time-Consistent Approximations

3.1 Introduction

Let us consider now the problem (2.3) in which the dynamic measure of risk has the following form

$$\varrho(Z_1, Z_2, \ldots, Z_T) = \rho_{1,T}(Z_1 + Z_2 + \cdots + Z_T), \tag{3.1}$$

with a coherent measure of risk $\rho_{1,T} : \mathcal{Z}_T \to \mathbb{R}$. We are not assuming time consistency, and thus we cannot take advantage of the representations developed in sections 2.3 and 2.4. However, the dual representation of the measure $\rho_{1,T}(\cdot)$ is still possible:

$$\rho_{1,T}(Z_1 + Z_2 + \cdots + Z_T) = \max_{q \in \mathcal{D}_{1,T}} \langle\, q, Z_1 + Z_2 + \cdots + Z_T \rangle. \tag{3.2}$$

This allows us to equivalently express (2.3) as a min-max problem:

$$\min_{x \in I \cap F} \max_{q \in \mathcal{D}_{1,T}} \big\langle\, q, \langle c_1, x_1\rangle + \langle c_2, x_2\rangle + \cdots + \langle c_T, x_T\rangle \,\big\rangle. \tag{3.3}$$

The only difference from (2.25) is that the set $\mathcal{D}_{1,T}$ cannot be, in general, expressed as a composition of multikernels, as in (2.24). We assume that the "original" probability distribution p on Ω_T is an element of $\mathcal{D}_{1,T}$. This condition is satisfied for all practically relevant coherent measures of risk. It is equivalent to the requirement that

$$\rho_{1,T}(Z_1 + Z_2 + \cdots + Z_T) \geq \mathbb{E}\big[Z_1 + Z_2 + \cdots + Z_T\big]$$

for all $Z_1, Z_2, \ldots, Z_T$. Now, we are ready to dive into the details of our algorithm for the generation of time-consistent approximations.

3.2 A Time-Consistent Cutting Plane Method

The main idea of our approach extends the classical cutting-plane method to our setting, by using the subgradient information about the measure $\rho_{1,T}(\cdot)$ in a new way which

exploits time-consistency. In a standard cutting plane method, the convex polyhedral approximation of problem (3.3) would have the form:

$$\min_{x\in I\cap F}\max_{q\in\mathcal{D}_{1,T}^{(k)}}\langle\, q, Z_1+Z_2+\cdots+Z_T\rangle, \tag{3.4}$$

where

$$\mathcal{D}_{1,T}^{(k)}=\operatorname{conv}\big\{\mu^{(j)},\ j=0,1\ldots,k\big\}, \tag{3.5}$$

and $\mu^{(j)}$ are the elements of $\mathcal{D}_{1,T}$ collected at iterations $j=0,1,\ldots,k$. The initial $\mu^{(0)}=p$, and at later iterations we set

$$\mu^{(k)}\in\partial\rho_{1,T}(Z_1^k+Z_2^k+\cdots+Z_T^k), \tag{3.6}$$

where $Z_t^k=\langle c_t,x_t^k\rangle$, $t=1,\ldots,T$, are costs at the optimal solution of problem (3.4). Observe that the approximate problems (3.4) are not, in general, time-consistent, even if the original problem was.

Our idea is to approximate the set $\mathcal{D}_{1,T}$ in (3.3) by a composition of multikernels

$$\mathcal{D}_{1,T}\simeq\mathcal{A}_1^{(k)}\circ\mathcal{A}_2^{(k)}\circ\cdots\circ\mathcal{A}_{T-1}^{(k)} \tag{3.7}$$

where k is the iteration number. As a result, the measure of risk $\varrho(Z_1,Z_2,\ldots,Z_T)$ is approximated by a time-consistent measure

$$\tilde{\varrho}^{(k)}(Z_1,Z_2,\ldots,Z_T)=\max_{q\in\mathcal{A}_1^{(k)}\circ\cdots\circ\mathcal{A}_{T-1}^{(k)}}\langle\, q, Z_1+Z_2+\cdots+Z_T\rangle. \tag{3.8}$$

The multikernels $\mathcal{A}_1^{(k)}$, $\mathcal{A}_2^{(k)}$, …,$\mathcal{A}_{T-1}^{(k)}$ are constructed in an iterative fashion. At iteration k of the method, the subgradient (3.6), instead of being used directly to construct the convex hull (3.5), is *projected* on stages $t=T-1,\ldots,1$ to obtain the node measures $\mu_t^{(k)}(\nu)$, $\nu\in\Omega_t$. The projection procedure is described in line 17 of Algorithm 1. It calculates for each node ν at level t its probability $w_t(\nu)$ implied by $\mu^{(k)}$, and the vector of conditional probabilities $\mu_t^{(k)}(\nu)$ for its children in $C(\nu)$. Then the multikernels $\mathcal{A}_t^{(k)}$ are represented as a collections of convex polyhedral sets:

$$\mathcal{A}_t^{(k)}(\nu)=\operatorname{conv}\big\{\mu_t^{(j)}(\nu),\ j=0,1\ldots,k\big\},\quad \nu\in\Omega_t,\quad t=1,\ldots,T-1. \tag{3.9}$$

In the running of the algorithm, the objects that are added to the convex hulls $\mathcal{A}_t^{(k)}(\nu)$ are only conditional distributions on the set of children of node ν. The resulting approximation of problem (2.3),

$$\min_{x \in I \cap F} \tilde{\varrho}^{(k)}\big(\langle c_1, x_1\rangle, \langle c_2, x_2\rangle, \ldots, \langle c_T, x_T\rangle\big), \tag{3.10}$$

is time-consistent and can be solved by the decomposition method of section 2.4.

The method is presented in detail in Algorithm 1. We call it the *time-consistent cutting plane method* to stress the fact that all approximate problems are time-consistent, as opposed to the standard cutting plane method.

Algorithm 1 Time-Consistent Cutting Plane Method

$k \leftarrow 0$
for all $t \in \{1, \ldots, T-1\}$ **do**
  for all $\nu \in \Omega_t$ **do**
    $\mathcal{A}_t^0(\nu) \leftarrow \emptyset$
  end for
end for
$\mu^{(0)} \leftarrow p$
repeat
  $k \leftarrow k + 1$
  for all $\nu \in \Omega_T$ **do**
    $w_T(\nu) \leftarrow \mu^{(k-1)}(\nu)$
  end for
  for $t = T-1, \ldots, 1$ **do**
    for all $\nu \in \Omega_t$ **do**
      $w_t(\nu) \leftarrow \big\| w_{t+1}^{C(\nu)} \big\|_1$
      if $w_t(\nu) > 0$ **then**
        $\mu_t(\nu) \leftarrow \frac{1}{w_t(\nu)} w_{t+1}^{C(\nu)}$
        $\mathcal{A}_t^{(k)}(\nu) \leftarrow \operatorname{conv}\big(\mathcal{A}_t^{(k-1)}(\nu) \cup \{\mu_t(\nu)\}\big)$
      else
        $\mathcal{A}_t^{(k)}(\nu) \leftarrow \mathcal{A}_t^{(k-1)}(\nu)$
      end if
    end for
  end for
  Find solution $x^{(k)}$ of problem (3.10)
  $\varrho\big(\langle c_1, x_1\rangle, \langle c_2, x_2\rangle, \ldots, \langle c_T, x_T\rangle\big) \leftarrow \max_{q \in \mathcal{D}_{1,T}} \big\langle q, \langle c_1, x_1^{(k)}\rangle, \langle c_2, x_2^{(k)}\rangle, \ldots, \langle c_T, x_T^{(k)}\rangle\big\rangle$
  $\mu^{(k)} \leftarrow \arg\max_{q \in \mathcal{D}_{1,T}} \big\langle q, \langle c_1, x_1^{(k)}\rangle, \langle c_2, x_2^{(k)}\rangle, \ldots, \langle c_T, x_T^{(k)}\rangle\big\rangle$
until $\varrho\big(\langle c_1, x_1^{(k)}\rangle, \langle c_2, x_2^{(k)}\rangle, \ldots, \langle c_T, x_T^{(k)}\rangle\big) \leq \tilde{\varrho}^{(k)}\big(\langle c_1, x_1^{(k)}\rangle, \langle c_2, x_2^{(k)}\rangle, \ldots, \langle c_T, x_T^{(k)}\rangle\big)$

Theorem 12. *Suppose the measure* (3.1) *is time-consistent, and problem* (3.3) *has a*

nonempty and compact feasible set $I \cap F$. Then every accumulation point of the sequence $\{x^{(k)}\}$ generated by Algorithm 1 is a solution of problem (3.3).

Proof. As the measure (3.1) is time-consistent, we have

$$\mathcal{D}_{1,T} = \mathcal{D}_1 \circ \mathcal{D}_2 \circ \cdots \circ \mathcal{D}_{T-1}, \tag{3.11}$$

where $\mathcal{D}_t : \Omega_t \rightrightarrows \mathcal{P}(\Omega_{t+1})$, $t = 1, \ldots, T-1$ are convex closed multikernels satisfying the local property (2.22). Suppose $\mu \in \mathcal{D}_{1,T}$. Then kernels $\mu_t \ll \mathcal{D}_t$, $t = 1, \ldots, T-1$ exist, such that

$$\mu = \mu_1 \circ \mu_2 \circ \cdots \circ \mu_{T-1}. \tag{3.12}$$

Consider a node $\nu \in \Omega_{T-1}$. It follows from (3.12) and the local property (2.22) for $\mathcal{D}_{T-1}$ that the vector $\mu^{C(\nu)}$ with coordinates $\mu(\eta)$, $\eta \in C(\nu)$, can be calculated as follows:

$$\mu^{C(\nu)} = \big[\mu_1 \circ \mu_2 \circ \cdots \circ \mu_{T-2}\big](\nu)\, \mu_{T-1}(\nu).$$

If $\mu^{C(\nu)} \neq 0$, then

$$\mu_{T-1}(\nu) = \frac{\mu^{C(\nu)}}{\big\|\mu^{C(\nu)}\big\|_1} \in \mathcal{D}_{T-1}.$$

In any case, the sum

$$w_{T-1}(\nu) = \big\|\mu^{C(\nu)}\big\|_1$$

is the total mass of node ν resulting from μ. Proceeding in this way, we show that all measures calculated in line 17 of Algorithm 1 are elements of the corresponding sets $\mathcal{D}_t$, $t = 1, \ldots, T-1$. Consequently,

$$\mathcal{A}_t^{(k)} \subseteq \mathcal{D}_t, \quad , t = 1, \ldots, T-1, \quad k = 0, 1, 2, \ldots.$$

Therefore, for every $k = 0, 1, 2, \ldots$ problem 3.10 is a convex relaxation of problem (3.3). The main difference from the cutting plane relaxation (3.4) is that instead of adding just one subgradient μ to the convex hull (3.9), we add also a large number of *implied* subgradients, which can be deduced from the multikernel composition (3.11). The remaining part of the proof is identical to the convergence proof of the classical cutting plane method (see, e.g. [47, Thm. 7.7]). □

Further simplifications of the method can be achieved under the assumption that the multikernels $\mathcal{D}_t$ in (3.11) are *homogeneous*, that is, $\mathcal{D}_t(\nu) = \mathcal{D}_t(\nu')$ for all $\nu, \nu' \in \Omega_t$, and all $t = 1, \dots, T-1$. In this case, instead of constructing different approximations $\mathcal{A}_t^{(k)}(\nu)$ for different nodes $\nu \in \Omega_t$, we can share the information among the nodes at level t, and approximate $\mathcal{D}_t(\nu)$ with one common set $\bar{\mathcal{A}}_t$. Algorithm 1 simplifies significantly by replacing line 18 with the formula:

$$\bar{\mathcal{A}}_t^{(k)}(\nu) \leftarrow \begin{cases} \operatorname{conv}\big(\bar{\mathcal{A}}_t^{(k-1)}(\nu) \cup \{\mu_t(\nu)\}\big) & \text{if } \nu \text{ is the first node in } \Omega_t, \\ \operatorname{conv}\big(\bar{\mathcal{A}}_t^{(k)}(\nu) \cup \{\mu_t(\nu)\}\big) & \text{for all other nodes in } \Omega_t. \end{cases}$$

Convergence of this version of the method follows can be proved identically to Theorem 12.

3.3 Application to Time-Inconsistent Problems

Let us now consider the case when the risk measure (3.1) in problem (2.3) is not time-consistent. Algorithm 1 can still be applied in such a situation. All subproblems (3.10) solved in successive iterations of the method are time-consistent, and thus the method provides a time-consistent approximation of the original problem.

Denote

$$Z^{(k)} = \big(\langle c_1, x_1^{(k)}\rangle, \langle c_2, x_2^{(k)}\rangle, \dots, \langle c_T, x_T^{(k)}\rangle\big). \tag{3.13}$$

By the construction of the method, $\mathcal{A}_t^{(k+1)}(\nu) \supseteq \mathcal{A}_t^{(k)}(\nu)$, and thus

$$\tilde{\varrho}^{(k+1)}\big(Z^{(k+1)}\big) \geq \tilde{\varrho}^{(k)}\big(Z^{(k)}\big), \quad k = 1, 2, \dots.$$

However, the time-consistent approximations $\tilde{\varrho}^{(k)}(\cdot)$ are not, in general, lower approximations of the original risk measure $\varrho(\cdot)$.

The next proposition proves that the method is still well-defined.

Theorem 13. *Suppose problem* (3.3) *has a nonempty and compact feasible set* $I \cap F$. *Then Algorithm 1 either stops after finitely many steps, or generates an infinite sequence* $\{x^{(k)}\}$ *such that*

$$\lim_{k\to\infty} \big[\varrho\big(Z^{(k)}\big) - \tilde{\varrho}^{(k)}\big(Z^{(k)}\big)\big] = 0.$$

Proof. For $\varepsilon > 0$ we define

$$\mathcal{K}_\varepsilon = \big\{k : \varrho\big(Z^{(k)}\big) \geq \tilde{\varrho}^{(k)}\big(Z^{(k)}\big) + \varepsilon\big\}.$$

Our assertion is equivalent to the fact that $\mathcal{K}_\varepsilon$ is finite for every $\varepsilon > 0$.

Let $k_1, k_2 \in \mathcal{K}_\varepsilon$, $k_1 < k_2$. Since $\varrho\big(Z^{(k_1)}\big) \geq \tilde{\varrho}^{(k_1)}\big(Z^{(k)}\big) + \varepsilon$, Algorithm 1 will not stop and the measure $\mu^{(k_1)}$ will be used to update the sets $\mathcal{A}_t^{(k_1+1)}$, $t = 1, \ldots, T-1$. As a result, at all iterations $j = k_1 + 1, k_1 + 2, \ldots$ we shall have

$$\mu^{(k_1)} \in \mathcal{A}_1^{(j)} \circ \mathcal{A}_2^{(j)} \circ \cdots \circ \mathcal{A}_{T-1}^{(j)}.$$

Therefore,

$$\tilde{\varrho}^{(j)}\big(Z^{(j)}\big) \geq \big\langle \mu^{(k_1)}, Z^{(j)} \big\rangle, \quad j = k_1 + 1, k_1 + 2, \ldots$$

As $k_2 \in \mathcal{K}_\varepsilon$ we obtain

$$\varrho\big(Z^{(k_2)}\big) \geq \tilde{\varrho}^{(k_2)}\big(Z^{(k_2)}\big) + \varepsilon \geq \big\langle \mu^{(k_1)}, Z^{(k_2)} \big\rangle + \varepsilon.$$

Since $\varrho\big(Z^{(k_1)}\big) = \big\langle \mu^{(k_1)}, Z^{(k_1)} \big\rangle$ we can rewrite the last inequality as follows:

$$\varrho\big(Z^{(k_2)}\big) - \varrho\big(Z^{(k_1)}\big) \geq \big\langle \mu^{(k_1)}, Z^{(k_2)} - Z^{(k_1)} \big\rangle + \varepsilon. \tag{3.14}$$

Owing to the translation property of $\varrho(\cdot)$, we have the estimate

$$\varrho\big(Z^{(k_2)}\big) - \varrho\big(Z^{(k_1)}\big) \leq \big\| Z^{(k_2)} - Z^{(k_1)} \big\|_\infty. \tag{3.15}$$

Moreover,

$$\Big| \big\langle \mu^{(k_1)}, Z^{(k_2)} - Z^{(k_1)} \big\rangle \Big| \leq \big\| \mu^{(k_1)} \big\|_1 \big\| Z^{(k_2)} - Z^{(k_1)} \big\|_\infty = \big\| Z^{(k_2)} - Z^{(k_1)} \big\|_\infty, \tag{3.16}$$

because $\mu^{(k_1)}$ is a probability measure. Combining inequalities (3.14),(3.15), and (3.16), we conclude that

$$\big\| Z^{(k_2)} - Z^{(k_1)} \big\|_\infty \geq \frac{\varepsilon}{2}. \tag{3.17}$$

As the feasible set $I \cap F$ is compact, the values (3.13) live in a compact set as well. Therefore, only a finite subset of them may satisfy inequality (3.17). □

It follows that if the stopping test in line 27 of Algorithm 1 is verified with accuracy $\varepsilon > 0$, the method stops after finitely many steps. The last point $x^{(k)}$ obtained is the minimizer of a time-consistent dynamic measure of risk $\tilde{\varrho}^{(k)}\big(Z(\cdot)\big)$ and $\tilde{\varrho}^{(k)}\big(Z^{(k)}\big) \geq \varrho\big(Z^{(k)}\big) - \varepsilon$. Therefore, the value $\tilde{\varrho}^{(k)}\big(Z^{(k)}\big)$ is a *time-consistent upper bound* on the optimal value of problem (2.3).

3.3.1 Non-parametric Cutting Plane Example

In this section we demonstrate an iteration of the non-parametric cutting plane method applied to time-inconsistent problems. We consider a two-stage decision tree with a probability measure p as given in the original example of time inconsistency of Section 1.3. We can see from Algorithm 1 that $\mu^{(0)} = p$. Therefore,

$$\begin{aligned} &\mu_2(\nu_1, \eta_1) = 0.3,\ \mu_2(\nu_1, \eta_2) = 0.7 \\ &\mathcal{A}_2^{(1)}(\nu_2) = \operatorname{conv}\{\mu_2(\nu_1)\} = \operatorname{conv}\{(0.3, 0.7)\} \end{aligned} \tag{3.18}$$

and similarly,

$$\begin{aligned} &\mu_2(\nu_2, \eta_3) = 0.3,\ \mu_2(\nu_2, \eta_4) = 0.7 \\ &\mathcal{A}_2^{(1)}(\nu_2) = \operatorname{conv}\{\mu_2(\nu_2)\} = \operatorname{conv}\{(0.3, 0.7)\} \end{aligned} \tag{3.19}$$

Further,

$$\begin{aligned} &\mu_1(\nu_0, \nu_1) = 0.3,\ \mu_1(\nu_0, \nu_2) = 0.7 \\ &\mathcal{A}_1^{(1)}(\nu_0) = \operatorname{conv}\{\mu_1(\nu_0)\} = \operatorname{conv}\{(0.3, 0.7)\} \end{aligned} \tag{3.20}$$

For the sake of simplicity, we only consider a final stage cost Z_3. This is sufficient, since first and second stage costs would be measurable at $T = 3$. We can measure the risk associated with costs incurred on the entire tree using a coherent risk measure $\rho_{1,3} : \mathcal{Z}_3 \to \mathbb{R}$. In this example we choose $\rho_{1,3}(\cdot)$ to be a mean-upper semideviation function with $\varkappa_{1,3} = 0.5$. Thus, $\rho_{1,3}(\cdot)$ is not a time-consistent risk measure, as it cannot be represented as a composition of one step conditional risk measures. After determining $\mu^{(1)}$ and $\mathcal{A}^{(1)}$, we solve the following problem at line 24 in Algorithm 1:

$$\min_{x \in I \cap F} \tilde{\varrho}^{(1)}\big(\langle c_3, x_3 \rangle\big) \tag{3.21}$$

Since, each of the multikernels $\mathcal{A}_t^{(1)}, t = 1, 2$ contains only a single one-step probability measure corresponding to the original measure p, we know that

$$\begin{aligned} \tilde{\varrho}^{(1)}(Z_3) &= \max_{q \in \mathcal{A}_1^{(1)} \circ \mathcal{A}_2^{(1)}} \langle\, q, Z_3 \rangle \\ &= \mathbb{E}_P[Z_3] \end{aligned} \tag{3.22}$$

Hence, at the first iteration, we find $x^{(1)} \in I \cap F$ such that expected cost is minimized.

$$x^{(1)} \leftarrow \arg\min_{x \in I \cap F} \mathbb{E}_P\big[\langle c_3, x_3 \rangle\big] \tag{3.23}$$

Now, suppose that the policy $x^{(1)}$ results in random cost $Z_3^{(1)}$ that is identical to the cost Z of the original example of time inconsistency of Section 1.3. Thus, $Z_3^{(1)\eta_1} = 80,\ Z_3^{(1)\eta_2} = 105, Z_3^{(1)\eta_3} = 103,$ and $Z_3^{(1)\eta_4} = 98$. This is illustrated in Figure 3.1. We know that the original probability measure p is such that $p_{\eta_1} = 0.09$,

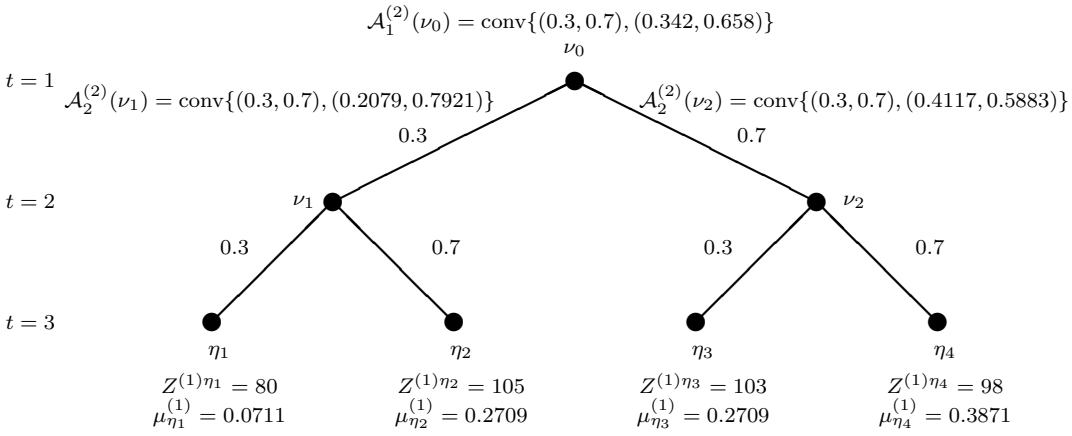

Figure 3.1: Non-parametric time-consistent cutting plane method.

$p_{\eta_2} = p_{\eta_3} = 0.21,$ and $p_{\eta_4} = 0.49$. Since $\rho_{1,3}(\cdot)$ is a mean-upper semideviation function with $\varkappa_{1,3} = 0.5$, we can use equation (1.13) to find its dual set of probability measures $\mathcal{D}_{1,3}$.

$$
\begin{aligned}
D_{1,3} &= \left\{ \mu : \frac{\mu_\eta}{p_\eta} = 1 + h_\eta - \sum_{m \in \Omega_3} h_m p_m,\ 0 \le h_\eta \le \varkappa,\ \nu \in \Omega_3 \right\} \\
&= \left\{ \mu : \begin{array}{l}
\mu_{\eta_1} = p_{\eta_1}(1 + h_{\eta_1} - p_{\eta_1} h_{\eta_1} - p_{\eta_2} h_{\eta_2} - p_{\eta_3} h_{\eta_3} - p_{\eta_4} h_{\eta_4}) \\
\mu_{\eta_2} = p_{\eta_2}(1 + h_{\eta_2} - p_{\eta_1} h_{\eta_1} - p_{\eta_2} h_{\eta_2} - p_{\eta_3} h_{\eta_3} - p_{\eta_4} h_{\eta_4}) \\
\mu_{\eta_3} = p_{\eta_3}(1 + h_{\eta_3} - p_{\eta_1} h_{\eta_1} - p_{\eta_2} h_{\eta_2} - p_{\eta_3} h_{\eta_3} - p_{\eta_4} h_{\eta_4}) \\
\mu_{\eta_4} = p_{\eta_4}(1 + h_{\eta_4} - p_{\eta_1} h_{\eta_1} - p_{\eta_2} h_{\eta_2} - p_{\eta_3} h_{\eta_3} - p_{\eta_4} h_{\eta_4}) \\
0 \le h_{\eta_1} \le \varkappa_{1,3} \\
0 \le h_{\eta_2} \le \varkappa_{1,3} \\
0 \le h_{\eta_3} \le \varkappa_{1,3} \\
0 \le h_{\eta_4} \le \varkappa_{1,3}
\end{array} \right\} \\
&= \left\{ \mu : \begin{array}{l}
\mu_{\eta_1} = 0.09 \cdot (1 + h_{\eta_1} - 0.09 \cdot h_{\eta_1} - 0.21 \cdot h_{\eta_2} - 0.21 \cdot h_{\eta_3} - 0.49 \cdot h_{\eta_4}) \\
\mu_{\eta_2} = 0.21 \cdot (1 + h_{\eta_2} - 0.09 \cdot h_{\eta_1} - 0.21 \cdot h_{\eta_2} - 0.21 \cdot h_{\eta_3} - 0.49 \cdot h_{\eta_4}) \\
\mu_{\eta_3} = 0.21 \cdot (1 + h_{\eta_3} - 0.09 \cdot h_{\eta_1} - 0.21 \cdot h_{\eta_2} - 0.21 \cdot h_{\eta_3} - 0.49 \cdot h_{\eta_4}) \\
\mu_{\eta_4} = 0.49 \cdot (1 + h_{\eta_4} - 0.09 \cdot h_{\eta_1} - 0.21 \cdot h_{\eta_2} - 0.21 \cdot h_{\eta_3} - 0.49 \cdot h_{\eta_4}) \\
0 \le h_{\eta_1} \le 0.5 \\
0 \le h_{\eta_2} \le 0.5 \\
0 \le h_{\eta_3} \le 0.5 \\
0 \le h_{\eta_4} \le 0.5
\end{array} \right\} \\
&= \left\{ \mu : \begin{array}{l}
\mu_{\eta_1} = 0.09 + 0.0819 \cdot h_{\eta_1} - 0.0189 \cdot h_{\eta_2} - 0.0189 \cdot h_{\eta_3} - 0.0441 \cdot h_{\eta_4} \\
\mu_{\eta_2} = 0.21 - 0.0189 \cdot h_{\eta_1} + 0.1659 \cdot h_{\eta_2} - 0.0441 \cdot h_{\eta_3} - 0.1029 \cdot h_{\eta_4} \\
\mu_{\eta_3} = 0.21 - 0.0189 \cdot h_{\eta_1} - 0.0441 \cdot h_{\eta_2} + 0.1659 \cdot h_{\eta_3} - 0.1029 \cdot h_{\eta_4} \\
\mu_{\eta_4} = 0.49 - 0.0441 \cdot h_{\eta_1} - 0.1029 \cdot h_{\eta_2} - 0.1029 \cdot h_{\eta_3} + 0.2499 \cdot h_{\eta_4} \\
0 \le h_{\eta_1} \le 0.5 \\
0 \le h_{\eta_2} \le 0.5 \\
0 \le h_{\eta_3} \le 0.5 \\
0 \le h_{\eta_4} \le 0.5
\end{array} \right\}
\end{aligned}
\tag{3.24}
$$

At line 26 in Algorithm 1, we compute a new probability measure $\mu^{(1)}$ as

$$\begin{aligned}\mu^{(1)} &= \arg\max_{q\in\mathcal{D}_{1,3}} \left\langle q, \langle c_3, x_3^{(1)}\rangle \right\rangle \\ &= \arg\max_{q\in\mathcal{D}_{1,3}} \left\langle q, Z_3^{(1)} \right\rangle\end{aligned} \tag{3.25}$$

Thus we solve the problem:

$$\begin{aligned}&\max \left\{80\mu_{\eta_1} + 105\mu_{\eta_2} + 103\mu_{\eta_3} + 98\mu_{\eta_4}\right\} \\ &\text{s.t.} \\ &\mu_{\eta_1} = 0.09 + 0.0819 \cdot h_{\eta_1} - 0.0189 \cdot h_{\eta_2} - 0.0189 \cdot h_{\eta_3} - 0.0441 \cdot h_{\eta_4} \\ &\mu_{\eta_2} = 0.21 - 0.0189 \cdot h_{\eta_1} + 0.1659 \cdot h_{\eta_2} - 0.0441 \cdot h_{\eta_3} - 0.1029 \cdot h_{\eta_4} \\ &\mu_{\eta_3} = 0.21 - 0.0189 \cdot h_{\eta_1} - 0.0441 \cdot h_{\eta_2} + 0.1659 \cdot h_{\eta_3} - 0.1029 \cdot h_{\eta_4} \\ &\mu_{\eta_4} = 0.49 - 0.0441 \cdot h_{\eta_1} - 0.1029 \cdot h_{\eta_2} - 0.1029 \cdot h_{\eta_3} + 0.2499 \cdot h_{\eta_4} \\ &0 \le h_{\eta_1} \le 0.5 \\ &0 \le h_{\eta_2} \le 0.5 \\ &0 \le h_{\eta_3} \le 0.5 \\ &0 \le h_{\eta_4} \le 0.5\end{aligned} \tag{3.26}$$

Hence, we find a solution $\mu^{(1)}$ such that $\mu_{\eta_1}^{(1)} = 0.0711, \mu_{\eta_2}^{(1)} = 0.2709, \mu_{\eta_3}^{(1)} = 0.2709$ and $\mu_{\eta_4}^{(1)} = 0.3871$. At the next iteration, we set $k = 2$, and compute

$$\begin{aligned}\mu_2(\nu_1, \eta_1) &= \frac{0.0711}{0.0711 + 0.2709} = 0.2079 \\ \mu_2(\nu_1, \eta_2) &= \frac{0.2709}{0.0711 + 0.2709} = 0.7921 \\ \mathcal{A}_2^{(2)}(\nu_1) &= \text{conv}\{(0.3, 0.7), (0.2079, 0.7921)\}\end{aligned} \tag{3.27}$$

Further,

$$\begin{aligned}\mu_2(\nu_2, \eta_3) &= \frac{0.2709}{0.2709 + 0.3871} = 0.4117 \\ \mu_2(\nu_2, \eta_4) &= \frac{0.3871}{0.2709 + 0.3871} = 0.5883 \\ \mathcal{A}_2^{(2)}(\nu_2) &= \text{conv}\{(0.3, 0.7), (0.4117, 0.5883)\}\end{aligned} \tag{3.28}$$

And additionally,

$$\begin{aligned}\mu_1(\nu_0, \nu_1) &= \frac{0.0711 + 0.2709}{1} = 0.342 \\ \mu_1(\nu_0, \nu_2) &= \frac{0.2709 + 0.3871}{1} = 0.658 \\ \mathcal{A}_1^{(2)}(\nu_0) &= \text{conv}\{(0.3, 0.7), (0.342, 0.658)\}\end{aligned} \tag{3.29}$$

Thus we can construct a new time-consistent approximation $\tilde{\varrho}^{(2)}(\cdot)$ of the original function $\rho_{1,3}(\cdot)$,

$$\tilde{\varrho}^{(2)}(Z_3) = \max_{q \in \mathcal{A}_1^{(2)} \circ \mathcal{A}_2^{(2)}} \langle\, q, Z_3 \rangle. \tag{3.30}$$

Now, we solve problem (3.10) for the function $\tilde{\varrho}^{(2)}(Z_3)$ to find a new policy $x^{(2)}$. Then we use the new policy to find a new probability measure $\mu^{(2)}$, and repeat until the stoping condition is satisfied.

3.4 Parametric Time-Consistent Approximations

Consider now the situation when we specify the functional form of the conditional measures of risk $\tilde{\rho}_t(\cdot)$ in the time-consistent approximation of the original risk measure:

$$\rho_{1,T}(Z_1 + Z_2 + \cdots + Z_T) \simeq \tilde{\rho}_1\Big(\tilde{\rho}_2\big(\cdots \tilde{\rho}_{T-1}(Z_1 + Z_2 + \cdots + Z_T)\cdots\big)\Big).$$

This results in restricting the functional form of the multikernels $\mathcal{A}_t^{(k)}$ in the composition formula (3.7). Under this restriction, we can still use Algorithm 1 in a suitable form.

The main difference is that we cannot use the convex hull formula (3.9) in line 18, but rather compute the smallest set $\mathcal{A}_t^{(k)}(\nu)$ containing $\big\{\mu_t^{(j)}(\nu),\ j = 0, 1 \ldots, k-1\big\}$ within the specified parametric family of sets.

To illustrate our approach, consider the case when all node risk measures $\tilde{\rho}^{\nu}(\cdot)$ are restricted to have the mean-semideviation form:

$$\tilde{\rho}^{\nu}\big(Z^{C(\nu)}\big) = \sum_{\eta \in C(\nu)} p_{\nu\eta} Z^{\eta} + \varkappa \sum_{\eta \in C(\nu)} p_{\nu\eta} \Big(Z^{\eta} - \sum_{m \in C(\nu)} p_{\nu m} Z^{m} \Big)_{+}, \tag{3.31}$$

with $\varkappa(\nu) \in [0, 1]$. It is well known (see, e.g., [50, Ex. 4.2]) that the corresponding multikernel is composed of sets

$$A_t^{\varkappa} = \partial \tilde{\rho}^{\nu}(0) = \Big\{ \mu : \frac{\mu_{\nu\eta}}{p_{\nu\eta}} = 1 + h_\eta - \sum_{m \in C(\nu)} h_m p_{\nu m},\ 0 \le h_\eta \le \varkappa \Big\}. \tag{3.32}$$

As the set $A_t^{\varkappa}$ grows when $\varkappa$ increases, the problem of specifying the smallest set $\mathcal{A}_t^{(k)}(\nu)$ containing $\big\{\mu_t^{(j)}(\nu),\ j = 0, 1 \ldots, k-1\big\}$ reduces to finding the smallest value $\varkappa$ such that $\mu_t^{(j)}(\nu) \in A_t^{\varkappa}(\nu)$ for all $j = 0, 1, \ldots, k-1$.

This estimation is done recursively in Algorithm 1, and thus it is sufficient to solve it for one measure: $\mu^{(j)}$, as in line 18 of Algorithm 1. The smallest value of $\varkappa$ is then the optimal value of the following linear programming problem:

$$\begin{aligned} \min_{h,\varkappa} \quad & \varkappa \\ \text{s.t.} \quad & h_\eta - \sum_{m \in C(\nu)} h_m p_{\nu m} = \frac{\mu^{(j)}_{\nu\eta}}{p_{\nu\eta}} - 1, \quad \eta \in C(\nu), \\ & 0 \le h_\eta \le \varkappa, \quad \eta \in C(\nu). \end{aligned} \tag{3.33}$$

If the optimal value of $\varkappa$ is larger than 1, estimation with a specified parametric family is not possible.

These observations allow us to modify Algorithm 1 as follows. For each node $\nu \in \Omega_t$ the sets $\mathcal{A}_t^{(k-1)}(\nu)$ are represented by their parameters $\varkappa^{(k-1)}(\nu)$. Initially, $\varkappa^{(0)}(\nu) = 0$ for all ν. In line 18, instead of taking the convex hull, we solve problem (3.33) to obtain the optimal value $\varkappa^{(k)}_{\min}(\nu)$, and we set

$$\varkappa^{(k)}(\nu) = \max\left(\varkappa^{(k-1)}(\nu), \varkappa^{(k)}_{\min}(\nu)\right).$$

Similarly to Theorem 12 we can prove that if the original measure of risk is indeed a composition of mean-semideviation conditional measures of risk, then the parametric version of Algorithm 1 finds the optimal solution of problem (3.3). If its not a member of the parametric family, the algorithm will have the property proved in Theorem 13. Proofs of these observations are almost identical to the proofs for the previous (non-parametric) versions.

3.4.1 Parametric Cutting Plane Example

We examine an iteration of the parametric time-consistent cutting plane method. We consider the same setup as in Section 3.3.1. Given a mean-upper semideviation function $\rho_{1,3}(Z)$ with $\varkappa_{1,3} = 0.5$ we construct a time-consistent approximation $\tilde{\rho}_1(\tilde{\rho}_2(Z))$ as a composition of to mean-upper semideviation functions. Again, for the sake of simplicity we only consider a final stage cost Z_3. We initialize $\mu^{(0)} = p$, and therefore

$$\mu_2^{(0)}(\nu_1, \eta_1) = 0.3, \ \mu_2^{(0)}(\nu_1, \eta_2) = 0.7 \tag{3.34}$$

Now, instead of using the convex hull formula of line 18 in Algorithm 1, we find $\varkappa^{(1)}(\nu_1)$ as the optimal value of the following linear programming problem:

$$\begin{aligned} \min_{h,\varkappa} \quad & \varkappa \\ \text{s.t.} \quad & h_{\eta_1} - h_{\eta_1} p_{\nu_1\eta_1} - h_{\eta_2} p_{\nu_1\eta_2} = \frac{\mu^{(0)}_{\nu_1\eta_1}}{p_{\nu_1\eta_1}} - 1, \\ & h_{\eta_2} - h_{\eta_1} p_{\nu_1\eta_1} - h_{\eta_2} p_{\nu_1\eta_2} = \frac{\mu^{(0)}_{\nu_1\eta_2}}{p_{\nu_1\eta_2}} - 1, \\ & 0 \le h_{\eta_1} \le \varkappa \\ & 0 \le h_{\eta_2} \le \varkappa \end{aligned} \tag{3.35}$$

Substituting, we get

$$\begin{aligned} \min_{h,\varkappa} \quad & \varkappa \\ \text{s.t.} \quad & h_{\eta_1} - 0.3 h_{\eta_1} - 0.7 h_{\eta_2} = \frac{0.3}{0.3} - 1, \\ & h_{\eta_2} - 0.3 h_{\eta_1} - 0.7 h_{\eta_2} = \frac{0.7}{0.7} - 1, \\ & 0 \le h_{\eta_1} \le \varkappa \\ & 0 \le h_{\eta_2} \le \varkappa \end{aligned} \tag{3.36}$$

which implies $\varkappa^{(1)}(\nu_1) = 0$.

Similarly,

$$\varkappa^{(1)}(\nu_2) = \varkappa^{(1)}(\nu_0) = 0$$

Now, we consider the time-consistent approximation to $\rho_{1,3}(Z)$

$$\tilde{\varrho}^{(1)}(Z) = \tilde{\rho}_1^{(1)}(\tilde{\rho_2}^{(1)}(Z)) \tag{3.37}$$

and we solve the approximate time-consistent problem at line 24 in Algorithm 1:

$$\min_{x \in I \cap F} \tilde{\varrho}^{(1)}\big(\langle c_3, x_3 \rangle\big) \tag{3.38}$$

Since, $\varkappa^{(1)}(\nu_0) = \varkappa^{(1)}(\nu_1) = \varkappa^{(1)}(\nu_2) = 0$, we know

$$\tilde{\varrho}^{(1)}(Z_3) = \mathbb{E}_P[Z_3] \tag{3.39}$$

Hence, similar to the non-parametric case, we minimize the expected cost:

$$x^{(1)} \leftarrow \operatorname*{arg\,min}_{x \in I \cap F} \mathbb{E}_P\big[\langle c_3, x_3 \rangle\big] \tag{3.40}$$

Let us again assume that the policy $x^{(1)}$ results in random cost $Z_3^{(1)}$ such that $Z_3^{(1)\eta_1} = 80,\ Z_3^{(1)\eta_2} = 105, Z_3^{(1)\eta_3} = 103,$ and $Z_3^{(1)\eta_4} = 98$. This is illustrated in Figure 3.2. We use $Z^{(1)}$ to compute a new probability measure $\mu^{(1)}$ at line 26 in Algorithm 1.

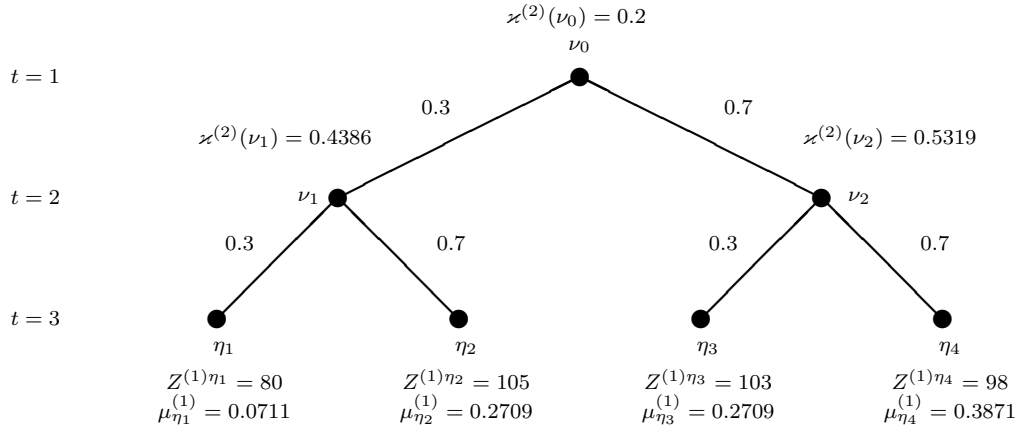

Figure 3.2: Parametric time-consistent cutting plane method.

$$\begin{aligned} \mu^{(1)} &= \underset{q \in \mathcal{D}_{1,3}}{\arg\max} \left\langle q, \langle c_3, x_3^{(1)} \rangle \right\rangle \\ &= \underset{q \in \mathcal{D}_{1,3}}{\arg\max} \left\langle q, Z_3^{(1)} \right\rangle \end{aligned} \tag{3.41}$$

where the dual set of probability measures $\mathcal{D}_{1,3}$ is the same as in Section 3.3.1. Hence we find the same solution $\mu^{(1)}$ as in Section 3.3.1: $\mu^{(1)}_{\eta_1} = 0.0711, \mu^{(1)}_{\eta_2} = 0.2709, \mu^{(1)}_{\eta_3} = 0.2709$ and $\mu^{(1)}_{\eta_4} = 0.3871$. Thus,

$$\begin{aligned} \mu_2^{(1)}(\nu_1, \eta_1) &= \frac{0.0711}{0.0711 + 0.2709} = 0.2079 \\ \mu_2^{(1)}(\nu_1, \eta_2) &= \frac{0.2709}{0.0711 + 0.2709} = 0.7921 \end{aligned} \tag{3.42}$$

In order to compute $\varkappa^{(2)}_{\min}(\nu_1)$, we consider the linear programming problem

$$\begin{aligned} \min_{h, \varkappa} \quad & \varkappa \\ \text{s.t.} \quad & h_{\eta_1} - h_{\eta_1} p_{\nu_1\eta_1} - h_{\eta_2} p_{\nu_1\eta_2} = \frac{\mu^{(1)}_{\nu_1\eta_1}}{p_{\nu_1\eta_1}} - 1, \\ & h_{\eta_2} - h_{\eta_1} p_{\nu_1\eta_1} - h_{\eta_2} p_{\nu_1\eta_2} = \frac{\mu^{(1)}_{\nu_1\eta_2}}{p_{\nu_1\eta_2}} - 1, \\ & 0 \le h_{\eta_1} \le \varkappa \\ & 0 \le h_{\eta_2} \le \varkappa \end{aligned} \tag{3.43}$$

After substituting the values of p and $\mu^{(1)}$, we get

$$\begin{aligned} \min_{h,\varkappa} \quad & \varkappa \\ \text{s.t.} \quad & h_{\eta_1} - 0.3h_{\eta_1} - 0.7h_{\eta_2} = \frac{0.2079}{0.3} - 1, \\ & h_{\eta_2} - 0.3h_{\eta_1} - 0.7h_{\eta_2} = \frac{0.7921}{0.7} - 1, \\ & 0 \leq h_{\eta_1} \leq \varkappa \\ & 0 \leq h_{\eta_2} \leq \varkappa \end{aligned} \tag{3.44}$$

and the optimal value is $\kappa^{(2)}_{\min}(\nu_1) = 0.4386$. Hence,

$$\begin{aligned} \varkappa^{(2)}(\nu_1) &= \max\left(\varkappa^{(1)}(\nu_1), \varkappa^{(2)}_{\min}(\nu_1)\right) \\ &= \max(0, 0.4386) \\ &= 0.4386 \end{aligned} \tag{3.45}$$

Therefore,

$$\mathcal{A}^{(2)}_2(\nu_1) = \mathcal{A}^{0.4386}_2$$

Now, let us consider node ν_2,

$$\begin{aligned} \mu^{(1)}_2(\nu_2, \eta_3) &= \frac{0.2709}{0.2709 + 0.3871} = 0.4117 \\ \mu^{(1)}_2(\nu_2, \eta_4) &= \frac{0.3871}{0.2709 + 0.3871} = 0.5883 \end{aligned} \tag{3.46}$$

$\varkappa^{(2)}_{\min}(\nu_2)$ is the optimal value of the linear programming problem

$$\begin{aligned} \min_{h,\varkappa} \quad & \varkappa \\ \text{s.t.} \quad & h_{\eta_3} - h_{\eta_3} p_{\nu_2\eta_3} - h_{\eta_4} p_{\nu_2\eta_4} = \frac{\mu^{(1)}_{\nu_2\eta_3}}{p_{\nu_2\eta_3}} - 1, \\ & h_{\eta_4} - h_{\eta_3} p_{\nu_2\eta_3} - h_{\eta_4} p_{\nu_2\eta_4} = \frac{\mu^{(1)}_{\nu_2\eta_4}}{p_{\nu_2\eta_4}} - 1, \\ & 0 \leq h_{\eta_3} \leq \varkappa \\ & 0 \leq h_{\eta_4} \leq \varkappa \end{aligned} \tag{3.47}$$

which can be rewritten as

$$\begin{aligned} \min_{h,\varkappa} \quad & \varkappa \\ \text{s.t.} \quad & h_{\eta_3} - 0.3h_{\eta_3} - 0.7h_{\eta_4} = \frac{0.4117}{0.3} - 1, \\ & h_{\eta_4} - 0.3h_{\eta_3} - 0.7h_{\eta_4} = \frac{0.5883}{0.7} - 1, \\ & 0 \leq h_{\eta_3} \leq \varkappa \\ & 0 \leq h_{\eta_4} \leq \varkappa \end{aligned} \tag{3.48}$$

We can compute the optimal value to be $\kappa^{(2)}_{\min}(\nu_1) = 0.5319$. Therefore,

$$\begin{aligned} \varkappa^{(2)}(\nu_2) &= \max\left(\varkappa^{(1)}(\nu_2), \varkappa^{(2)}_{\min}(\nu_2)\right) \\ &= \max(0, 0.5319) \\ &= 0.5319 \end{aligned} \tag{3.49}$$

Hence,

$$\mathcal{A}^{(2)}_2(\nu_2) = \mathcal{A}^{0.5319}_2$$

Finally, we also need to consider the root node ν_0,

$$\begin{aligned} \mu^{(1)}_2(\nu_0, \nu_1) &= \frac{0.0711 + 0.2709}{1} = 0.342 \\ \mu^{(1)}_2(\nu_0, \nu_2) &= \frac{0.2709 + 0.3871}{1} = 0.658 \end{aligned} \tag{3.50}$$

In order to find $\varkappa^{(2)}_{\min}(\nu_2)$ we consider the problem

$$\begin{aligned} \min_{h,\varkappa} \quad & \varkappa \\ \text{s.t.} \quad & h_{\nu_1} - h_{\nu_1} p_{\nu_0\nu_1} - h_{\nu_2} p_{\nu_0\nu_2} = \frac{\mu^{(1)}_{\nu_0\nu_1}}{p_{\nu_0\nu_1}} - 1, \\ & h_{\nu_2} - h_{\nu_1} p_{\nu_0\nu_1} - h_{\nu_2} p_{\nu_0\nu_2} = \frac{\mu^{(1)}_{\nu_0\nu_2}}{p_{\nu_0\nu_2}} - 1, \\ & 0 \leq h_{\nu_1} \leq \varkappa \\ & 0 \leq h_{\nu_2} \leq \varkappa \end{aligned} \tag{3.51}$$

After substitution, we get

$$\begin{aligned} \min_{h,\varkappa} \quad & \varkappa \\ \text{s.t.} \quad & h_{\nu_1} - 0.3h_{\nu_1} - 0.7h_{\nu_2} = \frac{0.342}{0.3} - 1, \\ & h_{\nu_2} - 0.3h_{\nu_1} - 0.7h_{\nu_2} = \frac{0.658}{0.7} - 1, \\ & 0 \leq h_{\nu_1} \leq \varkappa \\ & 0 \leq h_{\nu_2} \leq \varkappa \end{aligned} \tag{3.52}$$

The resulting optimal value is $\kappa^{(2)}_{\min}(\nu_0) = 0.2$. Hence,

$$\begin{aligned} \varkappa^{(2)}(\nu_2) &= \max\left(\varkappa^{(1)}(\nu_0), \varkappa^{(2)}_{\min}(\nu_0)\right) \\ &= \max(0, 0.2) \\ &= 0.2 \end{aligned} \tag{3.53}$$

And,

$$\mathcal{A}^{(2)}_2(\nu_2) = \mathcal{A}^{0.2}_2$$

Thus we can use the updated values $\varkappa^{(2)}$ to construct a new time-consistent approximation $\tilde{\varrho}^{(2)}(Z) = \tilde{\rho}^{(2)}_1(\tilde{\rho}^{(2)}_2(Z))$ of the original function $\rho_{1,3}(Z)$. Then we can find a new policy $x^{(2)}$ which would imply a random cost $Z^{(2)}$. Afterwards, we can compute a probability measure $\mu^{(2)}$, and continue with the next iteration.

Chapter 4

Universal Parametric Time-Consistent Dynamic Upper Bounds

In section 3.4 we presented a method for constructing parametric time-consistent upper bounds to $\rho_{1,T}(\cdot)$ by obtaining parameters $\varkappa^{(k)}(\nu)$ such that

$$\rho_{1,T}\big(Z_1^{(\ell)}+Z_2^{(\ell)}+\cdots+Z_T^{(\ell)}\big) \le \tilde{\rho}_1\Big(\tilde{\rho}_2\big(\cdots\tilde{\rho}_{T-1}(Z_1^{(\ell)}+Z_2^{(\ell)}+\cdots+Z_T^{(\ell)})\cdots\big)\Big), \quad \ell=1,2,\ldots,k.$$

As the successive policies $x^{(\ell)}$ and the resulting random outcomes $Z_2^{(\ell)}$ were obtained by minimizing the current time-consistent approximations, we also had an inequality for the optimal value of the original problem:

$$\min_{x\in I\cap F}\rho_{1,T}\big(Z_1(x)+Z_2(x)+\cdots+Z_T(x)\big) \le \tilde{\rho}_1\Big(\tilde{\rho}_2\big(\cdots\tilde{\rho}_{T-1}(Z_1^{(k)}+Z_2^{(k)}+\cdots+Z_T^{(k)})\cdots\big)\Big),$$

where k is the last iteration of the method.

In this section, we show that we can generate risk prices $\bar{\varkappa}(\nu), \nu\in\Omega_t$ such that

$$\rho_{1,T}(Z(x)) \le \tilde{\rho}_1\Big(\tilde{\rho}_2\big(\cdots\tilde{\rho}_{T-1}(Z(x))\cdots\big)\Big)$$

for any $Z(x)$ given by

$$Z(x) = \langle c_1, x_1\rangle + \langle c_2, x_2\rangle + \cdots + \langle c_T, x_T\rangle, \tag{4.1}$$

where

$$x\in\{I\cap F\}\subseteq\mathbb{R}^n, \quad n=\sum_{t=1}^{T} n_t.$$

We call the resulting upper bound a *universal parametric time-consistent bound*.

For an arbitrary $x\in I\cap F$ we define μ^x as

$$\mu^x = \arg\max_{q\in\mathcal{D}_{1,T}}\big\langle q, \langle c_1, x_1\rangle + \langle c_2, x_2\rangle + \cdots + \langle c_T, x_T\rangle\big\rangle$$

We denote with $\varkappa_{\min}(\nu, \mu)$ the optimal value of problem (3.33) when μ is used instead of $\mu^{(k)}$. Given $\nu \in \Omega_t$, we would like to find the parameters $\bar{\varkappa}(\nu)$ that provide the best possible upper bounds. Hence, the following should hold:

$$\bar{\varkappa}(\nu) = \max_{x \in I \cap F} \varkappa_{\min}(\nu, \mu_t^x) \tag{4.2}$$

Unfortunately, the set $I \cap F$ is not finite, in general, and it is not immediately obvious how the above maximum can be computed.

4.1 Universal Parametric Time-Consistent Upper Bounds by Scenario Enumeration

One possible approach would be to notice that if $\nu \in \Omega_T$, then

$$\mu^x(\nu) = p_\nu + \lambda^x(\nu) - p_\nu \sum_{\eta \in \Omega_T} \lambda^x(\eta), \tag{4.3}$$

where

$$\lambda^x(\nu) = \begin{cases} \varkappa_{1,T} p_\nu & \text{if } Z^\nu(x) \geq \sum_{\eta \in \Omega_T} p_\eta Z^\eta(x), \\ 0 & \text{otherwise.} \end{cases} \tag{4.4}$$

Equations (4.3) and (4.4) imply that there are at most $2^{|\Omega_T|}$ possible distinct vectors μ^x. Hence, for very small scenario trees we could enumerate all sets of constraints of the form:

$$\begin{aligned} & Z^\nu(x) \geq \sum_{\eta \in \Omega_T} p_\eta Z^\eta(x), \quad \nu \in N_+, \\ & Z^\nu(x) + \epsilon \leq \sum_{\eta \in \Omega_T} p_\eta Z^\eta(x), \quad \nu \in \Omega_T \setminus N_+, \\ & x \in I \cap F, \end{aligned} \tag{4.5}$$

where $N_+ \subseteq \Omega_T$, and $\epsilon > 0$ is a given precision tolerance. Using this approach, we can find $\bar{\varkappa}(\nu)$ for $\nu \in \Omega_t$ by computing finitely many values $\varkappa_{\min}(\nu, \mu_t^x(\nu))$. We summarize the method in Algorithm 2.

Algorithm 2 can be applied to problems involving high-dimensional policies $x \in I \cap F$. However, its computational time grows exponentially with the cardinality of Ω_T and therefore the method would be appropriate only when the tree size is small.

Algorithm 2 Method for Time-Consistent Upper Bounds Using Scenario Enumeration

Fix $\epsilon > 0$.
$k \leftarrow 0$
for all $t = 1, \ldots, T-1$ **do**
  for all $\nu \in \Omega_t$ **do**
    $\bar{\varkappa}^{(0)}(\nu) \leftarrow 0$
  end for
end for
for all $N_+ \subseteq \Omega_T$ **do**
  $X \leftarrow \left\{ \begin{array}{l} x \in I \cap F, \\ Z^\nu(x) \geq \sum_{\eta \in \Omega_T} p_\eta Z^\eta(x), \ \nu \in N_+, \\ Z^\nu(x) + \epsilon \leq \sum_{\eta \in \Omega_T} p_\eta Z^\eta(x), \ \nu \in \Omega_T \setminus N_+ \end{array} \right\}$
  if $X \neq \emptyset$ **then**
    $k \leftarrow k + 1$
    Select $x \in X$
    $\mu^{(k)} \leftarrow \arg\max_{q \in \mathcal{D}_{1,T}} \left\langle q, \langle c_1, x_1 \rangle + \langle c_2, x_2 \rangle + \cdots + \langle c_T, x_T \rangle \right\rangle$
    for all $\nu \in \Omega_T$ **do**
      $w_T(\nu) \leftarrow \mu^{(k)}(\nu)$
    end for
    for all $t = T-1, \ldots, 1$ **do**
      for all $\nu \in \Omega_t$ **do**
        $w_t(\nu) \leftarrow \| w_{t+1}^{C(\nu)} \|_1$
        if $w_t(\nu) > 0$ **then**
          $\mu_t^{(k)}(\nu) \leftarrow \frac{1}{w_t(\nu)} w_{t+1}^{C(\nu)}$
          $\bar{\varkappa}^{(k)}(\nu) \leftarrow \max\left(\bar{\varkappa}^{(k-1)}(\nu), \varkappa_{\min}(\nu, \mu_t^{(k)}) \right)$
        end if
      end for
    end for
  end if
end for

4.1.1 An Example of Constructing Universal Time-Consistent Upper Bounds by Scenario Enumeration

In this section we demonstrate the use of Algorithm 2 for the construction of universal time-consistent upper bounds. Similarly to the original example of time inconsistency in Figure 1.2, we consider an instance with two random variables observed at the final time period $T = 3$. Given a mean-upper semideviation risk measure $\rho(Z(x))$ with $\varkappa_{1,3} = 0.5$, we want to construct a time-consistent function $\rho_1(\rho_2(Z(x)))$ which would provide an upper bound to $\rho(Z(x))$ for any policy $x \in I \cap F$, where $I \cap F = \{x_3 \in \mathbb{R}^2 : \ \langle \mathbf{e}^T, x_3 \rangle = 1, \ x \geq 0\}$. Thus, we are looking for the best time-consistent upper bound that holds for any convex combination of the given random costs. Our setup is illustrated in Figure 4.1.

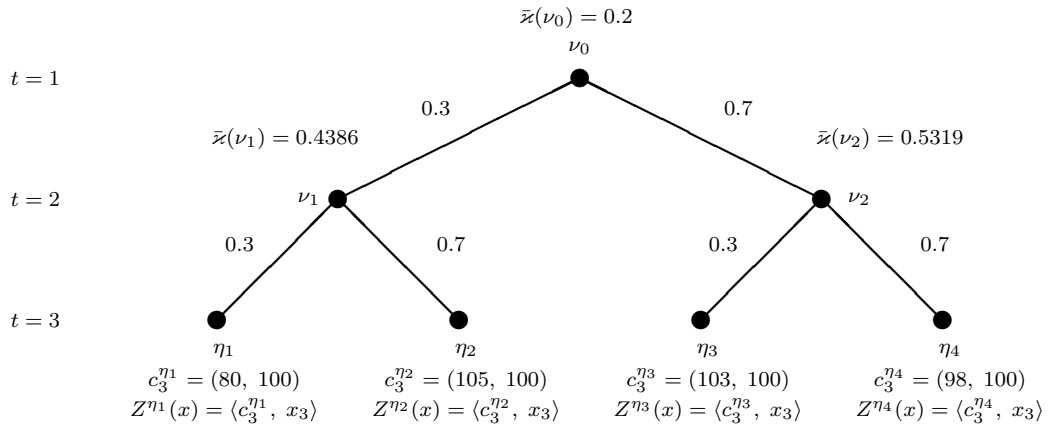

Figure 4.1: Universal time-consistent upper bounds.

At the beginning of Algorithm 2 we set $\epsilon = 0.001$ and initialize $\bar{\varkappa}(\nu_0) = \bar{\varkappa}(\nu_1) = \bar{\varkappa}(\nu_2) = 0$. Now, we need to examine all possible subsets $N_+ \subseteq \Omega_T$.

Let us begin with $N_+ = \{\eta_1, \eta_2, \eta_3, \eta_4\}$. We need to check for a feasible solution to the following system of equations:

$$
\begin{aligned}
X &= \left\{ \begin{array}{l} x \in I \cap F, \\ Z^{\nu}(x) \geq \sum_{\eta \in \Omega_T} p_{\eta} Z^{\eta}(x),\ \nu \in N_+, \\ Z^{\nu}(x) + \epsilon \leq \sum_{\eta \in \Omega_T} p_{\eta} Z^{\eta}(x),\ \nu \in \Omega_T \setminus N_+ \end{array} \right\} \\
&= \left\{ \begin{array}{l} \langle \mathbf{e}, x_3 \rangle = 1, \\ Z^{\nu}(x) \geq \sum_{\eta \in \Omega_T} p_{\eta} Z^{\eta}(x),\ \nu \in \{\eta_1, \eta_2, \eta_3, \eta_4\}, \\ x_3 \geq 0 \\ x_3 \in \mathbb{R}^2 \end{array} \right\} \\
&= \left\{ \begin{array}{l} x_3^1 + x_3^2 = 1, \\ 80x_3^1 + 100x_3^2 \geq 98.9x_3^1 + 100x_3^2, \\ 105x_3^1 + 100x_3^2 \geq 98.9x_3^1 + 100x_3^2, \\ 103x_3^1 + 100x_3^2 \geq 98.9x_3^1 + 100x_3^2, \\ 98x_3^1 + 100x_3^2 \geq 98.9x_3^1 + 100x_3^2, \\ x_3^1, x_3^2 \geq 0 \end{array} \right\}
\end{aligned} \tag{4.6}
$$

Clearly, $x_3^1 = 0, x_3^2 = 1$ is such that $x \in X$. Since $N_+ = \Omega_T$, we know

$$
\begin{aligned}
\lambda^{(1)}(\eta_1) &= \varkappa_{1,3} p_{\eta_1} = 0.045 \\
\lambda^{(1)}(\eta_2) &= \varkappa_{1,3} p_{\eta_2} = 0.105 \\
\lambda^{(1)}(\eta_3) &= \varkappa_{1,3} p_{\eta_3} = 0.105 \\
\lambda^{(1)}(\eta_4) &= \varkappa_{1,3} p_{\eta_4} = 0.245
\end{aligned} \tag{4.7}
$$

Therefore,

$$
\begin{aligned}
\mu^{(1)}(\eta_1) &= p_{\eta_1} + \lambda^{(1)}(\eta_1) - p_{\eta_1} \sum_{\eta \in \Omega_T} \lambda^{(1)}(\eta) \\
&= 0.09 + 0.045 - 0.09(0.045 + 0.105 + 0.105 + 0.245) \\
&= 0.09 + 0.045 - 0.045 \\
&= 0.09
\end{aligned} \tag{4.8}
$$

Further,

$$\begin{aligned}\mu^{(1)}(\eta_2) &= p_{\eta_2} + \lambda^{(1)}(\eta_2) - p_{\eta_2} \sum_{\eta \in \Omega_T} \lambda^{(1)}(\eta) \\ &= 0.21 + 0.105 - 0.21(0.045 + 0.105 + 0.105 + 0.245) \\ &= 0.21 + 0.105 - 0.105 \\ &= 0.21\end{aligned} \tag{4.9}$$

And similarly,

$$\begin{aligned}\mu^{(1)}(\eta_3) &= p_{\eta_3} + \lambda^{(1)}(\eta_3) - p_{\eta_3} \sum_{\eta \in \Omega_T} \lambda^{(1)}(\eta) \\ &= 0.21 + 0.105 - 0.21(0.045 + 0.105 + 0.105 + 0.245) \\ &= 0.21 + 0.105 - 0.105 \\ &= 0.21\end{aligned} \tag{4.10}$$

Finally,

$$\begin{aligned}\mu^{(1)}(\eta_4) &= p_{\eta_4} + \lambda^{(1)}(\eta_4) - p_{\eta_4} \sum_{\eta \in \Omega_T} \lambda^{(1)}(\eta) \\ &= 0.49 + 0.245 - 0.49(0.045 + 0.105 + 0.105 + 0.245) \\ &= 0.49 + 0.245 - 0.245 \\ &= 0.49\end{aligned} \tag{4.11}$$

Thus, when $N_+ = \{\eta_1, \eta_2, \eta_3, \eta_4\}$, the resulting probability measure $\mu^{(1)}$ coincides with the original probability measure p. Similarly to the first iteration of the parametric cutting plane method example in Section 3.4.1, we infer that

$$\mu_2^{(1)}(\nu_1, \eta_1) = 0.3,\ \mu_2^{(1)}(\nu_1, \eta_2) = 0.7 \tag{4.12}$$

Now we can find $\varkappa_{\min}^{(1)}(\nu_1)$ as the optimal value of the following linear programming

problem:

$$\begin{aligned}
\min_{h,\varkappa} \quad & \varkappa \\
\text{s.t.} \quad & h_{\eta_1} - h_{\eta_1} p_{\nu_1\eta_1} - h_{\eta_2} p_{\nu_1\eta_2} = \frac{\mu^{(1)}_{\nu_1\eta_1}}{p_{\nu_1\eta_1}} - 1, \\
& h_{\eta_2} - h_{\eta_1} p_{\nu_1\eta_1} - h_{\eta_2} p_{\nu_1\eta_2} = \frac{\mu^{(1)}_{\nu_1\eta_2}}{p_{\nu_1\eta_2}} - 1, \\
& 0 \le h_{\eta_1} \le \varkappa \\
& 0 \le h_{\eta_2} \le \varkappa
\end{aligned} \tag{4.13}$$

After substitution, we get

$$\begin{aligned}
\min_{h,\varkappa} \quad & \varkappa \\
\text{s.t.} \quad & h_{\eta_1} - 0.3h_{\eta_1} - 0.7h_{\eta_2} = \frac{0.3}{0.3} - 1, \\
& h_{\eta_2} - 0.3h_{\eta_1} - 0.7h_{\eta_2} = \frac{0.7}{0.7} - 1, \\
& 0 \le h_{\eta_1} \le \varkappa \\
& 0 \le h_{\eta_2} \le \varkappa
\end{aligned} \tag{4.14}$$

which implies $\varkappa^{(1)}_{\min}(\nu_1, \mu^{(1)}_2) = 0$. Hence

$$\begin{aligned}
\bar{\varkappa}^{(1)}(\nu_1) &= \max\{\bar{\varkappa}^{(1)}(\nu_1), \varkappa^{(0)}_{\min}(\nu_1, \mu^{(1)}_2)\} \\
&= \max\{0, 0\} \\
&= 0
\end{aligned} \tag{4.15}$$

Similarly, we can show

$$\bar{\varkappa}^{(1)}(\nu_0) = \bar{\varkappa}^{(1)}(\nu_2) = 0$$

Next we can choose another subset $N_+ = \{\eta_1, \eta_2, \eta_3\} \subseteq \Omega_T$. Hence, we are looking for a feasible solution to the following system:

$$
\begin{aligned}
X &= \left\{ \begin{array}{l} x \in I \cap F, \\ Z^{\nu}(x) \geq \sum_{\eta \in \Omega_T} p_{\eta} Z^{\eta}(x),\ \nu \in N_+, \\ Z^{\nu}(x) + \epsilon \leq \sum_{\eta \in \Omega_T} p_{\eta} Z^{\eta}(x),\ \nu \in \Omega_T \setminus N_+ \end{array} \right\} \\
&= \left\{ \begin{array}{l} \langle \mathbf{e}, x_3 \rangle = 1, \\ Z^{\nu}(x) \geq \sum_{\eta \in \Omega_T} p_{\eta} Z^{\eta}(x),\ \nu \in \{\eta_1, \eta_2, \eta_3\}, \\ Z^{\nu}(x) + \epsilon \leq \sum_{\eta \in \Omega_T} p_{\eta} Z^{\eta}(x),\ \nu \in \{\eta_4\}, \\ x_3 \geq 0 \\ x_3 \in \mathbb{R}^2 \end{array} \right\} \\
&= \left\{ \begin{array}{l} x_3^1 + x_3^2 = 1, \\ 80x_3^1 + 100x_3^2 \geq 98.9x_3^1 + 100x_3^2, \\ 105x_3^1 + 100x_3^2 \geq 98.9x_3^1 + 100x_3^2, \\ 103x_3^1 + 100x_3^2 \geq 98.9x_3^1 + 100x_3^2, \\ 98x_3^1 + 100x_3^2 + 0.001 \leq 98.9x_3^1 + 100x_3^2, \\ x_3^1, x_3^2 \geq 0 \end{array} \right\}
\end{aligned} \tag{4.16}
$$

Since the system is infeasible, we know that $X = \emptyset$.

We continue by choosing another subset $N_+ = \{\eta_2, \eta_3\} \subseteq \Omega_T$. In this case we have

$$
\begin{aligned}
X &= \left\{ \begin{array}{l} x \in I \cap F, \\ Z^{\nu}(x) \geq \sum_{\eta \in \Omega_T} p_{\eta} Z^{\eta}(x),\ \nu \in N_+, \\ Z^{\nu}(x) + \epsilon \leq \sum_{\eta \in \Omega_T} p_{\eta} Z^{\eta}(x),\ \nu \in \Omega_T \setminus N_+ \end{array} \right\} \\
&= \left\{ \begin{array}{l} \langle \mathbf{e}, x_3 \rangle = 1, \\ Z^{\nu}(x) \geq \sum_{\eta \in \Omega_T} p_{\eta} Z^{\eta}(x),\ \nu \in \{\eta_2, \eta_3\}, \\ Z^{\nu}(x) + \epsilon \leq \sum_{\eta \in \Omega_T} p_{\eta} Z^{\eta}(x),\ \nu \in \{\eta_1, \eta_4\}, \\ x_3 \geq 0 \\ x_3 \in \mathbb{R}^2 \end{array} \right\} \\
&= \left\{ \begin{array}{l} x_3^1 + x_3^2 = 1, \\ 80x_3^1 + 100x_3^2 + 0.001 \leq 98.9x_3^1 + 100x_3^2, \\ 105x_3^1 + 100x_3^2 \geq 98.9x_3^1 + 100x_3^2, \\ 103x_3^1 + 100x_3^2 \geq 98.9x_3^1 + 100x_3^2, \\ 98x_3^1 + 100x_3^2 + 0.001 \leq 98.9x_3^1 + 100x_3^2, \\ x_3^1, x_3^2 \geq 0 \end{array} \right\}
\end{aligned} \tag{4.17}
$$

We can check that $x_3^1 = 0.0011$ and $x_3^2 = 0.9989$ is a feasible solution. Since $N_+ = \{\eta_2, \eta_3\}$, we consider $\lambda^{(2)}$ such that

$$
\begin{aligned}
\lambda^{(2)}(\eta_1) &= 0 \\
\lambda^{(2)}(\eta_2) &= \varkappa_{1,3} p_{\eta_2} = 0.105 \\
\lambda^{(2)}(\eta_3) &= \varkappa_{1,3} p_{\eta_3} = 0.105 \\
\lambda^{(2)}(\eta_4) &= 0
\end{aligned} \tag{4.18}
$$

Hence,

$$
\begin{aligned}
\mu^{(2)}(\eta_1) &= p_{\eta_1} + \lambda^{(2)}(\eta_1) - p_{\eta_1} \sum_{\eta \in \Omega_T} \lambda^{(2)}(\eta) \\
&= 0.09 + 0 - 0.09(0 + 0.105 + 0.105 + 0) \\
&= 0.0711
\end{aligned} \tag{4.19}
$$

$$\begin{aligned}\mu^{(2)}(\eta_2) &= p_{\eta_2} + \lambda^{(2)}(\eta_2) - p_{\eta_2} \sum_{\eta \in \Omega_T} \lambda^{(2)}(\eta) \\ &= 0.21 + 0.105 - 0.21(0 + 0.105 + 0.105 + 0) \\ &= 0.2709\end{aligned} \tag{4.20}$$

$$\begin{aligned}\mu^{(2)}(\eta_3) &= p_{\eta_3} + \lambda^{(2)}(\eta_3) - p_{\eta_3} \sum_{\eta \in \Omega_T} \lambda^{(2)}(\eta) \\ &= 0.21 + 0.105 - 0.21(0 + 0.105 + 0.105 + 0) \\ &= 0.2709\end{aligned} \tag{4.21}$$

$$\begin{aligned}\mu^{(2)}(\eta_4) &= p_{\eta_4} + \lambda^{(2)}(\eta_4) - p_{\eta_4} \sum_{\eta \in \Omega_T} \lambda^{(2)}(\eta) \\ &= 0.49 + 0 - 0.49(0 + 0.105 + 0.105 + 0) \\ &= 0.3871\end{aligned} \tag{4.22}$$

Notice that the probability measure $\mu^{(2)}$ is the same as the measure $\mu^{(1)}$ in the example in Section 3.4.1, and therefore the resulting $\varkappa^{(2)}_{\min}$ values are also the same. Hence,

$$\begin{aligned}\bar{\varkappa}^{(2)}(\nu_0) &= \max\{\bar{\varkappa}^{(1)}(\nu_0), \varkappa^{(2)}_{\min}(\nu_0, \mu^{(2)}_1)\} = \max\{0, 0.2\} = 0.2 \\ \bar{\varkappa}^{(2)}(\nu_1) &= \max\{\bar{\varkappa}^{(1)}(\nu_1), \varkappa^{(2)}_{\min}(\nu_1, \mu^{(2)}_2)\} = \max\{0, 0.4386\} = 0.4386 \\ \bar{\varkappa}^{(2)}(\nu_2) &= \max\{\bar{\varkappa}^{(1)}(\nu_2), \varkappa^{(2)}_{\min}(\nu_2, \mu^{(2)}_2)\} = \max\{0, 0.5319\} = 0.5319\end{aligned}$$

All remaining subsets $N_+ \subseteq \Omega_T$ generate infeasible linear systems and no additional updates would be performed. Hence, if we set $\bar{\varkappa}(\nu_i) = \bar{\varkappa}^{(2)}(\nu_i),\ i = 0, 1, 2$, then the function $\rho_1(\rho_2(Z(x)))$ would be an upper bound to $\rho_{1,3}(Z(x))$ for any policy $x \in I \cap F$.

4.2 Universal Parametric Time-Consistent Upper Bounds by Policy Enumeration

Algorithm 2 would be appropriate when the size of the scenario tree is relatively small. In this section we propose an alternative method which could be applied to instances with large Ω_T. We assume that $I \cap F$ is a bounded polyhedral set having the following representation:

$$I \cap F = \{x \in \mathbb{R}^n : Ax = b,\ x \geq 0\},$$

where $A \in \mathbb{R}^{r\times n}$ has r linearly independent rows. Moreover, we also assume that the row space of A does not include the span of $\{\mathbf{e}_j^T : j \in J\}$ for any $J \subseteq \{1,\dots,n\}$, $|J| \geq 1$, i.e. none of the entries of x are fixed for $x \in I \cap F$. Further, we also consider the matrix $L \in \mathbb{R}^{|\Omega_T|\times n}$ of mean-adjusted losses (or costs). The row L_ν corresponding to $\nu \in \Omega_T$ is defined as,

$$L_\nu = \Big(c_1^\nu - \sum_{\eta\in\Omega_T} p_\eta c_1^\eta, c_2^\nu - \sum_{\eta\in\Omega_T} p_\eta c_2^\eta, \dots, c_T^\nu - \sum_{\eta\in\Omega_T} p_\eta c_T^\eta\Big),$$

where c_t^ν is the $\mathcal{F}_t$-measurable vector of random costs corresponding to $\nu \in \Omega_T$. Before we delve into further details, we introduce the following regularity assumption.

A1 *Linear independence:*

If $\nu_1, \nu_2, \dots, \nu_s \in \Omega_T$ and $j_1, j_2, \dots, j_t \in \{1, 2, \dots, n\}$ are such that $s + t = n - r$, then

$$\operatorname{rank}\left(\begin{bmatrix} L_{\nu_1}^T & \cdots & L_{\nu_s}^T & \mathbf{e}_{j_1} & \cdots & \mathbf{e}_{j_t} & A^T \end{bmatrix}\right) = n$$

Notice that the regularity assumption would hold almost certainly if the entries of A and L were generated by sampling at random from a continuous distribution.

Theorem 14. *If $\nu \in \Omega_t$ and $\bar{\varkappa}(\nu)$ is generated by Algorithm 3 using matrices A and L that satisfy the regularity assumption, then*

$$\bar{\varkappa}(\nu) = \max_{x\in I\cap F} \varkappa_{\min}(\nu, \mu_t^x). \tag{4.24}$$

Proof. First, we show that if $x \in I \cap F$, then $\mu^x = \mu^{(k)}$ for some $k \in \mathbb{N}$.
Let $x \in I \cap F$, and denote $N_+^x = \{\nu \in \Omega_T : \lambda^x(\nu) = \varkappa_{1,T} p_\nu\}$. Then, x is a feasible solution to the following linear system

$$\begin{aligned} &L_\nu x \geq 0, \quad \nu \in N_+^x, \\ &L_\nu x \leq 0, \quad \nu \in \Omega_T \setminus N_+^x, \\ &Ax = b, \\ &x \geq 0. \end{aligned} \tag{4.25}$$

By the theory of linear programming, we know that since $I \cap F$ is a polytope there must also exist a basic feasible solution $y \in \mathbb{R}^n$, with at least $n - r$ of the inequalities in the

Algorithm 3 Method for Time-Consistent Upper Bounds Using Policy Enumeration

for all $t = 1, \dots, T-1$ **do**
  for all $\nu \in \Omega_t$ **do**
    $\bar{\varkappa}^{(0)}(\nu) \leftarrow 0$
  end for
end for
$k \leftarrow 1$
for all $\{\nu_1, \dots, \nu_s\} \subseteq \Omega_T$ and $\{j_1, \dots, j_t\} \subseteq \{1, \dots, n\}$ such that $s + t = n - r$ **do**
  Let $y \in \mathbb{R}^n$ be the solution to the following linear system

$$\begin{aligned} L_{\nu_i} y &= 0, \quad i = 1, \dots, s, \\ \mathbf{e}_{j_i}^T y &= 0, \quad i = 1, \dots, t, \\ Ay &= b. \end{aligned} \tag{4.23}$$

  if $y \geq 0$ **then**
    for all $\nu \in \Omega_T$ **do**
      $\lambda^y(\nu) \leftarrow \begin{cases} \varkappa_{1,T} p_\nu & \text{if } Z^\nu(y) \geq \sum_{\eta \in \Omega_T} p_\eta Z^\eta(y) \\ 0 & \text{otherwise} \end{cases}$
    end for
    for all $N_+ \subseteq \{\nu_1, \dots, \nu_s\}$ **do**
      for all $\nu \in \Omega_T$ **do**
        $\lambda^{(k)}(\nu) \leftarrow \begin{cases} \varkappa_{1,T} p_\nu & \text{if } \nu \in N_+ \\ 0 & \text{if } \nu \in \{\nu_1, \dots, \nu_s\} \setminus N_+ \\ \lambda^y(\nu) & \text{otherwise} \end{cases}$
      end for
      if $\exists x \in I \cap F : \lambda^x(\nu) = \lambda^{(k)}(\nu),\ \forall \nu \in \Omega_T$ **then**
        for all $\nu \in \Omega_T$ **do**
          $\mu^{(k)}(\nu) \leftarrow p_\nu + \lambda^{(k)}(\nu) - p_\nu \sum_{\eta \in \Omega_T} \lambda^{(k)}(\eta)$
        end for
        for all $t = T-1, \dots, 1$ **do**
          for all $\nu \in \Omega_t$ **do**
            $w_t(\nu) \leftarrow \| w_{t+1}^{C(\nu)} \|_1$
            if $w_t(\nu) > 0$ **then**
              $\mu_t^{(k)}(\nu) \leftarrow \frac{1}{w_t(\nu)} w_{t+1}^{C(\nu)}$
              $\bar{\varkappa}(\nu) \leftarrow \max\left(\bar{\varkappa}(\nu), \varkappa_{\min}(\nu, \mu_t^{(k)})\right)$
            end if
          end for
        end for
        $k \leftarrow k + 1$
      end if
    end for
  end if
end for

above system holding with equality. Let $N_0 = \{\nu : \langle L_\nu, y\rangle = 0\}$. Then $\langle L_\nu, y\rangle > 0$ for $\nu \in N_+^x$, $\nu \notin N_0$. Similarly, $\langle L_\nu, y\rangle < 0$ for $\nu \in N_-^x$, $\nu \notin N_0$. Hence, $\lambda^y(\nu) = \lambda^x(\nu)$ for all $\nu \notin N_0$. Further, N_0 can be partitioned into sets $N_+ = \{\nu \in N_0 : \lambda^x(\nu) = \varkappa_{1,T} p_\nu\}$ and $N_- = \{\nu \in N_0 : \lambda^x(\nu) = 0\}$. Since Algorithm 3 examines all basic feasible solutions, as well as all possible subsets N_+ and N_-, we know that there exists $k \in \mathbb{N}$ such that $\lambda^x = \lambda^{(k)}$, which implies $\mu^x = \mu^{(k)}$.

Therefore,

$$\bar{\varkappa}(\nu) \geq \max_{x \in I \cap F} \varkappa_{\min}(\nu, \mu_t^x).$$

Furthermore, the conditional statement at line 17 implies that for any $\mu^{(k)}$, there exists a point $x \in I \cap F$ such that $\mu^x = \mu^{(k)}$. Therefore,

$$\bar{\varkappa}(\nu) \leq \max_{x \in I \cap F} \varkappa_{\min}(\nu, \mu_t^x),$$

which completes the proof. □

The algorithm for policy enumeration can be extended to handle the case when the regularity assumption is not satisfied. However, such analysis would involve combinatorial problems that are beyond the scope of this work. In practice, one can ensure almost certain regularity by small random perturbations of L and A. The version presented above entails the solution of only $O\left(\binom{|\Omega_T| + n}{n - r}\right)$ systems of linear equations of size $n \times n$. When $n >> m$, it is preferable to the straightforward feasibility approach which involves the solution of $O(2^{|\Omega_T|})$ systems of linear inequalities.

Finally, for the root node $\nu = 1$ we can show that $\bar{\varkappa}(1) \leq \varkappa_{1,T}$.

Lemma 15. *If* $\varkappa_{1,T} \in [0, 1]$ *and* $\bar{\varkappa}(1) \in \mathbb{R}$ *is such that* $\bar{\varkappa}(1) = \max_{x \in I \cap F} \varkappa_{\min}(1, \mu_1^x)$, *then* $\bar{\varkappa}(1) \leq \varkappa_{1,T}$.

Proof. For any $x \in I \cap F$, $\mu_1^x \in \mathcal{D}_{1,T}$, which implies $\varkappa_{\min}(1, \mu_1^x) \leq \varkappa_{1,T}$. Therefore, $\bar{\varkappa}(1) \leq \varkappa_{1,T}$. □

4.2.1 An Example of Constructing Universal Time-Consistent Upper Bounds by Policy Enumeration

In this section we demonstrate how we can construct universal time-consistent upper bounds using Algorithm 3. We consider a mean-upper semideviation risk measure $\rho_{1,3}(Z(x))$ with $\varkappa_{1,3} = 0.5$, and two random variables observed at the final time period $T = 3$. We would like to create a time-consistent function $\rho_1(\rho_2(Z(x)))$ which would provide an upper bound to $\rho_{1,3}(Z(x))$ for any policy $x \in I \cap F$. In order to be consistent with Section 4.1.1 we set $I \cap F = \{x_3 \in \mathbb{R}^2 : \ \langle \mathbf{e}^T, x_3 \rangle = 1, \ x \geq 0\}$, and

$$\begin{aligned} c_3^{\eta_1} &= (80, \ 100) \\ c_3^{\eta_2} &= (105, \ 100) \\ c_3^{\eta_3} &= (103, \ 100) \\ c_3^{\eta_4} &= (98, \ 100) \end{aligned}$$

Thus we can compute the mean-adjusted costs $L_\nu, \ \nu \in \Omega_T$ to be

$$\begin{aligned} L_{\eta_1}(x) &= (-18.6, 0) \\ L_{\eta_2}(x) &= (6.4, 0) \\ L_{\eta_3}(x) &= (4.4, 0) \\ L_{\eta_4}(x) &= (-0.6, 0) \end{aligned}$$

This is illustrated in Figure 4.2. Before we can apply Algorithm 3, we need to make sure that the regularity condition is satisfied. Since

$$A^T = \begin{bmatrix} 1 \\ 1 \end{bmatrix}$$

we know that

$$\operatorname{rank}\left(\begin{bmatrix} L_\nu^T & A^T \end{bmatrix}\right) = 2, \ \nu \in \Omega_3$$

and

$$\operatorname{rank}\left(\begin{bmatrix} \mathbf{e}_j & A^T \end{bmatrix}\right) = 2, \ j \in \{1, 2\}$$

Hence we know that condition (A1) holds.

Therefore we can apply Algorithm 3 to the given instance. We initialize $\bar{\varkappa}(\nu_0) = \bar{\varkappa}(\nu_1) = \bar{\varkappa}(\nu_2) = 0$ and set $k = 1$. Now, suppose that the first linear system we consider

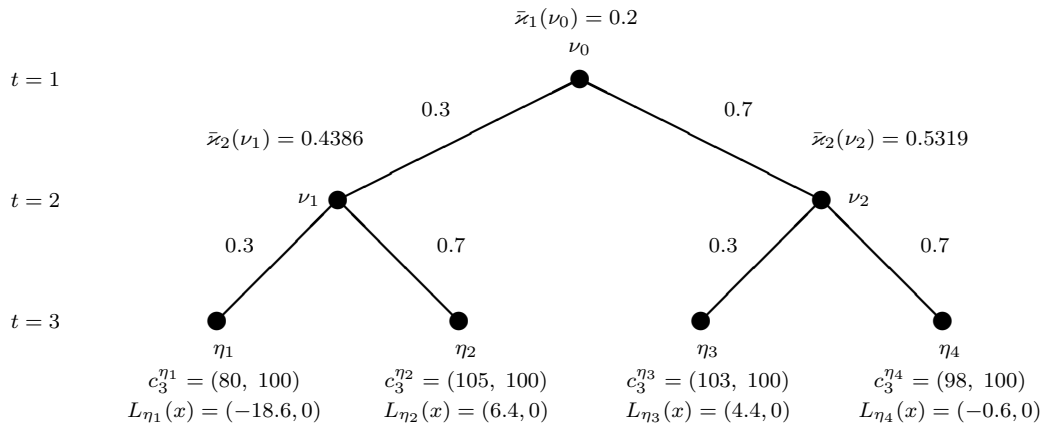

Figure 4.2: Universal time-consistent upper bounds with policy enumeration.

is

$$\begin{aligned} L_{\nu_1} y &= 0 \\ Ay &= b \end{aligned} \tag{4.26}$$

After substitution we get,

$$\begin{bmatrix} -18.6 & 0 \\ 1 & 1 \end{bmatrix} y = \begin{bmatrix} 0 \\ 1 \end{bmatrix} \tag{4.27}$$

which implies

$$y = \begin{bmatrix} 0 \\ 1 \end{bmatrix} \tag{4.28}$$

Since $y \geq 0$, we know that $y \in I \cap F$. Furthermore,

$$Z^{\eta_1}(y) = \begin{bmatrix} 80 & 100 \end{bmatrix} \begin{bmatrix} 0 \\ 1 \end{bmatrix} = 100 \tag{4.29}$$

Similarly,

$$Z^{\eta_2}(y) = Z^{\eta_3}(y) = Z^{\eta_4}(y) = 100$$

Finally, $Z^{\nu}(y) \geq \sum_{\eta \in \Omega_T} p_\eta Z^{\eta}(y),\ \nu \in \Omega_T$ implies that

$$\begin{aligned} \lambda^y(\eta_1) &= \varkappa_{1,3} p_{\eta_1} = 0.045 \\ \lambda^y(\eta_2) &= \varkappa_{1,3} p_{\eta_2} = 0.105 \\ \lambda^y(\eta_3) &= \varkappa_{1,3} p_{\eta_3} = 0.105 \\ \lambda^y(\eta_4) &= \varkappa_{1,3} p_{\eta_4} = 0.245 \end{aligned} \tag{4.30}$$

Next, let us choose $N_+ = \{\eta_1\}$. Then $\lambda^{(1)} = \lambda^y$, and therefore $\lambda^{(1)}$ satisfies the conditional statement at line 17. Notice that we encountered the same $\lambda^{(1)}$ in Section 4.1.1. Its corresponding $\mu^{(1)}$ is given by

$$\begin{aligned} \mu^{(1)}(\eta_1) &= 0.09 \\ \mu^{(1)}(\eta_2) &= 0.21 \\ \mu^{(1)}(\eta_3) &= 0.21 \\ \mu^{(1)}(\eta_4) &= 0.49 \end{aligned} \tag{4.31}$$

It implies

$$\varkappa^{(1)}_{\min}(\nu_0, \mu^{(1)}_1) = \varkappa^{(1)}_{\min}(\nu_1, \mu^{(1)}_2) = \varkappa^{(1)}_{\min}(\nu_2, \mu^{(1)}_2) = 0$$

Hence,

$$\bar{\varkappa}^{(1)}(\nu_0) = \bar{\varkappa}^{(1)}(\nu_1) = \bar{\varkappa}^{(1)}(\nu_2) = 0$$

Next we try $N_+ = \emptyset$. It results in the following $\lambda^{(2)}$:

$$\begin{aligned} \lambda^{(2)}(\eta_1) &= \varkappa_{1,3} p_{\eta_1} = 0 \\ \lambda^{(2)}(\eta_2) &= \varkappa_{1,3} p_{\eta_2} = 0.105 \\ \lambda^{(2)}(\eta_3) &= \varkappa_{1,3} p_{\eta_3} = 0.105 \\ \lambda^{(2)}(\eta_4) &= \varkappa_{1,3} p_{\eta_4} = 0.245 \end{aligned} \tag{4.32}$$

However, it turns out that this choice of $\lambda^{(2)}$ is not feasible since there does not exist $x \in I \cap F$ such that

$$\begin{aligned} Z^{\eta_1}(x) &< \textstyle\sum_{\eta \in \Omega_T} p_\eta Z^\eta(x) \\ Z^{\eta_2}(x) &\geq \textstyle\sum_{\eta \in \Omega_T} p_\eta Z^\eta(x) \\ Z^{\eta_3}(x) &\geq \textstyle\sum_{\eta \in \Omega_T} p_\eta Z^\eta(x) \\ Z^{\eta_4}(x) &\geq \textstyle\sum_{\eta \in \Omega_T} p_\eta Z^\eta(x) \end{aligned} \tag{4.33}$$

Indeed, we can verify that the system,

$$\begin{aligned} &80x^1_3 + 100x^2_3 < 98.9x^1_3 + 100x^2_3 \\ &105x^1_3 + 100x^2_3 \geq 98.9x^1_3 + 100x^2_3 \\ &103x^1_3 + 100x^2_3 \geq 98.9x^1_3 + 100x^2_3 \\ &98x^1_3 + 100x^2_3 \geq 98.9x^1_3 + 100x^2_3 \\ &x^1_3 + x^2_3 = 1 \\ &x^1_3, x^2_3 \geq 0 \end{aligned} \tag{4.34}$$

is infeasible. Thus, we need to revise our choice of $\lambda^{(2)}$. Since we have exhausted all possible choices of the subsets N_+ for the current y, we need to consider a new system of linear equations. Let us consider

$$\begin{aligned} \mathbf{e}_2^T y &= 0 \\ Ay &= b \end{aligned} \tag{4.35}$$

which implies,

$$\begin{bmatrix} 0 & 1 \\ 1 & 1 \end{bmatrix} y = \begin{bmatrix} 0 \\ 1 \end{bmatrix} \tag{4.36}$$

Hence,

$$y = \begin{bmatrix} 1 \\ 0 \end{bmatrix} \tag{4.37}$$

Clearly $y \geq 0$ and $y \in I \cap F$. We can compute the costs corresponding to the policy y for each scenario as,

$$Z^{\eta_1}(y) = \begin{bmatrix} 80 & 100 \end{bmatrix} \begin{bmatrix} 1 \\ 0 \end{bmatrix} = 80 \tag{4.38}$$

$$Z^{\eta_2}(y) = \begin{bmatrix} 105 & 100 \end{bmatrix} \begin{bmatrix} 1 \\ 0 \end{bmatrix} = 105 \tag{4.39}$$

$$Z^{\eta_3}(y) = \begin{bmatrix} 103 & 100 \end{bmatrix} \begin{bmatrix} 1 \\ 0 \end{bmatrix} = 103 \tag{4.40}$$

$$Z^{\eta_1}(y) = \begin{bmatrix} 98 & 100 \end{bmatrix} \begin{bmatrix} 1 \\ 0 \end{bmatrix} = 98 \tag{4.41}$$

Thus,

$$\begin{aligned} \sum_{\eta \in \Omega_T} p_\eta Z^\eta(y) &= 0.09 \cdot 80 + 0.21 \cdot 105 + 0.21 \cdot 103 + 0.49 \cdot 98 \\ &= 98.6 \end{aligned} \tag{4.42}$$

Hence,

$$\begin{aligned}\lambda^y(\eta_1) &= 0\\ \lambda^y(\eta_2) &= \varkappa_{1,3}p_{\eta_2} = 0.105\\ \lambda^y(\eta_3) &= \varkappa_{1,3}p_{\eta_3} = 0.105\\ \lambda^y(\eta_4) &= 0\end{aligned} \tag{4.43}$$

In this case, our only possible choice is $N_+ = \emptyset$. Thus we try $\lambda^{(2)} = \lambda^y$, which satisfies the conditional statement at line 17. As we have seen in previous examples, the corresponding $\mu^{(2)}$ is given by

$$\begin{aligned}\mu^{(2)}(\eta_1) &= 0.0711\\ \mu^{(2)}(\eta_2) &= 0.2709\\ \mu^{(2)}(\eta_3) &= 0.2709\\ \mu^{(2)}(\eta_4) &= 0.3871\end{aligned} \tag{4.44}$$

and it leads to the following $\bar{\varkappa}^{(2)}$ values:

$$\begin{aligned}\bar{\varkappa}^{(2)}(\nu_0) &= \max\{\bar{\varkappa}^{(1)}(\nu_0), \varkappa^{(2)}_{\min}(\nu_0, \mu^{(2)}_1)\} = \max\{0, 0.2\} = 0.2\\ \bar{\varkappa}^{(2)}(\nu_1) &= \max\{\bar{\varkappa}^{(1)}(\nu_1), \varkappa^{(2)}_{\min}(\nu_1, \mu^{(2)}_2)\} = \max\{0, 0.4386\} = 0.4386\\ \bar{\varkappa}^{(2)}(\nu_2) &= \max\{\bar{\varkappa}^{(1)}(\nu_2), \varkappa^{(2)}_{\min}(\nu_2, \mu^{(2)}_2)\} = \max\{0, 0.5319\} = 0.5319\end{aligned}$$

Since there are no additional sets N_+ for the current policy y, we need to continue by choosing another linear system. It turns out, that all of the remaining linear systems result in $\lambda^{(k)}$ identical to $\lambda^{(1)}$. Thus we know that if we set $\bar{\varkappa}(\nu_i) = \bar{\varkappa}^{(2)}(\nu_i),\ i = 0, 1, 2,$ then we would construct a universal upper bounding function $\rho_1(\rho_2(Z(x)))$ to the overall risk measure $\rho_{1,3}(Z(x))$ for an arbitrary policy $x \in I \cap F$.

Chapter 5

Numerical Illustration

In this chapter we present numerical experiments of the proposed methods for examples with the mean-semideviation risk measure applied to the total cost. The measure is not time-consistent. We consider the case when $T = 3$ and the number of children at the root node is finite. Moreover, in our scenario trees every node $\nu \in \Omega_2$ has the same number of children nodes $|C(\nu)|$.

The experiments were performed on a workstation equipped with two quadcore Intel Xeon E5520 @ 2.27GHz processors with hyperthreading enabled. We used IBM ILOG CPLEX 12.2 for the solution of linear programming problems. The workload was distributed by the MATLAB Parallel Computing Toolbox over 12 workers.

5.1 An Example with Two Assets

In this section we consider the scenario tree for two assets that we studied in Section 4.1.1 and Section 4.2.1. Our setup is illustrated in Figure 5.1. We apply the methods developed in Chapter 3 and Chapter 4 to construct time-consistent approximations to the mean-upper semideviation function $\rho_{1,3}(Z(x))$ for a range of risk-aversion parameters $\varkappa_{1,3} = \{0, 0.1, 0.2, 0.3, 0.4, 0.5\}$. We assume that the set of implementable and feasible policies is given by $I \cap F = \{x_3 \in \mathbb{R}^2 : \ \langle \mathbf{e}^T, x_3 \rangle = 1, \ x \geq 0\}$.

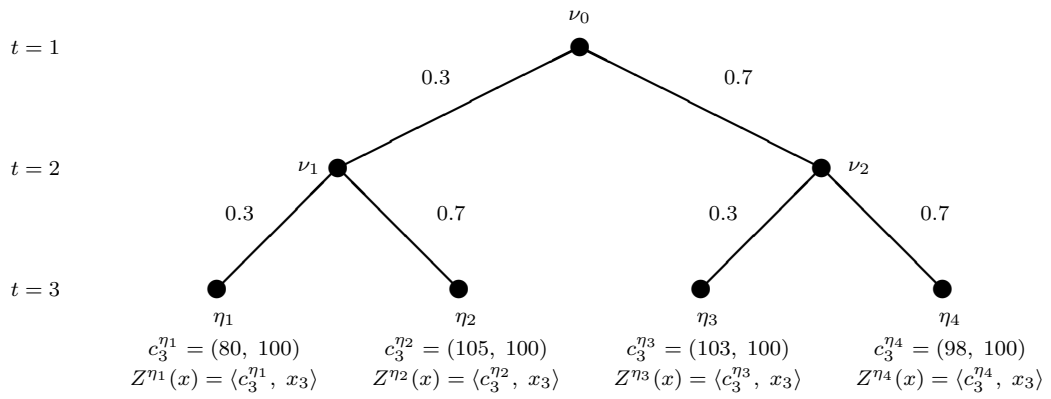

Figure 5.1: Two-stage scenario tree with two assets.

Both the non-parametric and the parametric time-consistent cutting plane methods converge after just two iterations for all values of $\varkappa_{1,3}$. Initially, both methods start with the original probability measure of the scenario tree shown in Figure 5.1 before generating the probability measures $\mu^{(1)}$ shown in Table 5.1.

$\mu^{(1)}$ \ $\varkappa_{1,3}$	0	0.1	0.2	0.3	0.4	0.5
$\mu_{\eta_1}^{(1)}$	0.0900	0.0862	0.0824	0.0787	0.0749	0.0711
$\mu_{\eta_2}^{(1)}$	0.2100	0.2222	0.2344	0.2465	0.2587	0.2709
$\mu_{\eta_3}^{(1)}$	0.2100	0.2222	0.2344	0.2465	0.2587	0.2709
$\mu_{\eta_4}^{(1)}$	0.4900	0.4694	0.4488	0.4283	0.4077	0.3871

Table 5.1: Probability measures computed in the first iteration of the time-consistent cutting plane method.

In the case of the parametric time-consistent cutting plane method, we also compute the risk-aversion coefficients $\varkappa^{(2)}$.

$\varkappa^{(2)}$ \ $\varkappa_{1,3}$	0	0.1	0.2	0.3	0.4	0.5
$\varkappa^{(2)}(\nu_0)$	0	0.0400	0.0800	0.1200	0.1600	0.2000
$\varkappa^{(2)}(\nu_1)$	0	0.0973	0.1894	0.2768	0.3597	0.4386
$\varkappa^{(2)}(\nu_1)$	0	0.1012	0.2049	0.3112	0.4202	0.5319

Table 5.2: Risk-aversion coefficients computed by the parametric time-consistent cutting plane method.

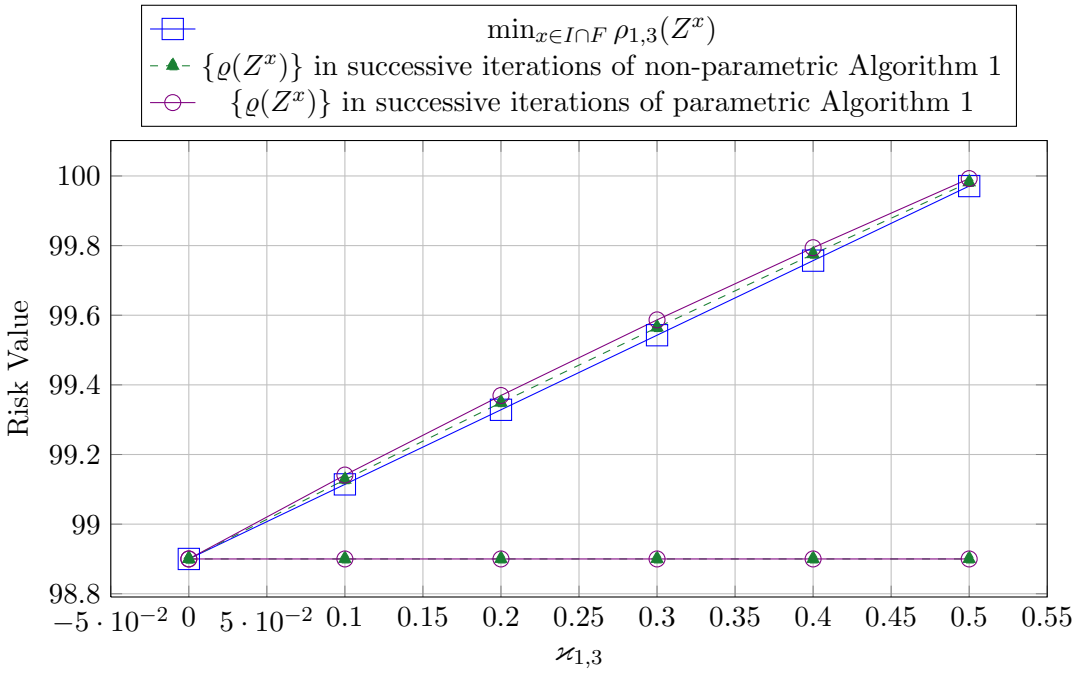

Figure 5.2: Numerical comparison of risk measures for $|x| = 2$ on a 2×2 scenario tree.

In general, the parametric time-consistent cutting plane method generates risk-aversion coefficients that are lower bounds to the coefficients generated by the universal upper bounding methods of Chapter 4. However, in this example the lower bound is tight, and the parameters of Table 5.1 coincide with the coefficents that we find with Algorithm 2 and Algorithm 3. For instances where this is not the case, please see the next section.

5.2 Randomly Generated Scenario Trees

Since the predictable translation equivariance axiom implies that all costs can be considered as final stage costs, we set $n_1 = n_2 = 0$, and hence $n_3 = n$. Furthermore, each entry of the cost vectors c_3^ν is generated by sampling uniformly at random on $[0, 100]$. In addition, the probability p_ν of occurence of scenario $\nu \in \Omega_3$ is drawn from the uniform $[0, 1]$ distribution and normalized so that $\sum_{\nu \in \Omega_T} p_\nu = 1$. Finally, we assume that the set of implementable and feasible policies is given by $I \cap F = \{x_3 \in \mathbb{R}^2 : \ \langle \mathbf{e}^T, x_3 \rangle = 1, \ x \geq 0\}$.

5.2.1 3×3 Scenario Tree with Ten Assets

In this section we consider a 3×3 scenario tree that was generated as described above. Our setup is illustrated in Figure 5.3. We apply the methods developed in Chapter 3 and Chapter 4 to construct time-consistent approximations to the mean-upper semideviation function $\rho_{1,3}(Z(x))$ for a range of risk-aversion parameters $\varkappa_{1,3}$.

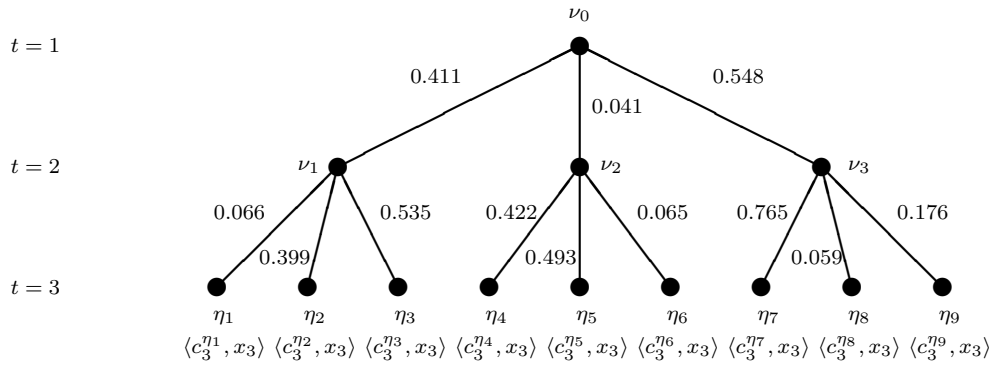

Figure 5.3: 3×3 scenario tree.

The instance that we examine consists of ten assets which result in different costs under each final stage scenario. The input data is given in Table 5.3.

$c_3^{\eta_1}$	$(59.415, 75.057, 80.896, 70.125, 32.670, 56.424, 64.541, 97.807, 61.303, 18.637)$
$c_3^{\eta_2}$	$(89.619, 90.638, 30.165, 90.592, 84.804, 27.235, 51.801, 48.627, 29.368, 34.447)$
$c_3^{\eta_3}$	$(27.885, 59.164, 96.904, 94.730, 12.188, 49.477, 31.332, 74.068, 88.708, 57.113)$
$c_3^{\eta_4}$	$(99.227, 96.227, 52.420, 91.846, 68.652, 82.635, 79.565, 57.115, 51.067, 41.332)$
$c_3^{\eta_5}$	$(20.801, 94.174, 23.668, 63.814, 37.475, 48.364, 53.672, 35.198, 98.098, 74.180)$
$c_3^{\eta_6}$	$(13.446, 83.016, 1.939, 24.154, 43.534, 58.147, 81.142, 81.629, 45.673, 53.794)$
$c_3^{\eta_7}$	$(16.150, 13.742, 58.555, 39.780, 88.429, 60.803, 25.508, 95.885, 37.916, 31.679)$
$c_3^{\eta_8}$	$(33.865, 68.479, 37.693, 96.237, 33.178, 18.713, 18.275, 41.719, 65.393, 28.677)$
$c_3^{\eta_9}$	$(77.712, 34.352, 18.048, 67.280, 30.746, 15.453, 48.824, 72.275, 74.429, 75.928)$

Table 5.3: Cost vectors for every final stage tree node.

Initially, the non-parametric time-consistent cutting plane method starts with the probability measure of the scenario tree of Figure 5.3. It converges in four iterations for all values of $\varkappa_{1,3}$ after examining the probability measures shown in Table 5.4.

$\mu^{(k)}$ \ $\varkappa_{1,3}$	0	0.1	0.2	0.3	0.4	0.5	0.6
$\mu^{(1)}_{\eta_1}$	0.0271	0.0288	0.0305	0.0323	0.0340	0.0357	0.0375
$\mu^{(1)}_{\eta_2}$	0.1640	0.1745	0.1850	0.1955	0.2060	0.2165	0.2271
$\mu^{(1)}_{\eta_3}$	0.2201	0.2122	0.2043	0.1964	0.1885	0.1806	0.1727
$\mu^{(1)}_{\eta_4}$	0.0185	0.0197	0.0209	0.0220	0.0232	0.0244	0.0256
$\mu^{(1)}_{\eta_5}$	0.0206	0.0219	0.0233	0.0246	0.0259	0.0272	0.0285
$\mu^{(1)}_{\eta_6}$	0.0027	0.0026	0.0025	0.0024	0.0023	0.0022	0.0021
$\mu^{(1)}_{\eta_7}$	0.4183	0.4033	0.3883	0.3733	0.3583	0.3432	0.3282
$\mu^{(1)}_{\eta_8}$	0.0322	0.0343	0.0364	0.0384	0.0405	0.0426	0.0446
$\mu^{(1)}_{\eta_9}$	0.0965	0.1027	0.1089	0.1151	0.1213	0.1275	0.1336
$\mu^{(2)}_{\eta_1}$	0.0271	0.0259	0.0247	0.0235	0.0224	0.0212	0.0200
$\mu^{(2)}_{\eta_2}$	0.1640	0.1732	0.1825	0.1918	0.2011	0.2103	0.2196
$\mu^{(2)}_{\eta_3}$	0.2201	0.2325	0.2449	0.2574	0.2698	0.2822	0.2947
$\mu^{(2)}_{\eta_4}$	0.0185	0.0195	0.0206	0.0216	0.0227	0.0237	0.0248
$\mu^{(2)}_{\eta_5}$	0.0206	0.0197	0.0188	0.0179	0.0170	0.0161	0.0152
$\mu^{(2)}_{\eta_6}$	0.0027	0.0026	0.0025	0.0024	0.0023	0.0021	0.0020
$\mu^{(2)}_{\eta_7}$	0.4183	0.4001	0.3819	0.3638	0.3456	0.3274	0.3092
$\mu^{(2)}_{\eta_8}$	0.0322	0.0341	0.0359	0.0377	0.0395	0.0414	0.0432
$\mu^{(2)}_{\eta_9}$	0.0965	0.0923	0.0881	0.0839	0.0797	0.0755	0.0713
$\mu^{(3)}_{\eta_1}$	0.0271	0.0288	0.0305	0.0323	0.0340	0.0226	0.0217
$\mu^{(3)}_{\eta_2}$	0.1640	0.1745	0.1850	0.1955	0.2060	0.2188	0.2297
$\mu^{(3)}_{\eta_3}$	0.2201	0.2122	0.2043	0.1964	0.1885	0.1835	0.1762
$\mu^{(3)}_{\eta_4}$	0.0185	0.0197	0.0209	0.0220	0.0232	0.0247	0.0259
$\mu^{(3)}_{\eta_5}$	0.0206	0.0219	0.0233	0.0246	0.0259	0.0275	0.0289
$\mu^{(3)}_{\eta_6}$	0.0027	0.0026	0.0025	0.0024	0.0023	0.0023	0.0022
$\mu^{(3)}_{\eta_7}$	0.4183	0.4033	0.3883	0.3733	0.3583	0.3489	0.3350
$\mu^{(3)}_{\eta_8}$	0.0322	0.0343	0.0364	0.0384	0.0405	0.0430	0.0452
$\mu^{(3)}_{\eta_9}$	0.0965	0.1027	0.1089	0.1151	0.1213	0.1288	0.1352

Table 5.4: Probability measures computed by the non-parametric time-consistent cutting plane method.

$\mu^{(k)}$ \ $\varkappa_{1,3}$	0	0.1	0.2	0.3	0.4	0.5	0.6
$\mu_{\eta_1}^{(1)}$	0.0271	0.0288	0.0305	0.0323	0.0340	0.0357	0.0375
$\mu_{\eta_2}^{(1)}$	0.1640	0.1745	0.1850	0.1955	0.2060	0.2165	0.2271
$\mu_{\eta_3}^{(1)}$	0.2201	0.2122	0.2043	0.1964	0.1885	0.1806	0.1727
$\mu_{\eta_4}^{(1)}$	0.0185	0.0197	0.0209	0.0220	0.0232	0.0244	0.0256
$\mu_{\eta_5}^{(1)}$	0.0206	0.0219	0.0233	0.0246	0.0259	0.0272	0.0285
$\mu_{\eta_6}^{(1)}$	0.0027	0.0026	0.0025	0.0024	0.0023	0.0022	0.0021
$\mu_{\eta_7}^{(1)}$	0.4183	0.4033	0.3883	0.3733	0.3583	0.3432	0.3282
$\mu_{\eta_8}^{(1)}$	0.0322	0.0343	0.0364	0.0384	0.0405	0.0426	0.0446
$\mu_{\eta_9}^{(1)}$	0.0965	0.1027	0.1089	0.1151	0.1213	0.1275	0.1336
$\mu_{\eta_1}^{(2)}$	0.0271	0.0288	0.0305	0.0323	0.0340	0.0357	0.0217
$\mu_{\eta_2}^{(2)}$	0.1640	0.1745	0.1850	0.1955	0.2060	0.2165	0.2297
$\mu_{\eta_3}^{(2)}$	0.2201	0.2122	0.2043	0.1964	0.1885	0.1806	0.1762
$\mu_{\eta_4}^{(2)}$	0.0185	0.0197	0.0209	0.0220	0.0232	0.0244	0.0259
$\mu_{\eta_5}^{(2)}$	0.0206	0.0219	0.0233	0.0246	0.0259	0.0272	0.0289
$\mu_{\eta_6}^{(2)}$	0.0027	0.0026	0.0025	0.0024	0.0023	0.0022	0.0022
$\mu_{\eta_7}^{(2)}$	0.4183	0.4033	0.3883	0.3733	0.3583	0.3432	0.3350
$\mu_{\eta_8}^{(2)}$	0.0322	0.0343	0.0364	0.0384	0.0405	0.0426	0.0452
$\mu_{\eta_9}^{(2)}$	0.0965	0.1027	0.1089	0.1151	0.1213	0.1275	0.1352
$\mu_{\eta_1}^{(3)}$	0.0271	0.0288	0.0305	0.0323	0.0340	0.0357	0.0181
$\mu_{\eta_2}^{(3)}$	0.1640	0.1745	0.1850	0.1955	0.2060	0.2165	0.2081
$\mu_{\eta_3}^{(3)}$	0.2201	0.2122	0.2043	0.1964	0.1885	0.1806	0.2792
$\mu_{\eta_4}^{(3)}$	0.0185	0.0197	0.0209	0.0220	0.0232	0.0244	0.0235
$\mu_{\eta_5}^{(3)}$	0.0206	0.0219	0.0233	0.0246	0.0259	0.0272	0.0262
$\mu_{\eta_6}^{(3)}$	0.0027	0.0026	0.0025	0.0024	0.0023	0.0022	0.0018
$\mu_{\eta_7}^{(3)}$	0.4183	0.4033	0.3883	0.3733	0.3583	0.3432	0.2798
$\mu_{\eta_8}^{(3)}$	0.0322	0.0343	0.0364	0.0384	0.0405	0.0426	0.0409
$\mu_{\eta_9}^{(3)}$	0.0965	0.1027	0.1089	0.1151	0.1213	0.1275	0.1225

Table 5.5: Probability measures computed by the parametric time-consistent cutting plane method.

The parametric time-consistent cutting plane method also starts with the probability measure shown in Figure 5.3. However, using Table 5.5 we can see that it does not examine the same probability measures as its non-parametric counterpart. Moreover, the parametric time-consistent cutting plane method also involves the computation of the risk-aversion coefficients $\varkappa^{(2)}$ shown in Table 5.6.

$\varkappa^{(k)}$ \ $\varkappa_{1,3}$	0	0.1	0.2	0.3	0.4	0.5	0.6
$\varkappa^{(2)}(\nu_0)$	0	0.0699	0.1399	0.2098	0.2798	0.3497	0.4197
$\varkappa^{(2)}(\nu_1)$	0	0.0990	0.1959	0.2908	0.3838	0.4749	0.5642
$\varkappa^{(2)}(\nu_2)$	0	0.0946	0.1793	0.2558	0.3251	0.3882	0.4459
$\varkappa^{(2)}(\nu_3)$	0	0.1013	0.2051	0.3115	0.4208	0.5329	0.6480
$\varkappa^{(3)}(\nu_0)$	0	0.0699	0.1399	0.2098	0.2798	0.3497	0.4197
$\varkappa^{(3)}(\nu_1)$	0	0.0990	0.1959	0.2908	0.3838	0.4749	0.5768
$\varkappa^{(3)}(\nu_2)$	0	0.0946	0.1793	0.2558	0.3251	0.3882	0.4459
$\varkappa^{(3)}(\nu_3)$	0	0.1013	0.2051	0.3115	0.4208	0.5329	0.6480
$\varkappa^{(4)}(\nu_0)$	0	0.0699	0.1399	0.2098	0.2798	0.3497	0.4197
$\varkappa^{(4)}(\nu_1)$	0	0.0990	0.1959	0.2908	0.3838	0.4749	0.5768
$\varkappa^{(4)}(\nu_2)$	0	0.0946	0.1793	0.2558	0.3251	0.3882	0.4879
$\varkappa^{(4)}(\nu_3)$	0	0.1013	0.2051	0.3115	0.4208	0.5329	0.7407

Table 5.6: Risk-aversion coefficients computed by the parametric time-consistent cutting plane method.

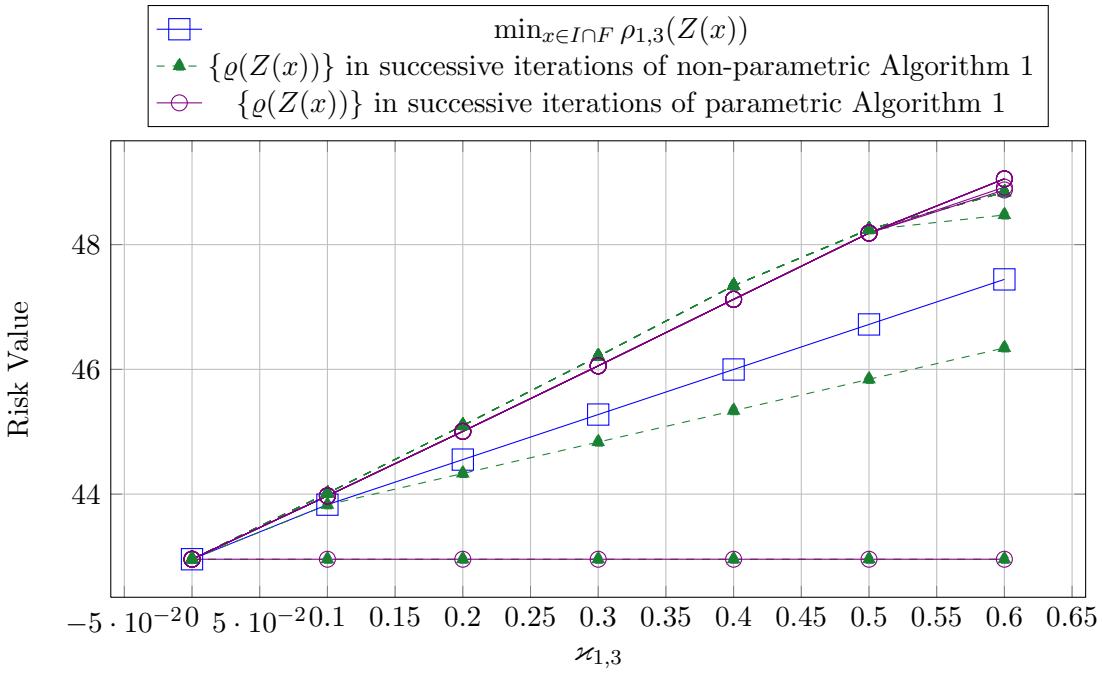

Figure 5.4: Time-consistent cutting plane approximations for $|x| = 10$ on a 3×3 scenario tree.

The risk value corresponding to the second iteration of the non-parametric cutting plane method would always be a lower bound on the risk value encountered in the second iteration of the parametric cutting plane method. This is due to the fact that both methods start with the same probability measure (given by the scenario tree), and the parametric cutting plane method imposes extra conditions on the geometry of the dual set. However, this observation cannot be extended past the second iteration, as can be seen in Figure 5.4.

Additionally, we can also construct universal time-consistent upper bounds. Since the given example has nine final stage scenarios and ten assets Algorithm 2 is preferable to Algorithm 3. The resulting values of the risk-aversion coefficients $\bar{\varkappa}$ are shown in Table 5.7.

$\bar{\varkappa}$ \ $\varkappa_{1,3}$	0	0.1	0.2	0.3	0.4	0.5	0.6
$\bar{\varkappa}(\nu_0)$	0	0.1000	0.2000	0.3000	0.4000	0.5000	0.6000
$\bar{\varkappa}(\nu_1)$	0	0.1056	0.2237	0.3566	0.5073	0.6798	0.8789
$\bar{\varkappa}(\nu_2)$	0	0.1069	0.2295	0.3718	0.5386	0.7371	0.9773
$\bar{\varkappa}(\nu_3)$	0	0.1045	0.2186	0.3440	0.4822	0.6354	0.8062

Table 5.7: Risk-aversion coefficients for the universal time-consistent upper bounds computed by Algorithm 2.

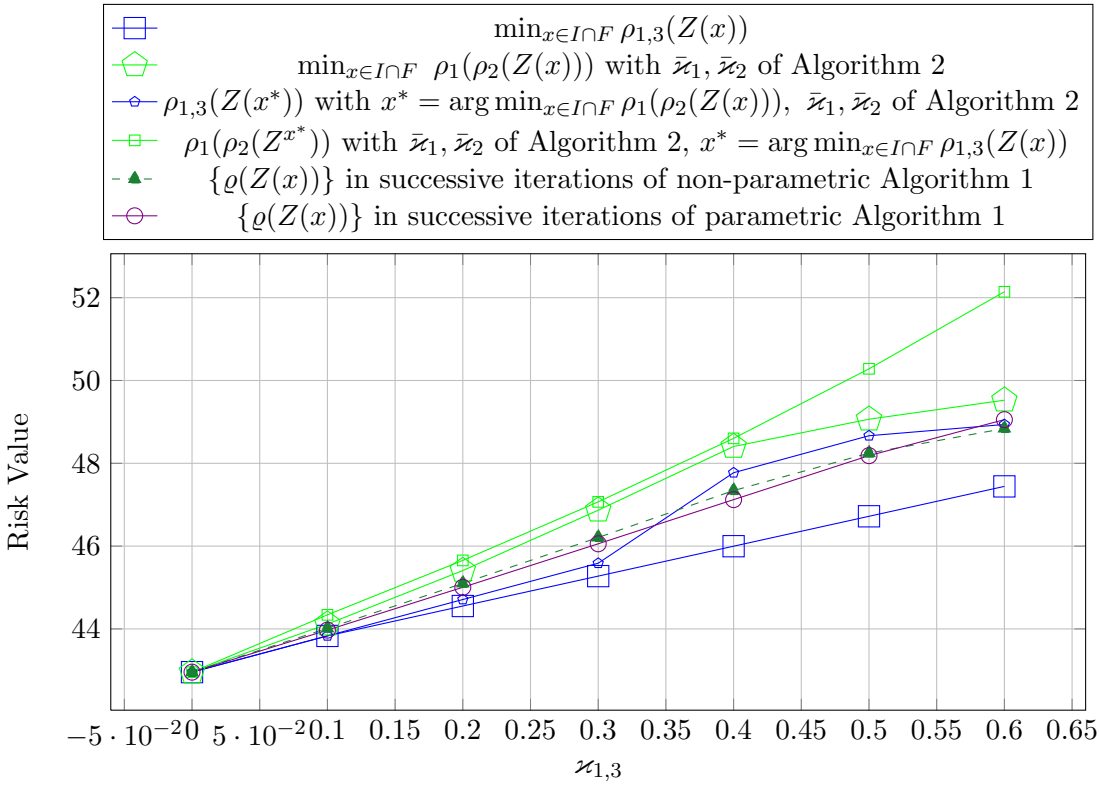

Figure 5.5: Universal time-consistent upper bounds for $|x| = 10$ on a 3×3 scenario tree.

We can see in Figure 5.5 that calculating the original time-inconsistent risk measure $\min\limits_{x\in I\cap F} \rho_{1,3}(Z(x))$ at the optimal solution of the universal time-consistent approximation $\min\limits_{x\in I\cap F} \rho_1(\rho_2(Z(x)))$ results in risk values that are also close to optimal.

Finally, we point out that if we are given a policy $y \in I \cap F$, then we can consider risk aversion coefficients $\varkappa_t(\nu) = \kappa_{\min}(\nu, \mu_t^y)$ for every $\nu \in \Omega_t$. Those risk coefficents would provide a time-consistent upper bound that holds only for the policy y. Such an approach might be useful when y is an optimal policy of the original problem $\min_{x \in I \cap F} \rho_{1,T}(Z(x))$ since it would provide a time-consistent approximation which is also an upper bound on the optimal risk value under the policy y. Before delving into further numerical experiments, we introduce the following notation. We use $\varkappa_t \lhd x$ to denote the case when $\varkappa_t(\nu) = \kappa_{\min}(\nu, \mu_t^x)$ for every $\nu \in \Omega_t$. We use this notation in Figure 5.6.

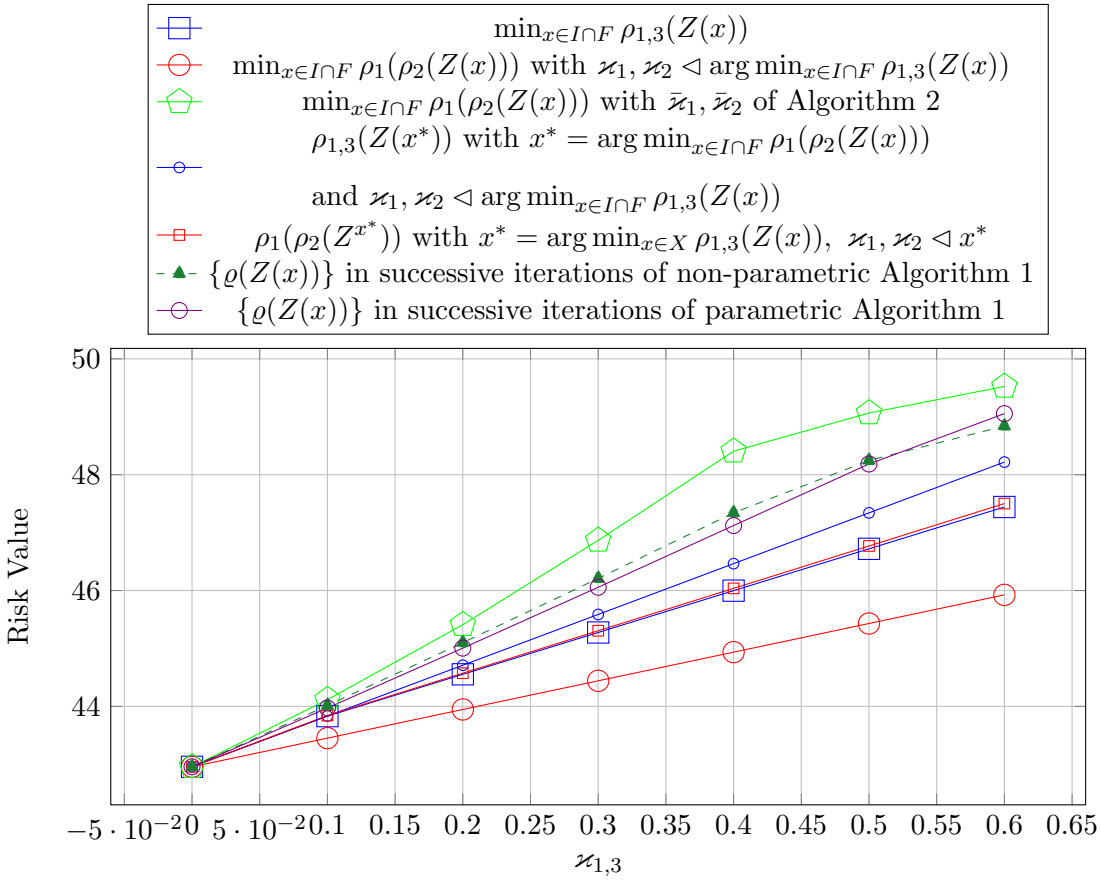

Figure 5.6: Numerical comparison of risk measures for $|x| = 10$ with a 3×3 scenario tree.

We can see in Figure 5.6 that when $\varkappa_1, \varkappa_2 \lhd x^*$, where $x^* = \arg\min_{x \in X} \rho_{1,3}(Z(x))$, then the time-consistent approximation $\rho_1(\rho_2(Z(x^*)))$ is a very close upper bound to the

optimal value of the overall risk measure $\min_{x \in X} \rho_{1,3}(Z(x))$. Finally, we emphasize that the small tree size of the current instance greatly affected its computability, as the total computational time of the three experiments in Figures 5.4, 5.5, and 5.6 was only 153 seconds.

5.2.2 5×5 Scenario Tree with Four Assets

In order to demonstrate the advatages of Algorithm 3 we briefly consider a 5×5 scenario tree. Although we do not provide a graphical illustration of the tree, we assume that its nodes are numbered analogously to Figure 5.3, with ν_0 being the root node, while $\nu_i,\ i = 1, \ldots, 5$ denote the nodes at time $t = 2$, and $\eta_i, i = 1, \ldots, 25$ are the nodes at the final time $t = 3$. The tree has probability and cost vectors as described in Table 5.8.

For comparison purposes, we compute the parametric and non-parametric time-consistent cutting plane approximations.

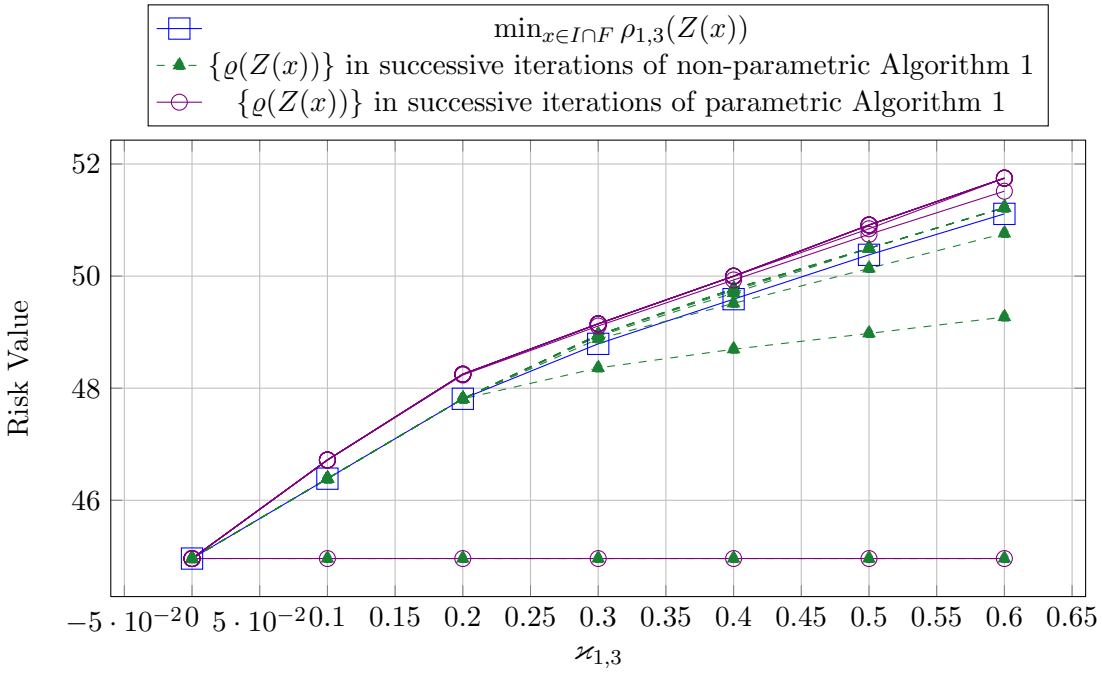

Figure 5.7: Time-consistent cutting plane methods for $|x| = 4$ on a 5×5 scenario tree.

Now, we can find the universal time-consistent upper bounds using Algorithm 3.

	p_η	c_3^η
η_1	0.0621	(64.5417, 74.0680, 34.4474, 96.2274)
η_2	0.0088	(1.9392, 37.4751, 79.5653, 81.6297)
η_3	0.0582	(74.1806, 13.7424, 18.0484, 33.1785)
η_4	0.0751	(25.5083, 72.2757, 28.6771, 66.6513)
η_5	0.0657	(75.0412, 98.8503, 56.9733, 10.5219)
η_6	0.0035	(51.8017, 61.3036, 57.1131, 94.1740)
η_7	0.0023	(91.8465, 43.5344, 53.6729, 51.0679)
η_8	0.0114	(53.7940, 68.4795, 39.7808, 30.7468)
η_9	0.0088	(18.2751, 37.9167, 75.9282, 7.8974)
η_{10}	0.0015	(17.8871, 76.7937, 49.7376, 41.1539)
η_{11}	0.0878	(31.3321, 29.3680, 99.2278, 83.0161)
η_{12}	0.0607	(63.8141, 82.6351, 81.1422, 98.0987)
η_{13}	0.0605	(16.1500, 34.3523, 96.2377, 60.8032)
η_{14}	0.0926	(48.8246, 65.3938, 24.9761, 31.9317)
η_{15}	0.0577	(27.7866, 71.6044, 40.0331, 73.9521)
η_{16}	0.0004	(97.8074, 88.7082, 20.8017, 52.4200)
η_{17}	0.0057	(24.1547, 48.3643, 57.1152, 45.6739)
η_{18}	0.0052	(33.8655, 58.5552, 67.2808, 18.7134)
η_{19}	0.0061	(95.8852, 74.4292, 72.8453, 75.2682)
η_{20}	0.0017	(8.7366, 55.6881, 35.6340, 13.7085)
η_{21}	0.0676	(48.6270, 18.6371, 13.4466, 23.6688)
η_{22}	0.0510	(68.6522, 58.1472, 35.1985, 41.3324)
η_{23}	0.0552	(77.7125, 37.6937, 88.4294, 15.4534)
η_{24}	0.0597	(41.7191, 31.6790, 11.6598, 32.3898)
η_{25}	0.0905	(35.4732, 49.1377, 1.0538, 98.1735)

Table 5.8: Probabilities and cost vectors for every final stage tree node.

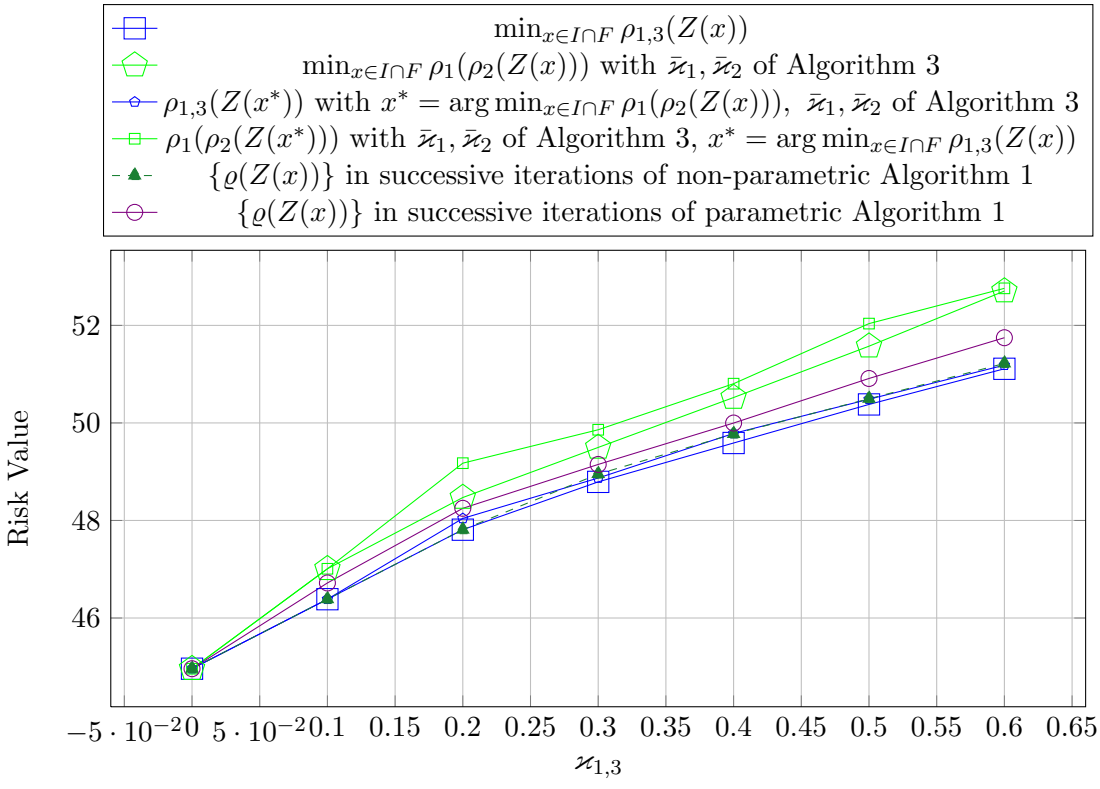

The use of Algorithm 2 for the experiment in Figure 5.8 would be impractical since it would entail the solution of 2^{25} linear programming problems for every $\varkappa_{1,3}$ value. However, due to the small value of $|x|$, we were able to complete the experiment in a matter of minutes using Algorithm 3. On all figures we repeat the the results of the parametric version of Algorithm 1 to illustrate the difference between the universal bounds and the bounds for the optimal value. Clearly, the universal bounds are worse than the parametric bounds, which are in turn worse than the non-parametric bounds. However, all methods closely approximate the original problem for a wide range of risk aversion coefficients. We also provide for comparison the results that would have been obtained if we knew the optimal solution $\hat{x}$ of the "true" problem. Finally, we calculate the "true" risk measure at the optimal solution x^* of the approximate time-consistent problem, to illustrate the accuracy of approximation. Moreover, the optimal solutions of the dynamic problems result in near-optimal objective values for the time-inconsistent formulation. The total computational time for the experiments in Figures 5.7, 5.8, and 5.9 was 423 seconds.

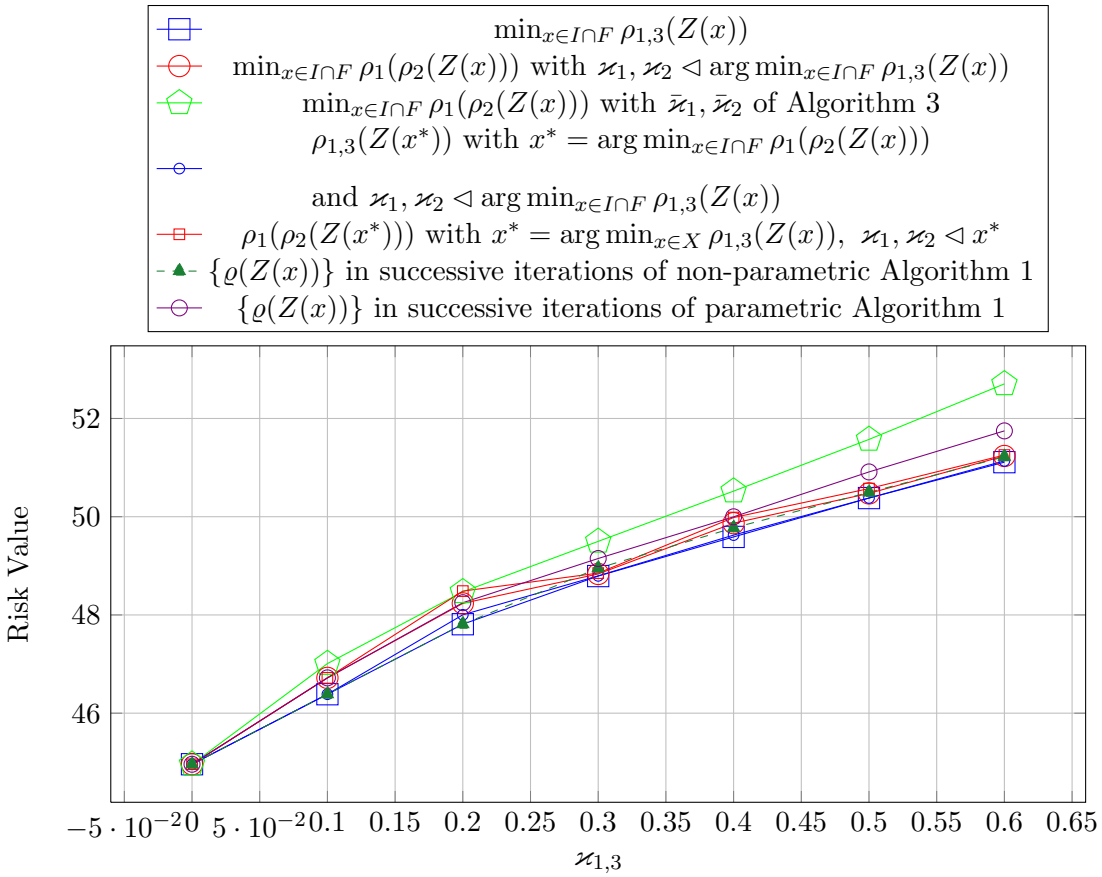

Figure 5.9: Numerical comparison of risk measures for $|x| = 4$ on a 5×5 scenario tree.

5.3 Time Consistency of the Dow Jones Industrial Average

The Dow Jones Industrial Average, or simply the Dow, is a stock market index that was named after former Wall Street Journal editor Charles Dow and statistician Edward Jones. The index comprises thirty large publicly owned companies and summarizes their stock market performance during a standard trading session. Created in 1896, the Dow is widely considered to be one of the most informative indicators of financial markets.

In this section we consider a two stage scenario tree for the stock returns of all companies forming the Dow. More specifically, we use a 4×4 scenario tree created with the multivariate GARCH scenario generation method of Gulten and Ruszczyński [24]. The model training data consists of daily stock price observations for the time period

between September 2, 2008 and November 30, 2011. The scenario trees are available at [23]. In its original form, the method produces scenarios for stock returns, and since we have adopted a cost interpretation we need to multiply the numerical output by -1 in order to make it useful for our purposes.

Under our setup, the time unit is one month which implies that the tree nodes of Ω_2 correspond to scenarios for one month ahead, and the nodes of Ω_3 correspond to scenarios for two months into the future. For the sake of readability, we measure the losses using basis points rather than small fractions.

We consider the following set of feasible and implementable policies $I \cap F = \{x_2 \in \mathbb{R}^{30}, x_3 \in \mathbb{R}^{30} : \ \langle \mathbf{e}^T, x_2 \rangle + \langle \mathbf{e}^T, x_3 \rangle = 1, \ x \geq 0\}$. Now, we can apply the methods of Chapter 3 and Chapter 4. We begin with the non-parametric and parametric cutting plane methods.

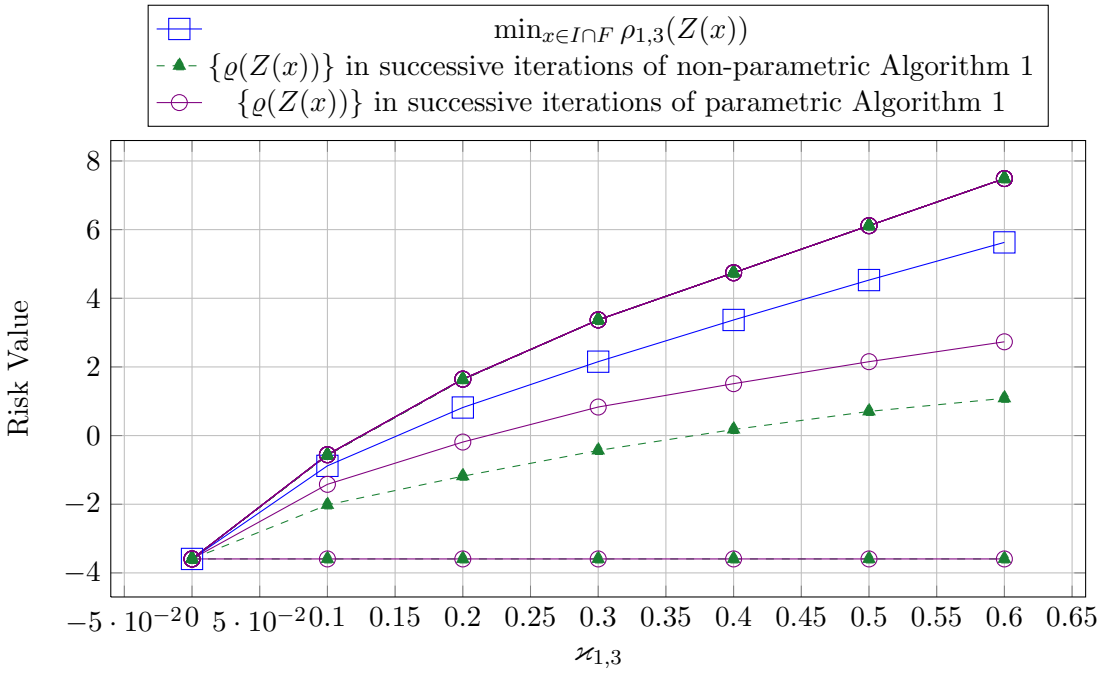

Figure 5.10: Time-consistent cutting plane approximations for $|x| = 60$ on a 4×4 scenario tree.

In Figure 5.10 the two versions of the time-consistent cutting plane method converge to very close values. Moreover, the time-consistent risk functions $\varrho(Z(x))$ closely approximate the original time-inconsistent mean-upper semideviation risk measure $\rho_{1,3}(Z(x))$.

Now, let us examine the universal time-consistent upper bounds.

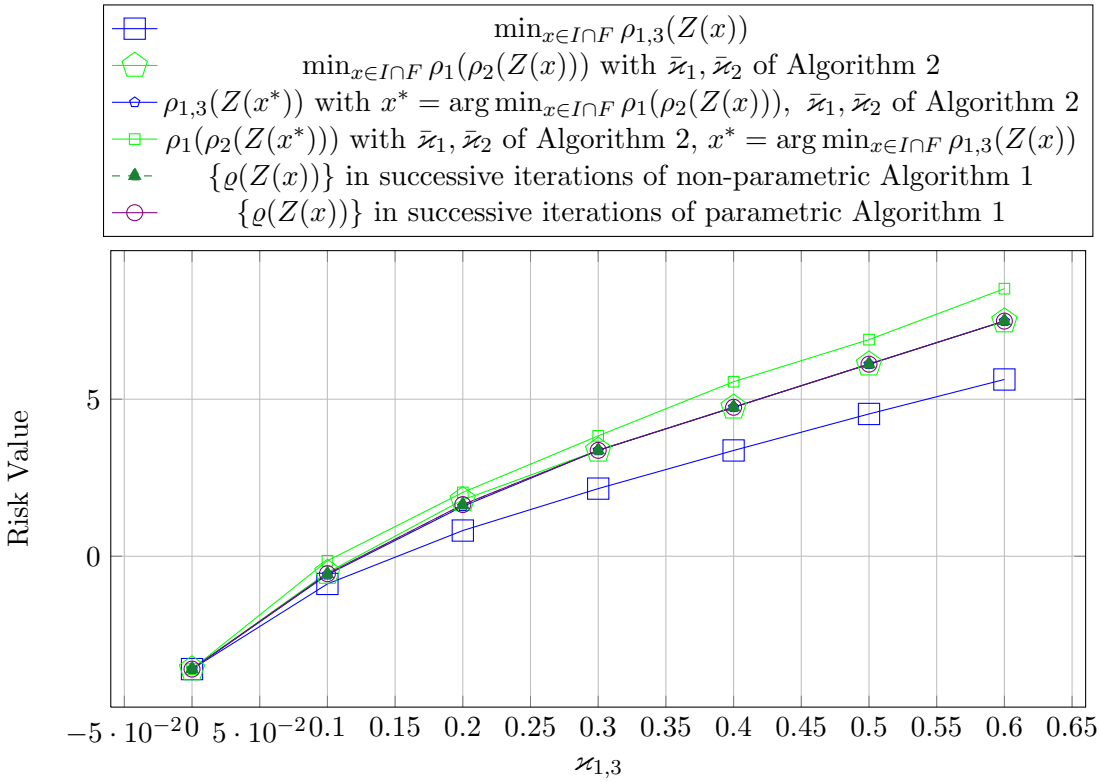

Figure 5.11: Universal time-consistent upper bounds for $|x| = 60$ on a 4×4 scenario tree.

We can see in Figure 5.11 that the optimal objective values of the universal time-consistent risk measures are very close to the optimal objective values of the time-consistent cutting plane methods. Such behavior is desirable in practice since Algorithm 1 can be applied to large problems where Algorithm 2 and Algorithm 3 would not be computationally feasible. Moreover, in Figure 5.12 we consider the construction of time-consistent approximations using only the optimal solution of the time-inconsistent problem $\min\limits_{x\in I\cap F}\rho_{1,3}(Z(x))$.

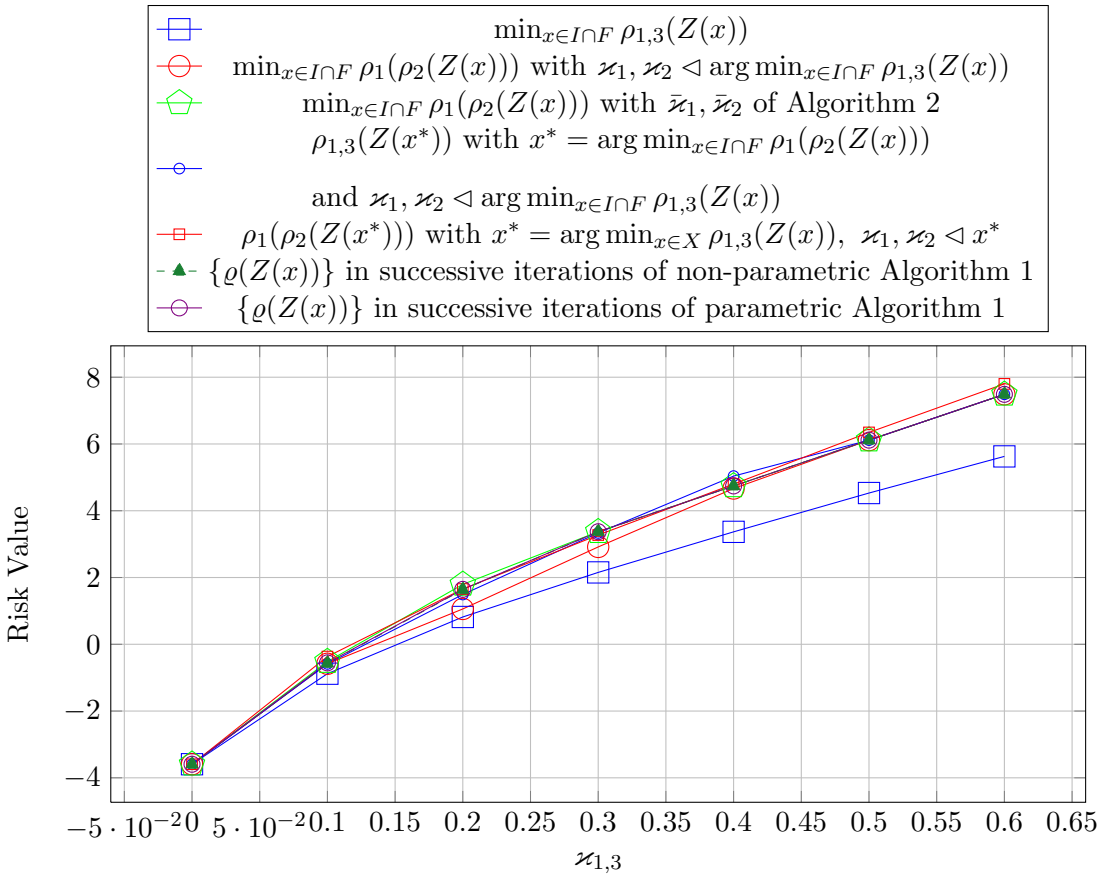

Figure 5.12: Numerical comparison of risk measures for $|x| = 60$ on a 4×4 scenario tree.

Again, the resulting time-consistent risk functions $\rho_1(\rho_2(Z(x)))$ where $\varkappa_1, \varkappa_2 \lhd \arg\min_{x\in I\cap F} \rho_{1,3}(Z(x))$ have optimal objective values that are very close to the universal time-consistent upper bounds. Furthermore, we mention that the completion of the three experiments in Figures 5.10, 5.11, and 5.12 took 997 seconds.

In conclusion, our numerical experiments indicate that the proposed algorithms generate close time-consistent approximations when used with a two-stage scenario tree for the monthly returns of the components of the Dow Jones Industrial Average. The results suggest that the methods can be successfully applied to practical problems, while maintaining the time-consistency of decisions, the interpretability of risk preferences and the computability of solutions.

Chapter 6

Conclusion

There is a great variety of possible methods that can be considered for the measurement of risk associated with uncertain outcomes. In order to improve the interpretability and usefulness of the notion of risk, researchers employ an axiomatic approach. Coherent risk measures are defined as functions of random variables that have the properties of subadditivity, monotonicity, translation equivariance and positive homogeneity. Furthermore, one can show that coherent risk measures are also convex, and therefore they adopt a dual representation.

In addition to making one-time decisions, practioners are often concerned with the evolution of risk over time. Still, the analysis of risk in a multi-period setting can be a treacherous excercise as identical risk preferences can imply vastly different decisions at different time periods. This phenomenon, commonly referred to as time-inconsistency, can present a significant obstacle to decision makers. Fortunately, one can avoid such discrepancies by using specially constructed functions known as time-consistent risk measures.

In our work we have explored the time-consistency of coherent risk measures in the framework of multistage risk-averse stochastic optimization problems on finite scenario trees. We have shown that dynamic time-consistent formulations can be used to approximate problems that have a single global coherent risk measure applied to the aggregated costs over all time periods.

We employed the duality of coherent risk measures to create a time-consistent cutting plane algorithm. In its original form, the method constructs non-parametric time-consistent approximations that are based on one-step conditional risk functions specified only by their dual representation. Furthermore, we showed that the result can be

extended to construct time-consistent approximations where every one-step measure belongs to a given parametric family. This is accomplished by restricting the functional form of the multikernels in the composition of risk measures, and finding the smallest sets of probability measures containing the convex hull of already discovered subgradients within the specified family of sets.

In addition, we also develop two methods for the construction of universal time-consistent upper bounding functions when the given global objective function is the mean-upper semideviation measure of risk. Our first approach is based on scenario enumeration which can be applied only to problems with a small number of final stage scenarios. Its greatest virtues are the straightforward implementation and the applicability to instances involving high-dimensional policies. Our second method involves policy enumeration which is suitable for problems with low-dimensional policies. However, it can be applied to larger trees than the scenario enumeration algorithm. Using the two methods, we are able to construct functions that provide time-consistent upper bounds to the global risk measure for any feasible policy.

In order to analyze the quality of the approximations generated by the proposed methods we conducted multiple computational experiments. We considered instances involving two-stage scenario trees with artificial data, as well as trees with stock return data for the components of the Dow Jones Industrial Average. In all cases, our time-consistent formulations yielded close approximations to the original problem for a wide range of risk aversion parameters.

In the future, we can consider several extensions of the current work. One possible avenue for exploration would be the study of time-consistent approximations for risk measures that lack coherency or convexity. In this direction, the Value at Risk function might be particularly attractive because of its wide use in practice. Another possibility would be the development of improvements of the current underlying model that would enhance the interpretability or computability of the resulting approximations. Such adjustments might be challenging as they could require fundamental changes to the proposed methodology.

References

[1] A. Ruszczyński A. Shapiro, D. Dentcheva. *Lectures on Stochastic Programming*. SIAM, Philadelphia, Pennsylvania, 2009.

[2] Carlo Acerbi and Dirk Tasche. Expected shortfall: a natural coherent alternative to value at risk. *Economic notes*, 31(2):379–388, 2002.

[3] P. Artzner, F. Delbaen, J. M. Eber, and D. Heath. Coherent measures of risk. *Mathematical finance*, 9(3):203–228, 1999.

[4] P. Artzner, F. Delbaen, J. M. Eber, D. Heath, and H. Ku. Coherent multiperiod risk adjusted values and Bellmans principle. *Annals of Operations Research*, 152:5–22, 2007.

[5] Philippe Artzner, Freddy Delbaen, Jean-Marc Eber, David Heath, and Hyejin Ku. Coherent multiperiod risk adjusted values and bellman's principle. *Annals of Operations Research*, 152(1):5–22, 2007.

[6] J.-P. Aubin and H. Frankowska. *Set-Valued Analysis*. Birkhäuser, Boston, 1990.

[7] Aharon Ben-Tal and Marc Teboulle. Expected utility, penalty functions, and duality in stochastic nonlinear programming. *Management Science*, 32(11):1445–1466, 1986.

[8] Aharon Ben-Tal and Marc Teboulle. An old-new concept of convex risk measures: The optimized certainty equivalent. *Mathematical Finance*, 17(3):449–476, 2007.

[9] J. R. Birge and F. Louveaux. *Introduction to Stochastic Programming*. Springer-Verlag, New York, NY, 1997.

[10] P. Cheridito, F. Delbaen, and M. Kupper. Dynamic monetary risk measures for bounded discrete-time processes. *Electronic Journal of Probability*, 11:57–106, 2006.

[11] Patrick Cheridito, Freddy Delbaen, and Michael Kupper. Dynamic monetary risk measures for bounded discrete-time processes. *Electronic Journal of Probability*, 11(3):57–106, 2006.

[12] Patrick Cheridito and Mitja Stadje. Time-inconsistency of var and time-consistent alternatives. *Finance Research Letters*, 6(1):40–46, 2009.

[13] R. A. Collado, D. Papp, and A. Ruszczyński. Scenario decomposition of risk-averse multistage stochastic programming problems. *Annals of Operations Research*, 200(1):147–170, 2012.

[14] Jon Danielsson, Bjørn N Jorgensen, Sarma Mandira, Gennady Samorodnitsky, and CG de Vries. Subadditivity re–examined: the case for value-at-risk. 2005.

[15] Freddy Delbaen. Coherent risk measures. *Blätter der DGVFM*, 24(4):733–739, 2000.

[16] Kai Detlefsen and Giacomo Scandolo. Conditional and dynamic convex risk measures. *Finance and Stochastics*, 9(4):539–561, 2005.

[17] H. Föllmer and A. Schied. *Stochastic Finance: An Introduction in Discrete Time*, volume 27 of *de Gruyter Studies in Mathematics*. Walter de Gruyter & Co., Berlin, 2nd edition, 2004.

[18] Hans Föllmer and Alexander Schied. Convex measures of risk and trading constraints. *Finance and Stochastics*, 6(4):429–447, 2002.

[19] Hans Follmer and Alexander Schied. Convex and coherent risk measures. *Encyclopedia of Quantitative Finance, John Wiley & Sons, Hoboken*, pages 355–363, 2010.

[20] M. Fritelli and E. Rosazza Gianin. Putting order in risk measures. *Journal of Banking and Finance*, 26:1473–1486, 2002.

[21] Marco Frittelli and E Rosazza Gianin. Dynamic convex risk measures. *Risk measures for the 21st century*, pages 227–248, 2004.

[22] Marco Frittelli and Emanuela Rosazza Gianin. Putting order in risk measures. *Journal of Banking & Finance*, 26(7):1473–1486, 2002.

[23] Sitki Gulten. Two-stage scenario trees for monthly stock returns. `http://www.asamov.com/monthly/`. Accessed: 2013-07-03.

[24] Sitki Gulten. *Two-Stage Portfolio Optimization with Higher-Order Conditional Measures of Risk*. PhD thesis, Rutgers University, 2013.

[25] Dan A Iancu, Marek Petrik, and Dharmashankar Subramanian. Tight approximations of dynamic risk measures.

[26] Rustam Ibragimov. Portfolio diversification and value at risk under thick-tailedness. *Harvard Institute of Economic Research Discussion Paper*, (2086), 2004.

[27] V. Kozmik and D. P. Morton. Risk-averse stochastic dual dynamic programming. *Optimization Online*, 2013.

[28] S. Kusuoka. On law invariant coherent risk measures. *Advances in mathematical economics*, 3(1):83–95, 2001.

[29] M. M. Fritelli and G. Scandolo. Risk measures and capital requirements for processes. *Mathematical Finance*, 16:589–612, 2006.

[30] Harry Markowitz. Portfolio selection*. *The journal of finance*, 7(1):77–91, 1952.

[31] Harry Markowitz. Portfolio selection: efficient diversification of investments. cowles foundation monograph no. 16, 1959.

[32] N. Miller and A. Ruszczyński. Risk-averse two-stage stochastic linear programming: modeling and decomposition. *Oper. Res.*, 59(1):125–132, 2011.

[33] Włodzimierz Ogryczak and Andrzej Ruszczyński. From stochastic dominance to mean-risk models: Semideviations as risk measures. *European Journal of Operational Research*, 116(1):33–50, 1999.

[34] Włodzimierz Ogryczak and Andrzej Ruszczyński. On consistency of stochastic dominance and mean–semideviation models. *Mathematical Programming*, 89(2):217–232, 2001.

[35] Irina Penner. Dynamic convex risk measures: time consistency, prudence, and sustainability. *Humboldt-Universität zu Berlin*, 2007.

[36] M. V. F. Pereira and L. M. V. G. Pinto. Multi-stage stochastic optimization applied to energy planning. *Mathematicsl Programming*, 52:359–375, 1991.

[37] G. Ch. Pflug and W. Römisch. *Modeling, Measuring and Managing Risk*. World Scientific, Singapore, 2007.

[38] Georg Ch Pflug. Some remarks on the value-at-risk and the conditional value-at-risk. In *Probabilistic constrained optimization*, pages 272–281. Springer, 2000.

[39] Georg Ch Pflug and Alois Pichler. Time consistency and temporal decomposition of positively homogeneous risk functionals. 2012.

[40] Georg Ch Pflug and Werner Römisch. *Modeling, measuring and managing risk*. World Scientific Singapore, 2007.

[41] A. B. Philpott and V. L. De Matos. Dynamic sampling algorithms for multistage stochastic programs with risk aversion. Technical report, Electric Power Optimization Centre, University of Auckland, 2011.

[42] F. Riedel. Dynamic coherent risk measures. *Stochastic Processes and Their Applications*, 112:185–200, 2004.

[43] R Tyrrell Rockafellar and Stanislav Uryasev. Conditional value-at-risk for general loss distributions. *Journal of Banking & Finance*, 26(7):1443–1471, 2002.

[44] Berend Roorda and Johannes M Schumacher. Time consistency conditions for acceptability measures, with an application to tail value at risk. *Insurance: Mathematics and Economics*, 40(2):209–230, 2007.

[45] Birgit Rudloff, Jörn Sass, and Ralf Wunderlich. Entropic risk constraints for utility maximization. *et al., Festschrift in celebration of Prof. Dr. Wilfried Greckschs 60th birthday. Aachen: Shaker Verlag. Berichte aus der Mathematik*, pages 149–180, 2008.

[46] A. Ruszczyński. Decomposition methods. In A. Ruszczyński and A. Shapiro, editors, *Stochastic Programming, Handbooks Oper. Res. Management Sci.*, pages 141–211. Elsevier, Amsterdam, 2003.

[47] A. Ruszczynski. *Nonlinear optimization*, volume 13. Princeton University Press, Princeton, New Jersey, 2006.

[48] A. Ruszczyński. Risk-averse dynamic programming for Markov decision processes. *Mathematical programming*, 125(2):235–261, 2010.

[49] A. Ruszczyński and A. Shapiro. Conditional risk mappings. *Mathematics of Operations Research*, 31(3):544–561, 2006.

[50] A. Ruszczyński and A. Shapiro. Optimization of convex risk functions. *Mathematics of Operations Research*, 31(3):433–452, 2006.

[51] A. Shapiro. On Kusuoka representation of law invariant risk measures.

[52] A. Shapiro. Analysis of stochastic dual dynamic programming method. *European J. Oper. Res.*, 209(1):63–72, 2011.

[53] Stefan Weber. Distribution-invariant risk measures, information, and dynamic consistency. *Mathematical Finance*, 16(2):419–441, 2006.

[54] Linwei Xin and Alexander Shapiro. Bounds for nested law invariant coherent risk measures. *Operations Research Letters*, 2012.

[55] Yasuhiro Yamai and Toshinao Yoshiba. On the validity of value-at-risk: comparative analyses with expected shortfall. *Monetary and Economic Studies*, 20(1):57–85, 2008.

Vita

Tsvetan Asamov

2008-2013 *Ph. D. in Operations Research*
RUTCOR, Rutgers University, NJ

2004-2008 *B. A. in Mathematics, Economics, Scientific Computing*
Kenyon College, OH

2012-2013 Graduate assistant, RUTCOR, Rutgers University

2010-2012 Teaching assistant, RUTCOR, Rutgers University

2008-2010 Fellow, RUTCOR, Rutgers University